Modeling and Control of Surge and Rotating Stall in Compressors

Dr.ing. thesis

Jan Tommy Gravdahl

Report 98-6-W
Department of Engineering Cybernetics
Norwegian University of Science and Technology
N-7034 Trondheim, Norway
1998

Abstract

This thesis contains new results in the field of modeling and control of rotating stall and surge in compressors.

A close coupled valve is included in the Moore-Greitzer compression system model and controllers for both surge and rotating stall is derived using backstepping. Disturbances, constant and time varying, are then taken into account, and non-linear controllers are derived. Stability results are given. Then, passivity is used to derive a simple surge control law for the close coupled valve. This proportional control law is shown to stabilize the system even in the presence of time varying disturbances in mass flow and pressure.

A novel model for an axial compression system with non-constant compressor speed is derived by extending the Moore-Greitzer model. Rotating stall and surge is studied in connection with acceleration of the compressor.

Finally, a model for a centrifugal compression system with time varying compressor speed is derived. The variable speed compressor characteristic is derived based on energy losses in the compressor components. Active control of surge in connection with varying speed is studied. Semi-global exponential stability of the compression system with both surge and speed control is proven.

The main results of this thesis have been presented at international conferences. Parts of the thesis has also been submitted for publication in international journals.

Preface and Acknowledgments

This thesis is submitted in partial fulfillment of the requirements for the degree of doktor ingeniør at the Norwegian University of Science and Technology (NTNU). The thesis is based on research done at the Department of Engineering Cybernetics during the period January 1995 through January 1998. It has been financed by a scholarship from the Research Council of Norway, under grant 107467/410.

I am grateful to my supervisor, Professor Dr.ing. Olav Egeland, for introducing me to the field of compressor control and control of mechanical systems in general. He has been a source of valuable advice, comments and inspiration throughout the work on this thesis and the papers on which it is based.

The staff at the department and my colleagues are acknowledged for creating a very pleasant environment in which to do research.

I would like to thank Dr.ing. Trygve Lauvdal with whom I shared an office for the past three years. Our office has been a very pleasant place to work, and we have had numerous useful and not-so-useful discussions. Trygve is also acknowledged for his proofreading of this thesis.

The help of Dr.ing. Erling Aarsand Johannesen, in the form of many constructive comments and proofreading, is greatfully acknowledged.

Finally, I would like to express my love and deepest gratitude to the three girls in my life: To my wife Gøril for her love, continued encouragement and support during the work on this thesis, and to my daughters Irja and Mina for their unconditional love.

Jan Tommy Gravdahl

March 1998, Trondheim, Norway

Contents

List of Figures

Chapter 1

Introduction

1.1 Introduction

This thesis presents results from an investigation on nonlinear compressor control where feedback is used to stabilize the compressor to the left of the surge line. The work is motivated by the fundamental instability problem of surge and rotating stall which limits the range of operation for compressors at low mass flows.

This instability problem has been extensively studied and industrial solutions based on *surge avoidance* are well established. These solutions are based on keeping the operating point to the right of the compressor surge line using a surge margin. There is a potential for 1) increasing the efficiency of compressors by allowing for operation closer to the surge line than what is the case in current systems, and 2) increasing the range of mass flows over which the compressor can operate stably. The increase in efficiency and mass flow range is in particular possible with compressor designs where the design is done with such controllers in mind. This, however, raises the need for control techniques, which stabilize the compressor also to the left of the surge line, as disturbances or set point changes may cause crossing of the surge line. This approach is known as *active surge control*. Active surge control is presently an area of very intense research activity, and is also the topic of this thesis.

1.2 Background

Compressors are used in a wide variety of applications. These includes turbojet engines used in aerospace propulsion, power generation using industrial gas turbines, turbocharging of internal combustion engines, pressurization of gas and fluids in the process industry, transport of fluids in pipelines and so on.

There are four general types of compressors: reciprocating, rotary, centrifugal and

axial. Some authors use the term radial compressor when refering to a centrifugal compressor. Reciprocating and rotary compressors work by the principle of reducing the volume of the gas, and will not be considered further in this thesis. Centrifugal and axial compressors, also known as turbocompressors or continuous flow compressors, work by the principle of accelerating the fluid to a high velocity and then converting this kinetic energy into potential energy, manifested by an increase in pressure, by decelerating the gas in diverging channels. In axial compressors the deceleration takes place in the stator blade passages, and in centrifugal compressor it takes place in the diffuser. One obvious difference between these two types of compressors is, in axial compressors, the flow leaves the compressor in the axial direction, whereas, in centrifugal compressors, the flows leaves the compressor in a direction perpendicular to the axis of the rotating shaft. In this thesis both types of continuous flow compressor will be studied. The literature on compressors in general is vast, and a basic introduction is given by e.g. Ferguson (1963) or Cohen *et al.* (1996), and more advanced topics are covered by e.g. Cumpsty (1989).

The useful range of operation of turbocompressors is limited, by choking at high mass flows when sonic velocity is reached in some component, and at low mass flows by the onset of two instabilities known as surge and rotating stall. Traditionally, these instabilities have been avoided by using control systems that prevent the operating point of the compressions system to enter the unstable regime to the left of the *surge line*, that is the stability boundary. A fundamentally different approach, known as active surge/stall control, is to use feedback to stabilize this unstable regime. This approach will be investigated in this thesis, and it will allow for both operation in the peak efficiency and pressure rise regions located in the neighborhood of the surge line, as well as an extension of the operating range of the compressor.

1.3 Stability of Compression Systems

Compression systems such as gas turbines can exhibit several types of instabilities: combustion instabilities, aeroelastic instabilities such as flutter and finally aerodynamic flow instabilities, which this study is restricted to.

Two types of aerodynamic flow instabilities can be encountered in compressors. These are known as *surge* and *rotating stall*. The instabilities limits the flow range in which the compressor can operate. Surge and rotating stall also restrict the performance (pressure rise) and efficiency of the compressor. According to de Jager (1995) this may lead to heating of the blades and to an increase in the exit temperature of the compressor.

1.3.1 Surge

Surge is an axisymmtrical oscillation of the flow through the compressor, and is characterized by a limit cycle in the compressor characteristic. An example of

such a characteristic is shown as the S-shaped curve in Figure 1.1. The dotted segment of the curve indicates that this section usually is an approximation of the physical system, as it is difficult to measure experimentally. Surge oscillations are in most applications unwanted, and can in extreme cases even damage the compressor. As discussed by Erskine and Hensman (1975) and Greitzer (1981), surge can also induce vibrations in other components of the compression system, such as e.g. connected piping. It is common to distinguish between at least two different types of surge: 1) Mild/Classic surge and 2) Deep surge. A combination of surge and rotating stall is known as modified surge. For more information on different types of surge, consult Greitzer (1981) or de Jager (1995).

The first of these types is a phenomenon with oscillations in both pressure and flow in the compressor system, while in the second type, the oscillations in mass flow have such a large amplitude, that flow reversal occurs in the compression system. A drawing of a typical deep surge cycle is shown in Figure 1.1. The cycle starts at (1) where the flow becomes unstable. It then jumps to the reversed flow characteristic (2) and follows this branch of the characteristic until approximately zero flow (3), and then jumps to (4) where it follows the characteristic to (1), and the cycle repeats. Surge can occur in both axial and centrifugal compressors.

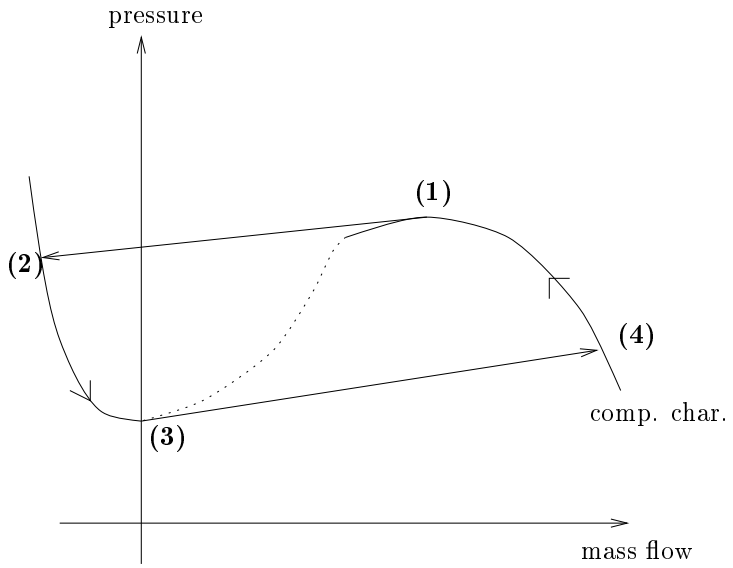

Figure 1.1: *Compressor characteristic with deep surge cycle, de Jager (1995).*

1.3.2 Rotating Stall

Rotating stall can occur in both axial and centrifugal compressors. Although rotating stall is known to occur in centrifugal compressors, see e.g. Emmons *et al.* (1955), there exists little theory on the subject, and according to de Jager (1995) its importance is still a matter of debate. In this thesis, only rotating stall in axial

compressors will be considered, and when it is referred to rotating stall it is to be understood that a axial compressor is considered.

Rotating stall is an instability where the circumferential flow pattern is disturbed. This is manifested through one or more *stall cells* of reduced, or stalled, flow propagate around the compressor annulus at a fraction, 20-70% according to Greitzer (1980), of the rotor speed. This leads to a reduction of the pressure rise of the compressor, and in the compressor map this corresponds to the compressor operating on the so called in-stall characteristic, see Figure 1.3.

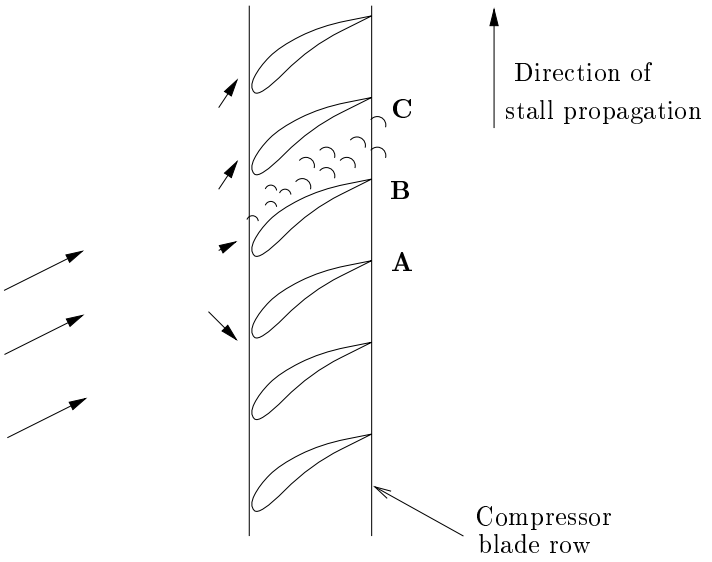

Figure 1.2: *Physical mechanism for inception of rotating stall, Emmons et.al. (1955).*

The basic explanation of the rotating stall mechanism was given by Emmons *et al.* (1955) and can be summarized as follows. Consider a row of axial compressor blades operating at a high angle of attack, as shown in Figure 1.2. Suppose that there is a non-uniformity in the inlet flow such that a locally higher angle of attack is produced on blade B which is enough to stall it. The flow now separates from the suction surface of the blade, producing a flow blockage between B and C. This blockage causes a diversion of the inlet flow away from B towards A and C, resulting in a increased angle of attack on C, causing it to stall. Thus the stall cell propagate along the blade row.

It is common to distinguish between at least two types of rotating stall, full-span and part-span. In full-span stall, the complete height of the annulus is stalled, while in part-span rotating stall a restricted region of the blade passage is stalled. Full-span stall is most likely to occur in high hub/tip ratio axial compressors. In addition we can have various degrees of rotating stall depending of the size of the area of the compressor annulus being blocked. In addition to the problem

related to reduced pressure rise due to rotating stall , there is also the problem of vibrations in the blades as stall cells rotate at a fraction of rotor speed. Thus, the blades passes in and out of regions of stalled flow which can, according to Horlock (1958), Greitzer (1981) and Pinsley *et al.* (1991), induce vibrations in the blades. Moreover, if a natural frequency of vibration of the blades coincides with the frequency at which the stall cell pass a blade, the result is resonance and possible mechanical failure due to fatigue.

Another consequence of rotating stall is the hysteresis occurring when trying to clear the stall by using the throttle. This phenomenon is depicted in Figure 1.3, and might be described in the following manner: Initially the compressor is operating stably (1), then a disturbance drives the equilibrium over the surge line resulting in rotating stall, and a operating point on the low pressure in-stall characteristic (2). By opening the throttle to clear the stall, result in a higher throttle opening than initially (3), before the operating point is back on the stable compressor characteristic (4). There are several degrees to how severe this hysteresis may be. This depends on the so called skewness of the compressor characteristic. This is treated in detail in recent papers by Wang and Krstić (1997*a*), Sepulchre and Kokotović (1996) and Protz and Paduano (1997).

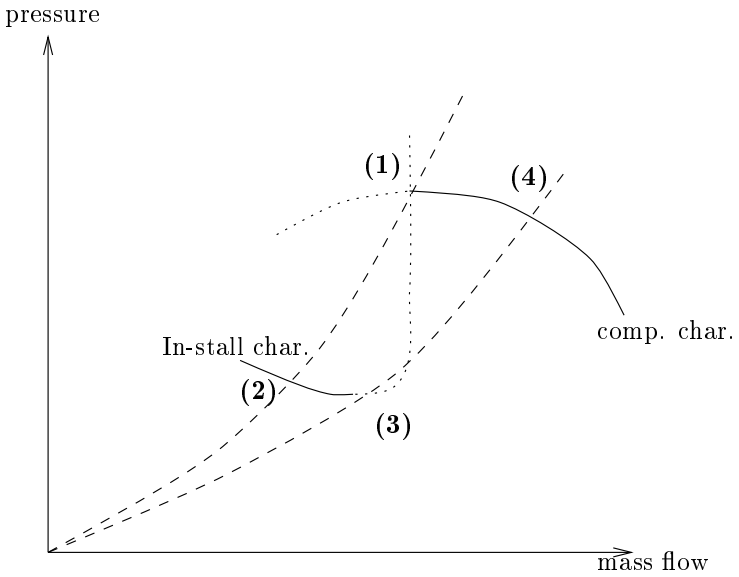

Figure 1.3: *Schematic drawing of hysteresis caused by rotating stall.*

1.3.3 Stability Analysis

As a rule, stall and surge occur at the local maximum of the compressor characteristic or at a point of the compressor characteristic with a certain positive slope. When linearizing the nonlinear surge model of Greitzer (1976*a*), one gets

a model similar to that of a damped linear oscillator. This surge model was also studied by Stenning (1980). Calculating the eigenvalues of the oscillator system, as done by Willems (1996) , reveals that the stability boundary is set by a relation between the slope of the compressor characteristic, the slope of the load line, and the Greitzer B-parameter. The surge point will be located some small distance to the left of the peak. According to Cumpsty (1989), the peak of the compressor characteristic provides a convenient working approximation for the surge point. The same conclusion is drawn by Stenning (1980), where it is also pointed out that rotating stall occurs at the peak of the compressor characteristic.

Another approach frequently used to investigate stability of compression systems is bifurcation analysis. For studies on this topic, consult McCaughan (1989), Liaw and Abed (1992) or Abed *et al.* (1993).

1.4 Modeling of Compression Systems

Low order models for surge in compression systems, both axial and centrifugal, have been proposed by many authors. A classical reference is Emmons *et al.* (1955). In the following, a *compression system* will refer to a system consisting of a compressor pressurizing incompressible fluid, which is discharged into a plenum volume which discharges via a throttle valve.

The compression system model of Greitzer (1976*a*) has been widely used for surge control design. It was derived for axial compression systems, but Hansen *et al.* (1981) showed that it is also applicable to centrifugal compressors. The model has two states, normalized mass flow and normalized pressure, and the compressor is treated as an actuator disc, with a third order polynomial flow/pressure rise characteristic. Other assumptions of this model are: one dimensional incompressible flow in the ducts, isentropic compression process in the plenum and no spatial variations of pressure in the plenum. Extensive experiments by Greitzer (1976*b*) and Hansen *et al.* (1981) confirm that although it is of low order compared to the complex phenomenon it models, the model is capable of describing both the qualitative and quantitative aspects of surge. The model was extended for centrifugal compressors with varying rotor speed by Fink *et al.* (1992). Many other models of compression systems have been presented in the literature, for an overview consult Willems (1996).

Based on the work of Moore (1984*b*), the Moore-Greitzer model was derived in Moore and Greitzer (1986). In developing this model, some of the assumptions made were: Large hub/tip ratio, irrotational and inviscid flow in the inlet duct, incompressible compressor mass flow, short throttle duct, small pressure rise compared to ambient conditions and constant rotor speed. A Galerkin procedure was used to approximate the PDEs describing the system dynamics by three ODEs. This three state model is capable of describing both surge and rotating stall, the third state being the stall amplitude. Many authors have extended and modified the model. Inclusion of higher order harmonics was studied by Mansoux *et al.* (1994), and other types of compressor characteristics was used by Wang and

Krstić (1997*a*).

An alternative model of rotating stall was presented by Paduano *et al.* (1995), where rotating stall was described as a traveling wave, and spatial Fourier analysis was used. Other models that are capable of demonstrating rotating stall are those of Eveker and Nett (1991) and Badmus *et al.* (1995), but these models do not include the stall amplitude as a state, but the presence of rotating stall is manifested as a pressure drop.

1.5 Control of Surge and Rotating Stall

1.5.1 Surge/Stall Avoidance

As mentioned above, the state of art in control of compressors was until about a decade ago, the method of surge avoidance, which is usually an open loop strategy according to de Jager (1995). The compressor is prevented from operating in a region near and beyond the surge line. This is achieved by e.g. recirculation of the flow or blowing off flow through a bleed valve. As the compressor characteristic and thus the surge line may be poorly known, it will often be necessary to have a fairly conservative *surge margin* between the surge line and the *surge avoidance line*. The compressor is then not allowed to operate between these two lines in the compressor map. Accounting for possible disturbances also affects the size of the surge margin.

The drawbacks of surge avoidance schemes are several: (1) Recycling and bleeding of compressed flow lower the efficiency of the system, (2) maximum efficiency and pressure rise may not be achievable at all, as they usually are achieved for mass flows close to the surge line and (3) the surge margin limits the transient performance of the compressor as acceleration of the machine tends to drive the state of the system towards the surge line.

An alternative to surge avoidance is *surge detection and avoidance*. Using this strategy, the drawbacks of the surge margin can be avoided by the activation of the controller if the onset of instabilities is detected. De Jager (1995) concludes that the main disadvantages of this strategy are problems associated with the detection of the instability onset and the necessity of large control forced and fast-acting control systems.

1.5.2 Active Surge/Stall Control

The approach of active surge/stall control aims at overcoming the drawbacks of surge avoidance, by stabilizing some part of the unstable area in the compressor map using feedback. This approach was introduced in the control literature by Epstein *et al.* (1989). In the last decade, the literature on feedback stabilization of compression systems has become extensive. This is partly due to the introduction, and success, of the Moore-Greitzer model.

In the literature on developments in the field of jet engines for aircraft propulsion, active stall/surge control is often said to become an important part of future engines. For details see e.g. Covert (1995), Ruffles (1996) or DeLaat *et al.* (1996). The term "smart engines" is often used when refering to these engines. Brown *et al.* (1997) reports of successfull in-flight experiments on a F-15 aircraft with active stall control on one engine. Experimental results on laboratory engines are reported by Paduano *et al.* (1993), Ffowcs Williams *et al.* (1993), Hynes *et al.* (1994) and Behnken and Murray (1997).

Among several possible actuators for stabilizing compression systems, the throttle valve as studied by Krstić *et al.* (1995*b*) and Badmus *et al.* (1996), or bleed valves as studied by Eveker and Nett (1991) or Murray (1997) has been the most commonly used, at least in the control literature. Other possibilities are variable inlet guide vanes as in Paduano *et al.* (1993), loudspeaker as in Ffowcs Williams and Huang (1989), tailored structures as in Gysling *et al.* (1991), recirculation as in Balchen and Mummé (1988), movable wall as in Epstein *et al.* (1989) or air injection as in Day (1993) and Behnken and Murray (1997). However, the use of a close-coupled valve (hereafter named CCV) was claimed by Simon *et al.* (1993) and van de Wal *et al.* (1997) to be among the most promising actuators for compressor surge control.

The methods used for designing surge and stall controllers vary. Linearization and complex-valued proportional control was used by Epstein *et al.* (1989), bifurcation theory by Liaw and Abed (1996), feedback linearization by Badmus *et al.* (1996), Lyapunov methods by Simon and Valavani (1991), backstepping by Krstić *et al.* (1995*b*) and $\mathcal{H}_\infty$ by van de Wal *et al.* (1997) and Weigl and Paduano (1997). In this thesis, backstepping, which is Lyapunov based, and passivity will be used.

Another important aspect of active surge and stall control is the disturbance rejection capabilities and robustness of the proposed controllers. Greitzer and Moore (1986) recognized that research is needed on modeling of disturbances in compression systems. The reason for this being that disturbances may initiate surge or rotating stall. Surge controllers with disturbance rejection was presented by Simon and Valavani (1991) and stall/surge controllers by Haddad *et al.* (1997), and stall/surge controllers for compressors with uncertain compressor characteristic was studied by Leonessa *et al.* (1997*b*).

1.6 Contributions of this Thesis

The contributions of this thesis can be summarized as follows:

- **Close coupled valve control of the Moore-Greitzer model:** Controllers for a close coupled valve in a Moore-Greitzer type compression system have been derived. The controllers allow for stabilization of rotating stall and surge to the left of the compressors surge line. The effect of constant and time varying disturbances has also been studied, and controllers have been derived that ensures avoidance of stall and surge when these disturbances are present in the compression system. The theory used is backstepping. This

work has been published in Gravdahl and Egeland (1997*c*) and Gravdahl and Egeland (1997*d*), and is also reported in Gravdahl and Egeland (1998*a*).

- **Passivity based surge control:** A surge control law has been derived for the Greitzer model using passivity and a input-output model. The resulting controller is very simple and is shown to render the system $\mathcal{L}_2$-stable also when disturbances are taken into account. Parts of this work has been published in Gravdahl and Egeland (1997*f*) and submitted in Gravdahl and Egeland (1998*c*).

- **Post stall modeling of axial compression systems with non-constant speed:** An extension of the Moore-Greitzer model has been derived to take non-constant compressor speed into account. This new model also includes higher harmonics of rotating stall. The work is published in Gravdahl and Egeland (1997*a*) and is also reported in Gravdahl and Egeland (1997*e*)

- **Centrifugal compressor modeling and control:** A speed dependent compressor characteristic for a centrifugal compressor has been derived by the use of energy transfer and losses in the compressor components. This characteristic has been used in a dynamic model of a compression system with time varying compressor speed, to derive controllers that simultaneously suppress surge and ensures that desired speed is reached. This work has been published in Gravdahl and Egeland (1997*g*) and Gravdahl and Egeland (1998*b*), and is also under consideration for publication in Gravdahl and Egeland (1997*b*).

The results reported of in this Thesis is also accepted for publication in Gravdahl (1998).

1.7 Outline of the Thesis

The outline of this thesis is as follows

- **Chapter 2:** The Moore-Greitzer model and the actuator used in this theses for surge/stall control, the close coupled valve, are presented. Using back-stepping, various controllers are derived. These includes controllers for surge with time varying and constant disturbances (in the later case an adaptive controller is derived) and controllers for rotating stall with time varying disturbances. Stability results are given for each controller.

- **Chapter 3:** Passivity is used to derive a surge control law. The controller is shown to maintain certain stability properties even if disturbances are considered.

- **Chapter 4:** An extension of the familiar Moore-Greitzer model is presented. This model includes Greitzer's B-parameters as a state, which is a consequence of relaxing the assumption of constant compressor speed.

- **Chapter 5:** Here a novel model for a compression system with a variable speed centrifugal compressor is derived. Using Lyapunov theory, controllers are derived that ensures suppression of surge and regulation of speed. The closed loop system is shown to be semi globally exponentially stable.
- **Chapter 6:** Conclusions
- Finally, references and five appendices are given at the end of the thesis. A nomenclature is given in Appendix A.

Chapter 2

Close Coupled Valve Control of Surge and Rotating Stall for the Moore-Greitzer Model

2.1 Introduction

In this chapter controllers for surge and rotating stall using a CCV is derived. Several possible actuators exists for stabilizing compression systems. Krstić *et al.* (1995*b*), Badmus *et al.* (1996) and others suggest using a variable throttle valve, Eveker and Nett (1991), Murray (1997) and others use bleed valves. These two actuators have been the most commonly used, at least in the control literature. However, there are many other possibilities: Paduano *et al.* (1993) use variable inlet guide vanes, a loudspeaker is used by Ffowcs Williams and Huang (1989), tailored structures in Gysling *et al.* (1991), recirculation is studied by Balchen and Mummé (1988), a movable wall in Epstein *et al.* (1989) and finally Day (1993) and Behnken and Murray (1997) employ air injection. However Simon *et al.* (1993) claimed that the use of a close-coupled valve (hereafter named CCV) is among the most promising actuators for active surge control.

The use of a CCV for control of compressor surge was studied by Dussourd *et al.* (1976), Greitzer (1981), Pinsley *et al.* (1991), Simon and Valavani (1991), Simon *et al.* (1993) and Jungowski *et al.* (1996). Experimental results of compressor surge control using a CCV was reported by Erskine and Hensman (1975) and Dussourd *et al.* (1977). Simon (1993) and Simon *et al.* (1993) compared, using linear theory, this strategy to a number of other possible methods of actuation and sensing. The conclusion was that the most promising method of surge control is to actuate the system with feedback from the mass flow measurement to a CCV or an injector. In

line with this conclusion are the recent results of van de Wal and Willems (1996) and van de Wal *et al.* (1997), where nonlinear controllers were derived based on $\mathcal{H}_\infty$ performance specifications.

Dussourd *et al.* (1976), Greitzer and Griswold (1976), Dussourd *et al.* (1977), Greitzer (1977) and Greitzer (1981) conclude that downstream components in compression systems have an impact on the onset of rotating stall. Dussourd *et al.* (1977) used a CCV to achieve a significant extension of flow range, and it was concluded that the CCV also affected the onset of rotating stall as well as surge. Osborn and Wagner (1970) report of experiments where rotating stall in an axial-flow fan rotor was suppressed, at the cost of a drop in efficiency, by a movable "door" close coupled downstream of the rotor. The door had a similar geometry to that of a axisymmetric nozzle, and the experimental setup simulated a turbofan engine. Greitzer (1977) found that a downstream nozzle shifted the point of onset of rotating stall to lower mass flows, however the effect was strongest for single cell, full span stall. The Moore-Greitzer model, which is going to be used in this chapter, assumes a high hub to tip ratio compressor, which is likely to exhibit full span stall. Moreover, Greitzer (1977) found that the stabilizing effect of the nozzle falls rapidly with increasing distance between compressor and nozzle, and thereby emphasizing the importance of close coupling between compressor and actuator, a point also made by Hendricks and Gysling (1994). Based on this, the CCV will in this thesis not only be used as an actuator to stabilize surge, but also rotating stall.

Simon and Valavani (1991) studied the stability of a compressor with CCV control by using a Lyapunov function termed the incremental energy. The control law developed by Simon and Valavani (1991) requires knowledge of the compressor characteristic, and additional adjustments to the controller dictated by the Lyapunov analysis is performed in order to avoid a discontinuous controller.

Here we will use the backstepping methodology of Krstić *et al.* (1995*a*) to derive a control law for a CCV which gives a GAS equilibrium beyond the original surge line. Simon and Valavani (1991) studied the effect on stability of disturbances in pressure rise. This will be considered also here, and in addition we will also consider disturbances in the plenum outflow. In the case of only pressure disturbances, we will derive a controller that only requires knowledge of an upper bound on the slope of the compressor characteristic in order to guarantee stability. Discontinuity is not a problem with this controller. Under mild assumptions on the disturbances, global uniform boundedness and convergence will be proven in the presence of both pressure and mass flow disturbances. Constant disturbances or offsets will also be considered.

Krstić and Kokotović (1995) and Krstić *et al.* (1995*b*) used backstepping to design anti surge and anti stall controllers. The actuator used was a variable throttle. Here, we use the pressure drop across the CCV as the control variable. Pinsley *et al.* (1991) pointed out that in compression systems with large B-parameter (to be defined), the use of a CCV is expected to be more effective than the use of the throttle in control of surge. In this case the flow through the throttle is less coupled with the flow through the compressor than is the case when the B-parameter is

small. Pinsley *et al.* (1991), Krstić and Kokotović (1995) and Krstić *et al.* (1995*b*) use feedback from mass flow and pressure. As will be shown, the application of the backstepping procedure to CCV surge and stall control, in the case of no mass flow disturbances, results in a control law which uses feedback from mass flow only.

As opposed to throttle control, CCV control modifies the compressor characteristic. This allows for, at the cost of a pressure loss over the valve, recovery from rotating stall beyond the surge line. Although the pressure rise achieved in the compression system with a steady pressure drop across the CCV is comparable with the pressure rise achieved when the machine is in rotating stall, the CCV approach is to prefer as the possibility for blade vibration and high temperatures is avoided.

2.2 Preliminaries

2.2.1 The Model of Moore and Greitzer

Several dynamic models for the unstable operation of compression systems have been proposed in the last decade, but the model of Moore and Greitzer (1986) stands out in the sense that rotating stall amplitude is included as a state, and not manifested as a pressure drop which is the case in the other models. The low

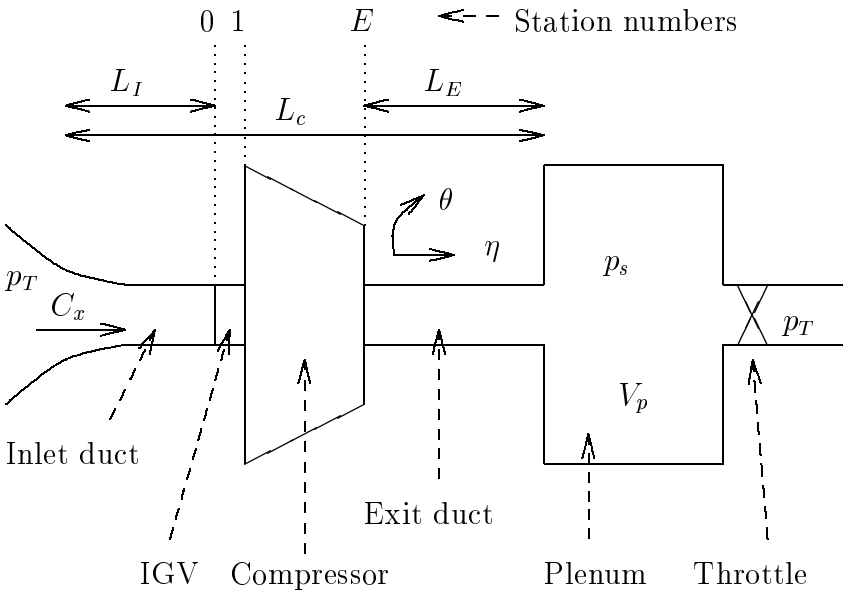

Figure 2.1: *Compression system. Figure taken from Moore and Greitzer (1986)*

order[1] model of Moore and Greitzer (1986) captures the post stall transients of a low speed axial compressor-plenum-throttle (see Figure 2.1) system. The main assumptions made by Moore and Greitzer (1986) in deriving the model are: large hub-to-tip ratio so that a two-dimensional description seems reasonable, incompressible compressor mass flow, compressible flow in the plenum, spatially uniform plenum pressure and short throttle duct. The three differential equations of the model arises from a Galerkin approximation of the local momentum balance, the annulus-averaged momentum balance and the mass balance of the plenum. A cubic compressor characteristic is assumed. The model is given by:

$$\begin{aligned}
\dot{\Psi} &= \frac{W/H}{4B^2}\left(\frac{\Phi}{W} - \frac{1}{W}\Phi_T(\Psi)\right)\frac{H}{l_c} \\
\dot{\Phi} &= \frac{H}{l_c}\left(-\frac{\Psi - \psi_{c0}}{H} - \frac{1}{2}\left(\frac{\Phi}{W} - 1\right)^3 + 1 + \frac{3}{2}\left(\frac{\Phi}{W} - 1\right)\left(1 - \frac{J}{2}\right)\right) \\
\dot{J} &= J\left(1 - \left(\frac{\Phi}{W} - 1\right)^2 - \frac{J}{4}\right)\varrho
\end{aligned} \tag{2.1}$$

where

- Φ is the annulus averaged mass flow coefficient (axial velocity divided by compressor speed), where the annulus average is defined as $\frac{1}{2\pi}\int_0^{2\pi}\phi(\xi,\theta)d\theta \triangleq \Phi(\xi)$, and $\phi(\xi,\theta)$ is the local mass flow coefficient,
- Ψ is the non dimensional plenum pressure or pressure coefficient (pressure divided by density and the square of compressor speed),
- J is the squared amplitude of rotating stall amplitude
- $\Phi_T(\Psi)$ is the throttle mass flow coefficient and
- l_c is the effective flow-passage nondimensional length of the compressor and ducts defined as
$$l_c \triangleq l_I + \frac{1}{a} + l_E, \tag{2.2}$$
where the positive constant a is the reciprocal time-lag parameter of the blade passage,

For a discussion of the employed nondimensionalization, consult Appendix B. The constant $B > 0$ is Greitzer's B-parameter defined by Greitzer (1976*a*) as

$$B \triangleq \frac{U}{2a_s}\sqrt{\frac{V_p}{A_c L_c}}, \tag{2.3}$$

where U is the constant compressor tangential speed (in m/s) at mean diameter, a_s is the speed of sound, V_p is the plenum volume, A_c is the flow area and L_c is

[1] "Low order" refers to the simplicity of the model, three states, compared to the complex fluid dynamic system it models

the length of ducts and compressor. The constant $\varrho > 0$ is defined as

$$\varrho = \frac{3aH}{(1+ma)W}, \tag{2.4}$$

where m is the compressor-duct flow parameter, H is the semi-height of the compressor characteristic and W is the semi-width of the compressor characteristic. The time variable ξ used throughout this chapter is also nondimensional, and is defined as

$$\xi \triangleq Ut/R \tag{2.5}$$

where t is the actual time and R is the mean compressor radius. The notation $\dot{\Phi}$ is to be understood as the derivative of Φ with respect to ξ, that is $\dot{\Phi} = \frac{d\Phi}{d\xi}$.

Relaxing the constant speed assumption is important for studying effects of set point changes, acceleration, deceleration, etc. A model taking variable speed into account will be developed in Chapter 4, but will not be considered further here.

In the case of pure surge, that is when $J \equiv 0$, the model reduces to that of Greitzer (1976*a*):

$$\begin{aligned} \dot{\Phi} &= \frac{1}{l_c}(\Psi_c(\Phi) - \Psi) \\ \dot{\Psi} &= \frac{1}{4B^2 l_c}(\Phi - \Phi_T(\Psi)). \end{aligned} \tag{2.6}$$

In Greitzer (1976*a*), the model was written

$$\begin{aligned} \dot{\Phi} &= B(\Psi_c(\Phi) - \Psi) \\ \dot{\Psi} &= \frac{1}{B}(\Phi - \Phi_T(\Psi)). \end{aligned}$$

The discrepancy in the constants is due to Greitzer (1976*a*) defining nondimensional time as $\xi = t\omega_H$ where ω_H is the Helmholtz frequency. Here, nondimensional time is defined according to (2.5), as was also done by Moore and Greitzer (1986). The model (2.6) was derived for axial compression systems, but it was demonstrated by Hansen *et al.* (1981) that the model also is applicable to centrifugal systems.

The pressure rise of the compressor is a nonlinear function of the mass flow. This function, $\Psi_c(\phi)$, is known as the compressor characteristic. Different expressions for this characteristic have been used, but one that has found widespread acceptance in the control literature is the cubic characteristic of Moore and Greitzer (1986):

$$\Psi_c(\phi) = \psi_{c0} + H\left(1 + \frac{3}{2}\left(\frac{\Phi}{W} - 1\right) - \frac{1}{2}\left(\frac{\Phi}{W} - 1\right)^3\right), \tag{2.7}$$

where the constant $\psi_{c0} > 0$ is the shut-off value of the compressor characteristic. The cubic characteristic with the parameters ψ_{c0}, W and H is shown in Figure 2.2. Mansoux *et al.* (1994), Sepulchre and Kokotović (1996) and Wang and Krstić (1997*a*) suggest other compressor characteristics for axial compressors, and

Hansen *et al.* (1981) presents an alternative polynomial characteristic for centrifugal compressors. However, the cubic seems to capture the general shape of the compressor characteristic of a large class of compressors. The nondimensionalization employed, transforms the usual family of curves in the compressor map, one for each compressor speed, to one single characteristic given by (2.7). Nisenfeld (1982) and Badmus *et al.* (1996) concludes that this is in fact a statement of the Fan law relation. The surge line, which passes through the local maxima of the family of curves is transformed to the local maximum of (2.7).

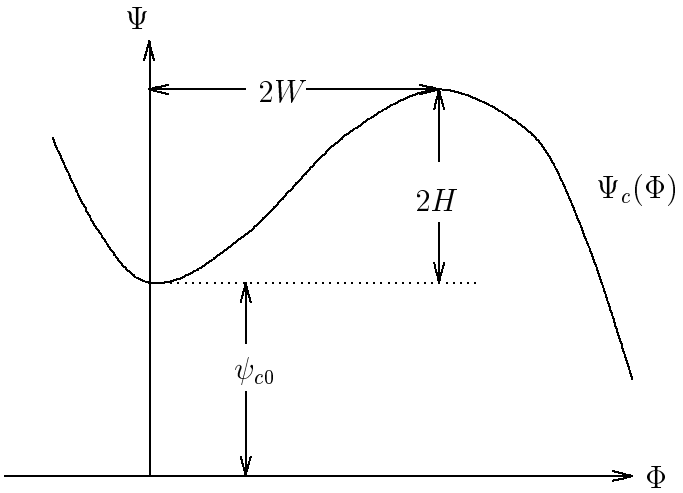

Figure 2.2: *Cubic compressor characteristic of Moore and Greitzer (1986). The constants W and H are known as the semi width and semi height, respectively.*

The throttle mass flow $\Phi_T(\Psi)$ is given by the throttle characteristic

$$\Phi_T(\Psi) = \gamma_T \sqrt{\Psi} \tag{2.8}$$

where γ_T is the throttle gain. The inverse throttle characteristic

$$\Psi_T(\Phi) = \Phi_T^{-1}(\Phi) = \frac{1}{\gamma_T^2}\Phi^2 \tag{2.9}$$

is shown in Figure 2.5.

2.2.2 Close Coupled Valve

A compressor in series with a CCV will be studied in the following. According to Simon and Valavani (1991), with "close-coupled" it is to be understood that the distance between the compressor outlet and the valve is so small that no significant mass storage can take place, see Figure 2.3.

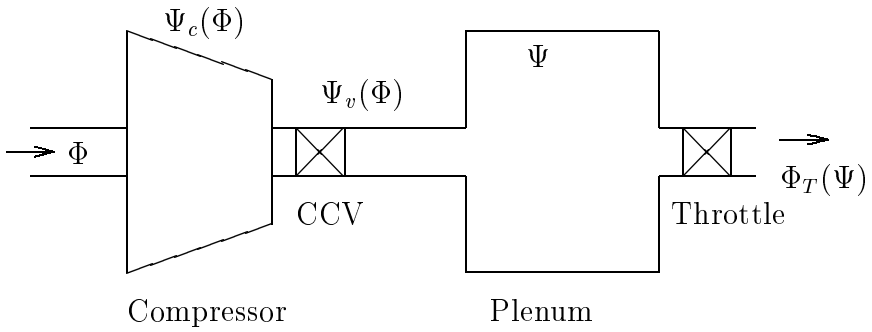

Figure 2.3: *Compression system with CCV*

The assumption of no mass storage between the compressor and the valve allows for the definition of an *equivalent* compressor. This term was introduced by Simon and Valavani (1991). The pressure rise over this equivalent compressor is the sum of the pressure rise over the compressor and the pressure drop over the valve. The pressure drop over the valve will be used as the control. This will allow for manipulation of the equivalent compressor characteristic, given by

$$\Psi_e(\Phi) = \Psi_c(\Phi) - \Psi_v(\Phi), \tag{2.10}$$

where $\Psi_c(\Phi)$ and $\Psi_v(\Phi)$ are the compressor pressure rise and valve pressure drop respectively and Φ is the axial mass flow coefficient. The motivation behind this, is that the slope of the compressor characteristic determines the stability properties of the equilibrium of the system, and this slope can be varied by varying the pressure drop over the CCV. The use of the CCV as an actuator for surge control is also elaborated upon in section 5.7, where the stabilizing effect of such a valve is discussed in connection with the destabilizing effect of incidence losses.

The CCV has a characteristic given by

$$\Psi_v(\Phi) = \frac{1}{\gamma^2}\Phi^2, \tag{2.11}$$

where $\gamma > 0$ is proportional to the valve opening. We now set out to repeat the modeling and Galerkin approximation of Moore and Greitzer (1986) with the equivalent characteristic Ψ_e replacing Ψ_c. Equation (5) in Moore and Greitzer (1986), which gives the pressure rise across the compressor, is modified according to

$$\underbrace{\frac{p_E - p_1}{\rho U^2} = N_s F(\phi) - \frac{1}{2a}\left(2\frac{\partial \phi}{\partial \xi} + \frac{\partial \phi}{\partial \theta}\right)}_{\text{Equation (5) in Moore and Greitzer (1986)}} - \Psi_v(\phi) \tag{2.12}$$

where p_1 and p_E is the static pressure at the entrance and exit of the equivalent compressor, ρ is the constant inlet density, U is the compressor speed at mean diameter, N_s is the number of compressor stages, $F(\phi)$ is the pressure rise coefficient

in the blade passage, and θ is the angular coordinate around the wheel. Equation (2.12) now gives the pressure rise over the equivalent compressor.

Using (2.12) as a starting point and following the derivation of Moore and Greitzer (1986), the following model is found[2]:

$$\begin{aligned}
\dot{\Psi} &= \frac{W/H}{4B^2}\left(\frac{\Phi}{W} - \frac{1}{W}\Phi_T(\Psi)\right)\frac{H}{l_c} \\
\dot{\Phi} &= \frac{H}{l_c}\Bigg(-\frac{\Psi-\psi_{c0}}{H} - \frac{1}{2}\left(\frac{\Phi}{W}-1\right)^3 + 1 \\
&\quad + \frac{3}{2}\left(\frac{\Phi}{W}-1\right)\left(1-\frac{J}{2}\right) - \frac{1}{\gamma^2}\left(\frac{W^2 J}{2H} + \frac{\Phi^2}{H}\right)\Bigg) \\
\dot{J} &= J\left(1 - \left(\frac{\Phi}{W}-1\right)^2 - \frac{J}{4} - \frac{1}{\gamma^2}\frac{4W\Phi}{3H}\right)\varrho,
\end{aligned} \tag{2.13}$$

which will be used in design of stall/surge controllers in this chapter. In the simpler case of pure surge, J is set to zero, and we are left with the model

$$\begin{aligned}
\dot{\Psi} &= \frac{1}{4B^2 l_c}(\Phi - \Phi_T(\psi)) \\
\dot{\Phi} &= \frac{1}{l_c}(\Psi_c(\Phi) - \Psi_v(\Phi) - \Psi)
\end{aligned} \tag{2.14}$$

which will used in the study of surge control.

2.2.3 Equilibria

The compressor is in equilibrium when $\dot{\Phi} = \dot{\Psi} = \dot{J} = 0$. If $J(0) = 0$ then $J \equiv 0$ and the equilibrium values ϕ_0 and ψ_0 are given by the intersection of $\Psi_e(\Phi)$ and the throttle characteristic. If $J(0) > 0$, and the throttle characteristic crosses Ψ_e to the left of the local maximum, the compressor may[3] enter rotating stall and the equilibrium values ϕ_0 and ψ_0 are given by the intersection of the throttle characteristic and the stall characteristic $\Psi_{es}(\Phi)$ which is found by analyzing the $\dot{J}$-equation of (2.13). It is seen that $\dot{J} = 0$ is satisfied for $J = 0$ or

$$J = J_e = 4\left(1 - \left(\frac{\Phi}{W}-1\right)^2 - \frac{1}{\gamma^2}\frac{4W\Phi}{3H}\right). \tag{2.15}$$

Inserting (2.15) in the $\dot{\Phi}$-equation of (2.13) and setting $\dot{\Phi} = 0$ gives the expression for $\Psi_{es}(\phi)$:

$$\Psi_{es}(\Phi) = \Psi_s(\Phi) + \frac{5}{H}\Psi_v(\Phi) - \frac{8W}{H\gamma^2}\left(1 - \frac{W^2}{3H^2\gamma^2}\right)\Phi, \tag{2.16}$$

[2]The complete derivation is shown in Appendix C.

[3]This depends on the numerical value of B. Greitzer and Moore (1986) showed that small B gives rotating stall, and large B gives surge.

where

$$\Psi_s(\Phi) = \psi_{c0} + H\left(1 - \frac{3}{2}\left(\frac{\Phi}{W} - 1\right) + \frac{5}{2}\left(\frac{\Phi}{W} - 1\right)^3\right) \tag{2.17}$$

is the stall characteristic found when the CCV is not present. In Figure 2.4 the various characteristics are shown. As can be seen, the throttle line intersects Ψ_c in a point of positive slope, that is in the unstable area of the compressor map, and the compressor would go into rotating stall or surge. By introducing the CCV, the throttle line crosses the equivalent characteristic Ψ_e in an area of negative slope. This new equilibrium is thus stable.

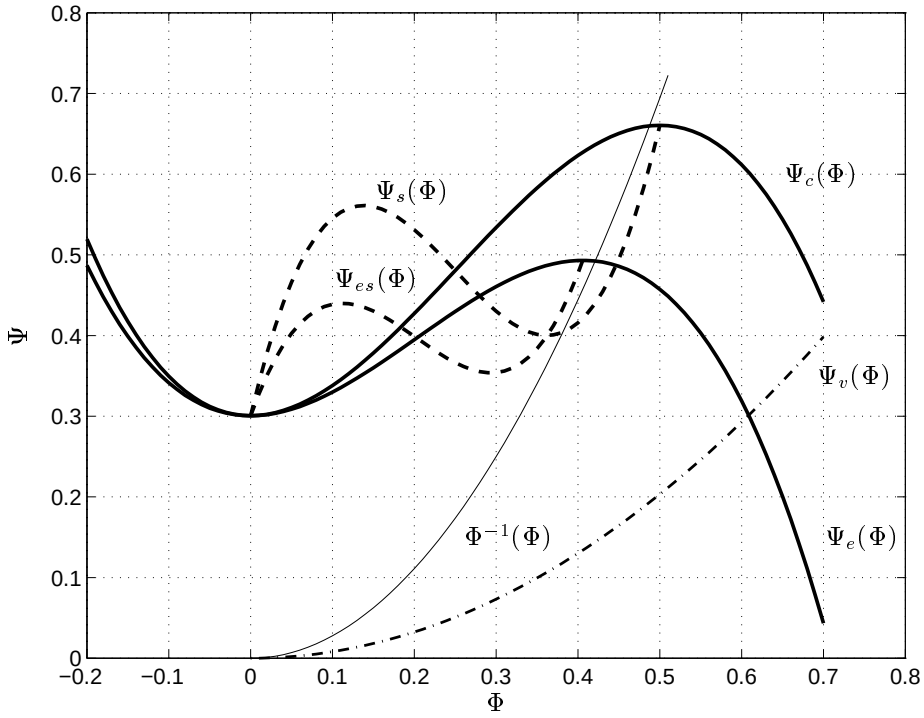

Figure 2.4: *Compressor and throttle characteristics.*

2.2.4 Change of Variables

The equilibrium of the compression system without the presence of the valve, is at the intersection of the compressor characteristic $\Psi_c(\Phi)$ and the throttle characteristic $\Phi_T(\Psi)$. When introducing the CCV into the system, the equilibrium is shifted to the intersection of the equivalent compressor characteristic $\Psi_e(\Phi)$ and the throttle characteristic $\Phi_T(\Psi)$. The equilibrium values are then related through

$$\psi_0 = \Phi_T^{-1}(\phi_0). \tag{2.18}$$

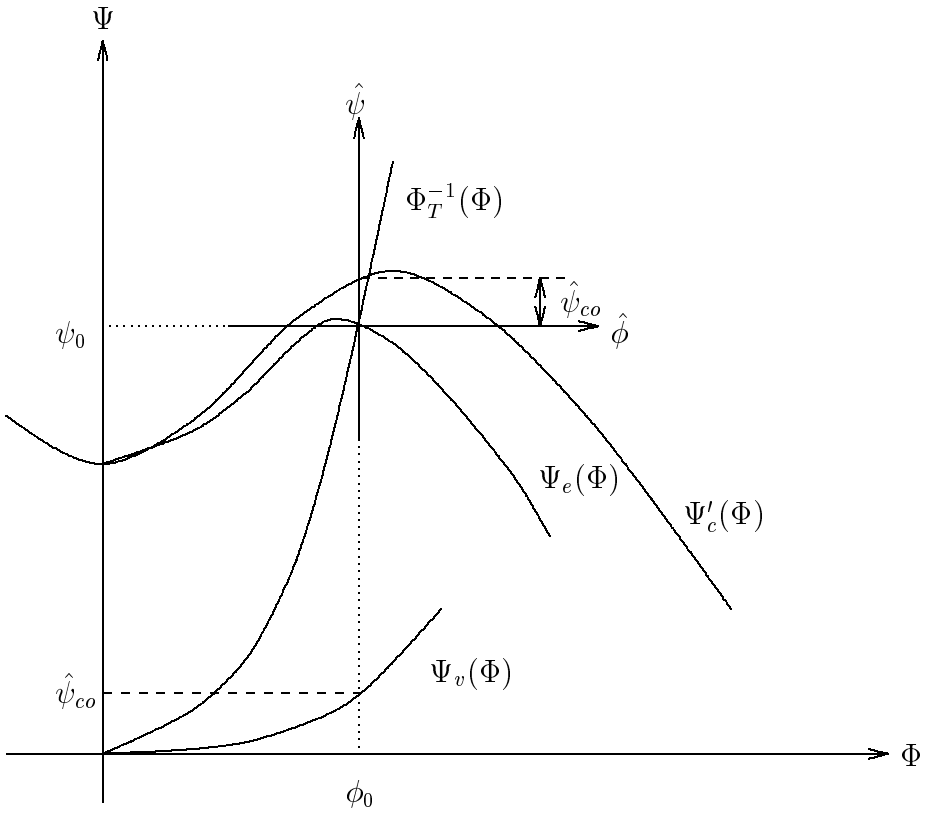

Figure 2.5: *Change of variables, principal drawing*

To prepare for the analysis of the system, it is desirable to perform a change of coordinates on the system equations so that the origin becomes the equilibrium under study. The new coordinates are defined as

$$\begin{aligned} \hat{\psi} &= \Psi - \psi_0 \\ \hat{\phi} &= \Phi - \phi_0. \end{aligned} \tag{2.19}$$

The system characteristics in the new coordinates are defined as

$$\begin{aligned} \hat{\Psi}_e(\hat{\phi}) &= \Psi_e(\hat{\phi} + \phi_0) - \Psi_e(\phi_0) \\ &= \Psi_e(\hat{\phi} + \phi_0) - \psi_0 && (2.20) \\ \hat{\Psi}_c'(\hat{\phi}) &= \Psi_c(\hat{\phi} + \phi_0) - \psi_0 && (2.21) \\ \hat{\Psi}_v(\hat{\phi}) &= \Psi_v(\hat{\phi} + \phi_0) - \psi_0 && (2.22) \\ \hat{\Phi}_T(\hat{\psi}) &= \Phi_T(\hat{\psi} + \psi_0) - \phi_0. && (2.23) \end{aligned}$$

Using (2.7), the transformed compressor characteristic (2.21) can be calculated as

$$\hat{\Psi}_c'(\hat{\phi}) = \hat{\psi}_{co} - k_3\hat{\phi}^3 - k_2\hat{\phi}^2 - k_1\hat{\phi}, \tag{2.24}$$

where

$$\begin{aligned}
\hat{\psi}_{co} &= \psi_{co} - \psi_0 - \frac{\phi_0^2 H}{2W^2}\left(\frac{\phi_0}{W} - 3\right), && (2.25)\\
k_1 &= \frac{3H\phi_0}{2W^2}\left(\frac{\phi_0}{W} - 2\right), && (2.26)\\
k_2 &= \frac{3H}{2W^2}\left(\frac{\phi_0}{W} - 1\right), && (2.27)\\
k_3 &= \frac{H}{2W^3}. && (2.28)
\end{aligned}$$

It can be recognized that $k_3 > 0$, while $k_1 \leq 0$ if the equilibrium is in the unstable region of the compressor map and $k_1 > 0$ otherwise. The sign of k_2 may vary. If $\phi_0 > W$ then $k_2 > 0$, and if $\phi_0 < W$ then $k_2 < 0$.

Using the definition of the equivalent compressor (2.10) and the definition of ψ_0 in (2.18), it can be shown that

$$\psi_0 = \psi_{co} - \frac{\phi_0^2 H}{2W^2}\left(\frac{\phi_0}{W} - 3\right) - \Psi_v(\phi_0). \tag{2.29}$$

Combining (2.29) with (2.25) we get the simple result

$$\hat{\psi}_{co} = \Psi_v(\phi_0), \tag{2.30}$$

which could have been seen directly from Figure 2.5.

The Moore-Greitzer model (2.13) can now be written in the new coordinates as

$$\begin{aligned}
\dot{\hat{\psi}} &= \frac{1}{4B^2 l_c}\left(\hat{\phi} - \hat{\Phi}_T(\hat{\psi})\right) && (2.31)\\
\dot{\hat{\phi}} &= \frac{1}{l_c}\left(\hat{\Psi}_c'(\hat{\phi}) - \hat{\psi} - \hat{\Psi}_v(\hat{\phi}) - \psi_0 - \frac{3H}{4}J\left(\frac{\Phi}{W} - 1\right) - \frac{W^2 J}{2\gamma^2}\right)\\
\dot{J} &= \varrho J\left[1 - \left(\frac{\Phi}{W} - 1\right)^2 - \frac{J}{4}\right] - \frac{4W\varrho}{3H\gamma^2}J\Phi,
\end{aligned}$$

By defining

$$\hat{\Psi}_c'(\hat{\phi}) = \Psi_v(\phi_0) + \hat{\Psi}_c(\hat{\phi}), \tag{2.32}$$

where

$$\hat{\Psi}_c(\hat{\phi}) \triangleq -k_3\hat{\phi}^3 - k_2\hat{\phi}^2 - k_1\hat{\phi}, \tag{2.33}$$

the model (2.31) can be written

$$\begin{aligned}
\dot{\hat{\psi}} &= \frac{1}{4B^2 l_c}\left(\hat{\phi} - \hat{\Phi}_T(\hat{\psi})\right) \\
\dot{\hat{\phi}} &= \frac{1}{l_c}\left(\hat{\Psi}_c(\hat{\phi}) - \hat{\psi} - u - \frac{3H}{4}J\left(\frac{\Phi}{W} - 1\right) - \frac{W^2 J}{2\gamma^2}\right) \\
\dot{J} &= \varrho J\left[1 - \left(\frac{\Phi}{W} - 1\right)^2 - \frac{J}{4}\right] - \frac{4W\varrho}{3H\gamma^2}J\Phi,
\end{aligned} \tag{2.34}$$

where the control u has been selected as

$$u = \hat{\Psi}_v(\hat{\phi}) + \psi_0 - \Psi_v(\phi_0) = \Psi_v(\Phi) - \Psi_v(\phi_0). \tag{2.35}$$

In the case of pure surge, the model (2.34) reduces to

$$\begin{aligned}
\dot{\hat{\psi}} &= \frac{1}{4B^2 l_c}(\hat{\phi} - \hat{\Phi}_T(\hat{\psi})) \\
\dot{\hat{\phi}} &= \frac{1}{l_c}(\hat{\Psi}_c(\hat{\phi}) - u - \hat{\psi})
\end{aligned} \tag{2.36}$$

Simon and Valavani (1991) suggested using the pressure drop across the valve as the control variable u. This approach will also be taken here. Our aim will be to design a control law u for the valve such that the compressor can be operated also on the left side of the original surge line without going into surge or rotating stall. That is, we are going to use feedback to move the surge line towards lower values of Φ, and thus expand the useful range of mass flows over which the compressor can be safely operated.

As the pressure difference across the valve always will be a pressure drop, the valve must be partially closed during stable operation in order for the control u to attain both positive and negative values. It is also evident that there must exist a pressure drop over the valve when the compressor is operated in a previously unstable area. The price paid for a larger operating range, is some pressure loss at low mass flows. A further discussion of the steady state pressure loss can be found in Simon and Valavani (1991).

2.2.5 Disturbances

As in all types of physical systems, disturbances will occur in the compression system. Greitzer and Moore (1986) stated that this is a topic that need more study, at least in the case of the disturbances initiating stall and surge. Some research have been done in this area. Hynes and Greitzer (1987), DeLaat *et al.* (1996) and others have studied the effect of circumferential inlet distortion on the stability properties, and Simon and Valavani (1991), Haddad *et al.* (1997) and others studied mass flow and pressure disturbances. From a control theory point of view it is also important to investigate what performance the closed loop system will have when disturbances is taken into account.

As in Simon and Valavani (1991), the effect of a pressure disturbance $\hat{\Psi}_d(\xi)$, and a flow disturbance $\hat{\Phi}_d(\xi)$ will be considered here. The pressure disturbance, which may arise from combustion induced fluctuations when considering the model of a gas turbine, will accelerate the flow. As pointed out by van de Wal and Willems (1996), the flow disturbances may arise from processes upstream of the compressor, other compressors in series or an air cleaner in the compressor duct. In the case of an aircraft jet engine, large angle of attack or altitude variations may cause mass flow disturbances according to van de Wal and Willems (1996) and DeLaat *et al.* (1996). Also, DeLaat *et al.* (1996) reports of a number of aircraft maneuvers (full-rudder sideslips, wind-up turns, etc.) causing inlet airflow disturbances in the jet engine of a F-15 fighter.

In the analysis of Simon and Valavani (1991) $\hat{\Phi}_d(\xi)$ is set to zero. Disturbances in stall/surge control is also studied by Haddad *et al.* (1997), with disturbances assumed to converge to zero. Here, both types of disturbances, mass flow and pressure, will be considered. The disturbances are time varying, and the only assumption made at this point is boundedness, that is $\|\hat{\Phi}_d\|_\infty$ and $\|\hat{\Psi}_d\|_\infty$ exists. In addition to time varying disturbances, constant, or slow varying, offsets will be introduced into the model. This is of particular interest when e.g. a constant negative mass flow disturbance pushes the equilibrium over the surge line, initiating surge or rotating stall. The offsets in mass flow and pressure rise is termed d_ϕ and d_ψ, respectively. The constant bias d_ψ in pressure can also be thought of as reflecting some uncertainty in the compressor characteristic $\hat{\Psi}_c(\hat{\phi})$, and likewise and the mass flow bias d_ϕ can be thought of as reflecting a uncertainty in the throttle characteristic $\hat{\Phi}(\hat{\psi})$. A study of surge/stall control for compressors with uncertain compressor characteristic was also done by Leonessa *et al.* (1997*b*). With these disturbances the model becomes:

$$\begin{aligned}
\dot{\hat{\psi}} &= \frac{1}{4B^2 l_c}\left(\hat{\phi} - \hat{\Phi}_T(\hat{\psi}) - \hat{\Phi}_d(\xi) - d_\phi\right) \qquad (2.37)\\
\dot{\hat{\phi}} &= \frac{1}{l_c}\left(-\hat{\psi} + \hat{\Psi}_c(\hat{\phi}) - \hat{\Psi}_v(\hat{\phi}) + \hat{\Psi}_d(\xi) + d_\psi\right.\\
&\quad \left. -\frac{3HJ}{4}\left(\frac{\Phi}{W} - 1\right) - \frac{W^2 J}{2\gamma^2}\right)\\
\dot{J} &= \varrho J\left(1 - \left(\frac{\Phi}{W} - 1\right)^2 - \frac{J}{4}\right) - \frac{4W\varrho}{3H\gamma^2} J\Phi,
\end{aligned}$$

and in the case of pure surge

$$\begin{aligned}
\dot{\hat{\psi}} &= \frac{1}{4B^2 l_c}\left(\hat{\phi} - \hat{\Phi}_T(\hat{\psi}) - \hat{\Phi}_d(\xi) - d_\phi\right) \qquad (2.38)\\
\dot{\hat{\phi}} &= \frac{1}{l_c}\left(-\hat{\psi} + \hat{\Psi}_c(\hat{\phi}) - \hat{\Psi}_v(\hat{\phi}) + \hat{\Psi}_d(\xi) + d_\psi\right). \qquad (2.39)
\end{aligned}$$

2.3 Surge Control

In this section controllers will be designed for the pure surge case. First the undisturbed case is studied, then disturbances are added, and finally adaption will be used to stabilize the system in the presence of constant disturbances.

2.3.1 Undisturbed Case

Theorem 2.1 *The controller*

$$u = c_2(\Phi - \phi_0), \tag{2.40}$$

where $c_2 > a_m$ and a_m is the maximum positive slope of the compressor characteristic $\hat{\Psi}_c(\hat{\phi})$, renders the equilibrium (ϕ_0, ψ_0) of (2.14) GAS. □

Proof: The backstepping methodology of Krstić *et al.* (1995*a*) will be employed in deriving the control law.

Step 1. Two error variables are defined as $z_1 = \hat{\psi}$ and $z_2 = \hat{\phi} - \alpha$. The control Lyapunov function (clf) for this step is chosen as

$$V_1 = 2B^2 l_c z_1^2 \tag{2.41}$$

with time derivative along the solution trajectories of (2.36) given by

$$\dot{V}_1 = z_1 \left(-\hat{\Phi}_T(z_1) + z_2 + \alpha \right). \tag{2.42}$$

The throttle is assumed passive, that is $\hat{\psi}\hat{\Phi}_T(\hat{\psi}) \geq 0 \; \forall \hat{\psi}$. We have

$$\hat{\psi}\hat{\Phi}_T(\hat{\psi}) \geq 0 \;\Rightarrow\; -z_1\hat{\Phi}_T(z_1) \leq 0 \tag{2.43}$$

As it is desirable to avoid cancelation of useful nonlinearities in (2.42), the stabilizing function α is not needed and accordingly $\alpha = 0$, which gives

$$\dot{V}_1 = -\hat{\Phi}_T(z_1)z_1 + z_1 z_2. \tag{2.44}$$

Although the virtual control α is not needed here, in the interest of consistency with the following sections, this notation is kept.

Step 2.The derivative of z_2 is

$$\dot{z}_2 = \frac{1}{l_c}\left(\hat{\Psi}_c(z_2) - z_1 - u \right). \tag{2.45}$$

The clf for this step is

$$V_2 = V_1 + \frac{l_c}{2} z_2^2 \tag{2.46}$$

with time derivative

$$\dot{V}_2 = -z_1\hat{\Phi}_T(z_1) + z_2\left(\hat{\Psi}_c(z_2) - u\right). \tag{2.47}$$

Notice that V_2 as defined by (2.46) is similar to the incremental energy of Simon and Valavani (1991).

Control law. The control variable u will be chosen so that (2.47) is made negative definite. To this end we define the *linear* control law

$$u = c_2 z_2, \tag{2.48}$$

where the controller gain $c_2 > 0$ is chosen so that

$$z_2\Psi_c(z_2) - c_2 z_2^2 < 0. \tag{2.49}$$

Using (2.33) this implies that c_2 must satisfy

$$-k_3 z_2^2\left(z_2^2 + \frac{k_2}{k_3}z_2 + \frac{k_1 + c_2}{k_3}\right) < 0. \tag{2.50}$$

Finding the roots of the above bracketed expression, it is seen that (2.50) is satisfied if c_2 is chosen according to

$$c_2 > \frac{k_2^2}{4k_3} - k_1. \tag{2.51}$$

Although (2.51) implies that the compressor characteristic must be known in order to determine c_2, it can be shown that the knowledge of a bound on the positive slope of the characteristic is sufficient. Differentiating (2.33) twice with respect to $\hat{\phi}$, reveals that the maximum positive slope occurs for

$$\hat{\phi} = \hat{\phi}_m = -\frac{k_2}{3k_3} \tag{2.52}$$

and is given by

$$a = \left.\frac{d\hat{\Psi}_c(\hat{\phi})}{d\hat{\phi}}\right|_{\hat{\phi}=\hat{\phi}_m} = \frac{k_2^2}{3k_3} - k_1 = \frac{3H}{2W}. \tag{2.53}$$

Assuming that only an upper bound a_m on the positive slope of $\hat{\Psi}_c(\hat{\phi})$ is known, a conservative condition for c_2 is

$$c_2 > a_m \geq a > \frac{k_2^2}{4k_3} - k_1. \tag{2.54}$$

Thus the price paid for not knowing the exact coefficients of the compressor characteristic is a somewhat conservative condition for the controller gain c_2. Notice also that no knowledge of Greitzer's B-parameter or its upper bound is required in formulating the controller. The final expression for $\dot{V}_2$ is then

$$\dot{V}_2 = -z_1\hat{\Phi}_T(z_1) + \hat{\Psi}_c(z_2)z_2 - c_2 z_2^2 = -W(z_1, z_2) \leq 0. \tag{2.55}$$

The closed loop system can be written as

$$\dot{z}_1 = \frac{1}{4B^2 l_c}(-\hat{\Phi}_T(z_1) + z_2) \tag{2.56}$$

$$\dot{z}_2 = \frac{1}{l_c}(-z_1 + \hat{\Psi}(z_2) - c_2 z_2). \tag{2.57}$$

It follows that the equilibrium point $z_1 = z_2 = 0$ is GAS, and the same result holds for the equilibrium (ϕ_0, ψ_0). □

Remark 2.1 *By combining (2.82) and (2.48), the following control law for the CCV gain is found:*

$$c_2(\Phi - \phi_0) = \Psi_v(\Phi) - \Psi_v(\phi_0) \tag{2.58}$$

$$\Downarrow$$

$$\gamma = \sqrt{\frac{\Phi + \phi_0}{c_2}}. \tag{2.59}$$

Notice that this control law requires measurement of mass flow only. □

Remark 2.2 *Although not showing stability, Bendixon's criterion can be used to show that the controller (2.48) guarantees that no limit cycles (surge oscillations) exists. Bendixon's criterion states (somewhat simplified) that no limit cycles exists in a dynamical system defined on a simply connected region $D \subset \mathbb{R}^2$ if the divergence of the system is not identically zero and does not change sign in D. For an exact statement of Bendixon's criterion and the proof, see any textbook on dynamical systems, e.g. Perko (1991). The divergence $\nabla \cdot \boldsymbol{f}$ of the system $\dot{\boldsymbol{x}} = \boldsymbol{f}(\boldsymbol{x})$ defined by (2.14) is*

$$\nabla \cdot \boldsymbol{f} = -\frac{1}{4B^2 l_c}\frac{\partial \hat{\Phi}_T(\hat{\psi})}{\partial \hat{\psi}} + \frac{1}{l_c}\left(\frac{\partial \hat{\psi}_c(\hat{\phi})}{\partial \hat{\phi}} - \frac{\partial u}{\partial \hat{\phi}}\right). \tag{2.60}$$

The slope of the throttle is always positive, so the first term in (2.60) is always negative. To make the second term also negative, it is sufficient that $\frac{\partial u}{\partial \hat{\phi}}$ dominates $\frac{\partial \hat{\psi}_c(\hat{\phi})}{\partial \hat{\phi}}$, which is exactly what is ensured by the controller in Theorem 2.1. Thus, according to Bendixon's criterion, no surge oscillations can exist for the closed loop system. □

2.3.2 Determination of ϕ_0

As a consequence of the controller (2.40) being designed after the system equations are transformed to the new coordinates, its implementation depends on knowledge of the equilibrium value ϕ_0. The equilibrium is located at the intersection of the

equivalent compressor characteristic $\Psi_e(\Phi)$ and the throttle characteristic Φ_T^{-1}. By combining (2.82), (2.40) and (2.59), it is seen that

$$\begin{aligned}\Psi_v(\phi_0) &= (u+\Psi_v(\phi_0))|_{\Phi=\phi_0} \\ &= \left(c_2(\Phi-\phi_0)+\frac{c_2}{\Phi+\phi_0}\phi_0^2\right)\Big|_{\Phi=\phi_0} \\ &= \frac{c_2\phi_0}{2}. \end{aligned} \tag{2.61}$$

At the equilibrium, we have

$$\Psi_c(\phi_0)-\Psi_v(\phi_0)=\frac{1}{\gamma^2}\phi_0^2, \tag{2.62}$$

or by using (2.61), ϕ_0 is found by solving the following 3rd order equation

$$\psi_{co}+H\left(1+\frac{3}{2}\left(\frac{\phi_0}{W}-1\right)-\frac{1}{2}\left(\frac{\phi_0}{W}-1\right)^3\right)-\frac{c_2\phi_0}{2}=\frac{2}{\gamma^2}\phi_0^2, \tag{2.63}$$

with respect to ϕ_0, and its value is to be used in the control law (2.40). Solving (2.63) requires knowledge of the compressor characteristic. If this is not the case, alternatives to finding ϕ_0 explicitly is, using an adaption scheme like the one suggested by Bazanella *et al.* (1997) or it is possible to use throttle control in addition to the CCV control to control ϕ using ϕ_0 as the reference. If none of these alternatives are attractive, an approximation for ϕ_0 can be used. In this case, asymptotic stability cannot be shown, but convergence to a set and avoidance of surge is easily shown. Defining $\Delta\phi$ as

$$\Delta\phi=\phi_0-\phi_{aprx}, \tag{2.64}$$

where ϕ_{aprx} is the approximation used for feedback, and ϕ_0 is the actual and unknown value of the equilibrium. By using the same Lyapunov function as is Theorem 2.1, and

$$u=c_2(\Phi-\phi_{aprx})=c_2(\Phi-\phi_0+\Delta\phi), \tag{2.65}$$

the time derivative of V_2 is found and upper bounded by

$$\dot{V}_2\leq -z_1\hat{\Phi}(z_1)+z_2(\hat{\Psi}_c(z_2)-c_2z_2)z_2-z_2c_2\Delta\phi. \tag{2.66}$$

Application of Young's inequality[4] to the last term in (2.66) gives

$$-z_2c_2\Delta\phi\leq\frac{c_2}{2}\left(\frac{z_2^2}{\eta_0}+(\Delta\phi)^2\eta_0\right), \tag{2.67}$$

[4] In its simplest form Young's inequality states that

$$\forall a,b\ :\ ab\leq\frac{1}{2}(\frac{a^2}{c}+cb^2)\ \ \forall c>0.$$

where η_0 is a constant, and it follows that

$$\begin{aligned}\dot{V}_2 &\leq -z_1\hat{\Phi}_T(z_1) + z_2(\hat{\Psi}_c(z_2) - c_2(1-\frac{1}{2\eta_0})z_2)z_2 + \eta_0(\Delta\phi)^2 \\ &= -W(z_1,z_2) + \eta_0(\Delta\phi)^2, \end{aligned} \tag{2.68}$$

where the definition of W is obvious. By choosing η_0 and c_2 such that

$$c_2(1-\frac{1}{2\eta_0}) > a_m, \tag{2.69}$$

is satisfied, it can be shown that $W(z_1,z_2)$ is radially unbound and positive definite. Thus, $\dot{V}_2 < 0$ outside a set $\mathcal{R}_\Delta$. This set can be found in the following manner: According to Krstić *et al.* (1995*a*), the fact that $V_2(z_1,z_2)$ and $W(z_1,z_2)$ is positive definite and radially unbounded, and $V_2(z_1,z_2)$ is smooth, implies that there exists class-$\mathcal{K}_\infty$ functions β_1, β_2 and β_3 such that

$$\beta_1(|\boldsymbol{z}|) \leq V_2(\boldsymbol{z}) \leq \beta_2(|\boldsymbol{z}|) \tag{2.70}$$

$$\beta_3(|\boldsymbol{z}|) \leq W(\boldsymbol{z}) \tag{2.71}$$

where $\boldsymbol{z} = (z_1 \;\; z_2)^{\mathrm{T}}$. Following the proof of Lemma 2.26 in Krstić *et al.* (1995*a*), we have that the states of the model are uniformly ultimately bounded, and that they converge to the residual set

$$\mathcal{R}_\Delta = \left\{ \boldsymbol{z} \;:\; |\boldsymbol{z}| \leq \beta_1^{-1} \circ \beta_2 \circ \beta_3^{-1}\left(\eta(\Delta\phi)^2\right) \right\}. \tag{2.72}$$

From (2.68) it follows that $\dot{V}_2$ is negative whenever $W(\boldsymbol{z}) > \eta_0(\Delta\phi)^2$. Combining this with (2.71) it can be concluded that

$$|\boldsymbol{z}(\xi)| > \beta_3^{-1}\left(\eta(\Delta\phi)^2\right) \;\Rightarrow\; \dot{V}_2 < 0. \tag{2.73}$$

This means that if $|\boldsymbol{z}(0)| \leq \beta_3^{-1}\left(\eta(\Delta\phi)^2\right)$, then

$$V_2(\boldsymbol{z}(\xi)) \leq \beta_2 \circ \beta_3^{-1}\left(\eta(\Delta\phi)^2\right), \tag{2.74}$$

which in turn implies that

$$|\boldsymbol{z}(\xi)| \leq \beta_1^{-1} \circ \beta_2 \circ \beta_3^{-1}\left(\eta(\Delta\phi)^2\right). \tag{2.75}$$

If, on the other hand $|\boldsymbol{z}(0)| > \beta_3^{-1}\left(\eta(\Delta\phi)^2\right)$, then $V_2(\boldsymbol{z}(\xi)) \leq V_2(\boldsymbol{z}(0))$, which implies

$$|\boldsymbol{z}(\xi)| \leq \beta_1^{-1} \circ \beta_2(|\boldsymbol{z}(0)|). \tag{2.76}$$

Combining (2.75) and (2.76) leads to the global uniform boundedness of $\boldsymbol{z}(\xi)$:

$$\|\boldsymbol{z}\|_\infty \leq \max\left\{\beta_1^{-1} \circ \beta_2 \circ \beta_3^{-1}\left(\eta(\Delta\phi)^2\right),\; \beta_1^{-1} \circ \beta_2(|\boldsymbol{z}(0)|)\right\}, \tag{2.77}$$

while (2.73) and (2.70) prove the convergence of $\boldsymbol{z}(\xi)$ to the residual set defined in (2.72).

It is trivial to establish the fact that no limit cycles, and hence surge oscillations, can exist inside this set using Bendixon's criterion. It is seen from (2.72), that the size of the set $\mathcal{R}_\Delta$ is dependent on the square of the equilibrium estimate error $\Delta\phi$ and the parameter η_0. A more accurate estimate ϕ_{aprx}, or a smaller value of η_0, both implies a smaller set. A smaller value of η_0 will, by equation (2.69), require a larger controller gain c_2, which is to be expected.

2.3.3 Time Varying Disturbances

First, time varying pressure disturbances will be considered. That is, $\hat{\Phi}_d(\xi)$, d_ϕ and d_ψ are set to zero as in Simon and Valavani (1991).

Theorem 2.2 (Time varying pressure disturbances)
The controller

$$u = (c_2 + d_2)(\Phi - \phi_0), \tag{2.78}$$

where c_2 is chosen as in Theorem 2.1, and $d_2 > 0$ guarantees that the states of the model (2.38) are globally uniformly bounded, and that they converge to a set. □

Proof: The controller will be derived using backstepping.

Step 1. Identical to Step 1 in proof of Theorem 2.1.

Step 2. The derivative of z_2 is

$$\dot{z}_2 = \frac{1}{l_c}\left(\hat{\Psi}_c(\hat{\phi}) - z_1 + \hat{\Psi}_d(\xi) - u\right). \tag{2.79}$$

V_2 is chosen as

$$V_2 = V_1 + \frac{l_c}{2} z_2^2 \tag{2.80}$$

where $\dot{V}_2$ can be bounded according to

$$\dot{V}_2 = -\hat{\Phi}_T(z_1) z_1 + z_2\left(\hat{\Psi}_c(\hat{\phi}) + \hat{\Psi}_d(\xi) - u\right). \tag{2.81}$$

Control law. To counteract the effect of the disturbance, a damping factor $d_2 > 0$ is included and u is chosen as

$$u = c_2 z_2 + d_2 z_2. \tag{2.82}$$

c_2 is chosen so that (2.54) is satisfied. Inserting (2.82) in (2.81) gives

$$\dot{V}_2 = -z_1 \hat{\Phi}_T(z_1) + \hat{\Psi}_c(z_2) z_2 - c_2 z_2^2 + \hat{\Psi}_d(\xi) z_2 - d_2 z_2^2. \tag{2.83}$$

Use of Young's inequality gives

$$z_2 \hat{\Psi}_d(\xi) \le d_2 z_2^2 + \frac{\hat{\Psi}_d^2(\xi)}{4 d_2} \le d_2 z_2^2 + \frac{\|\hat{\Psi}_d\|_\infty^2}{4 d_2}, \tag{2.84}$$

and $\dot{V}_2$ can be bounded according to

$$\dot{V}_2 \le -W(z_1, z_2) + \frac{\hat{\Psi}_d^2(\xi)}{4 d_2} \le -W(z_1, z_2) + \frac{1}{4 d_2}\|\hat{\Psi}_d\|_\infty^2 \tag{2.85}$$

where

$$W(z_1, z_2) = z_1 \hat{\Phi}(z_1) - (\hat{\Psi}_c(z_2) z_2 - c_2 z_2^2) \tag{2.86}$$

is radially unbounded and positive definite. This implies that $\dot{V}_2 < 0$ outside a set $\mathcal{R}_1$ in the $z_1 z_2$ plane.

By using (2.70) and (2.71) again, it follows from similar calculations as in (2.73)-(2.77), that $\boldsymbol{z}(\xi)$ is globally uniformly bounded and that $\boldsymbol{z}(\xi)$ converges to the residual set

$$\mathcal{R}_1 = \left\{ \boldsymbol{z} \ : \ |\boldsymbol{z}| \leq \beta_1^{-1} \circ \beta_2 \circ \beta_3^{-1} \left(\frac{\|\hat{\Psi}_d\|_\infty^2}{4 d_2} \right) \right\}. \tag{2.87}$$

□

Remark 2.3 *Notice that the controller (2.82) is essentially the same as (2.48), with the only difference being that (2.82) requires a larger gain in order to suppress the disturbance. Consequently, Remark 2.1 also applies here.* □

It is now shown that an additional assumption on the disturbance ensures that the controller (2.82) not only makes the states globally uniformly bounded, but also guarantees convergence to the origin.

Corollary 2.1 (Convergence to the origin)
If the disturbance term $\hat{\Psi}_d(\xi)$ is upper bounded by a monotonically decreasing non-negative function $\overline{\Psi}_d(\xi)$ such that

$$|\hat{\Psi}_d(\xi)| \leq \overline{\Psi}_d(\xi) \ \forall \xi \geq 0 \tag{2.88}$$

and

$$\lim_{\xi \to \infty} \overline{\Psi}_d(\xi) = 0, \tag{2.89}$$

the controller (2.82) ensures that the states of the model (2.38), with pressure disturbances, converge to the origin. □

Proof: Inspired by the calculations for a simple scalar system starting on page 75 in Krstić *et al.* (1995*a*) , we introduce the signal

$$s(\boldsymbol{z}, \xi) = V_2(\boldsymbol{z}) e^{c\xi}, \tag{2.90}$$

where $c > 0$ is a constant, for use in the proof:

$$\begin{aligned} \frac{d}{dt} s(\boldsymbol{z}, \xi) &= \frac{d}{dt} \left\{ V_2(\boldsymbol{z}) e^{c\xi} \right\} \\ &= \left(\dot{V}_2(\boldsymbol{z}) + c V_2(\boldsymbol{z}) \right) e^{c\xi} \\ &\leq \left(-W(\boldsymbol{z}) + \frac{\hat{\Psi}_d^2(\xi)}{4 d_2} + c V_2(\boldsymbol{z}) \right) e^{c\xi} \\ &\leq \left(-\beta_3(|\boldsymbol{z}|) + c \beta_2(|\boldsymbol{z}|) \right) e^{c\xi} + \frac{\hat{\Psi}_d^2(\xi)}{4 d_2} e^{c\xi}. \end{aligned} \tag{2.91}$$

By choosing c according to

$$c \leq \beta_2^{-1} \circ \beta_3(|\boldsymbol{z}|) \leq \beta_2^{-1} \circ \beta_3(\|\boldsymbol{z}\|_\infty), \tag{2.92}$$

where the existence of $\|\boldsymbol{z}\|_\infty$ follows from (2.87), (2.91) gives

$$\frac{d}{dt}\left\{V_2(\boldsymbol{z})e^{c\xi}\right\} \leq \frac{\hat{\Psi}_d^2(\xi)}{4d_2}e^{c\xi}. \tag{2.93}$$

By integrating (2.93) and using an argument similar to the one in the proof of lemma 2.24 in Krstić *et al.* (1995*a*), it can be shown that

$$V_2(\boldsymbol{z}(\xi)) \leq V_2(\boldsymbol{z}(0))e^{-c\xi} + \frac{1}{4cd_2}\left(\overline{\Psi}_d{}^2(0)e^{-\frac{c\xi}{2}} + \overline{\Psi}_d{}^2(\xi/2)\right). \tag{2.94}$$

Since $\lim_{\xi\to\infty} \overline{\Psi}_d{}^2(\xi/2) = 0$ it follows that

$$\lim_{\xi\to\infty} V_2(\boldsymbol{z}(\xi)) = 0. \tag{2.95}$$

As V_2 is positive definite it follows that

$$\lim_{\xi\to\infty} \boldsymbol{z}(\xi) = 0. \tag{2.96}$$

Thus we have shown that under the additional assumptions (2.88) and (2.89) on the disturbance term, $\boldsymbol{z}(\xi)$ converges to the origin. This also implies that $\hat{\phi}$ and $\hat{\psi}$ converge to the origin and that $\Phi(\xi)$ and $\Psi(\xi)$ converge to the point of intersection of the compressor and throttle characteristic. □

Notice that the positive constant c introduced in (2.90) is used for analysis only, and is *not* included in the implementation of the control law.

At this point we include the flow disturbance $\hat{\Phi}_d(\xi)$ in the analysis.

Theorem 2.3 (Time varying pressure and flow disturbances)
The controller

$$\begin{aligned} u &= c_2 z_2 - k_3\left(\alpha^3 + 3\alpha z_2^2\right) - k_2\hat{\phi}^2 - k_1\alpha \\ &\quad + \frac{d_1}{4B^2}\left(-\hat{\Phi}_T(z_1) + \hat{\phi}\right) + d_2 z_2\left(1 + \frac{d_1^2}{4B^2}\right), \end{aligned} \tag{2.97}$$

where $c_2 > |k_1|$ guarantees that the states of the model (2.37) with both mass flow disturbances and pressure disturbances is globally uniformly bounded and that they converge to a set. □

Proof: The backstepping procedure is as follows:

Step 1. As before two error variables z_1 and z_2 are defined as $z_1 = \hat{\psi}$ and $z_2 = \hat{\phi} - \alpha$. Again, V_1 is chosen as

$$V_1 = 2B^2 l_c z_1^2, \tag{2.98}$$

with time derivative

$$\dot{V}_1 = z_1 \left(-\hat{\Phi}_T(z_1) + z_2 - \hat{\Phi}_d(\xi) + \alpha \right), \tag{2.99}$$

where (2.37) is used. The virtual control α is chosen as

$$\alpha = -d_1 z_1, \tag{2.100}$$

where $-d_1 z_1$ is a damping term to be used to counteract the disturbance $\hat{\Phi}_d(\xi)$. $\dot{V}_1$ can now be written as

$$\dot{V}_1 = -d_1 z_1^2 + z_1 z_2 - \hat{\Phi}_d(\xi) z_1 - \hat{\Phi}_T(z_1) z_1, \tag{2.101}$$

and upper bounded according to

$$\dot{V}_1 \leq -\hat{\Phi}_T(z_1) z_1 + z_1 z_2 + \frac{\|\hat{\Phi}_d\|_\infty^2}{4d_1}. \tag{2.102}$$

To obtain the bound in (2.102), Young's inequality has been used to obtain

$$-\hat{\Phi}_d(\xi) z_1 \leq d_1 z_1^2 + \frac{\hat{\Phi}_d^2(\xi)}{4d_1} \leq d_1 z_1^2 + \frac{\|\hat{\Phi}_d\|_\infty^2}{4d_1}. \tag{2.103}$$

Step 2. The derivative of z_2 is

$$\begin{aligned} \dot{z}_2 &= \frac{1}{l_c} \left(\hat{\Psi}_c(\hat{\phi}) - z_1 + \hat{\Psi}_d(\xi) - \frac{\partial \alpha}{\partial z_1} \frac{1}{4B^2 l_c} \left(-\hat{\Phi}_T(z_1) + \hat{\phi} \right) \right. \\ &\quad \left. + \frac{1}{4B^2 l_c} \frac{\partial \alpha}{\partial z_1} \hat{\Phi}_d(\xi) - u \right). \end{aligned} \tag{2.104}$$

From (2.100) it is seen that

$$\frac{\partial \alpha}{\partial z_1} = -d_1. \tag{2.105}$$

V_2 is chosen as

$$V_2 = V_1 + \frac{l_c}{2} z_2^2. \tag{2.106}$$

Using (2.102) and (2.104), an upper bound on $\dot{V}_2$ is

$$\begin{aligned} \dot{V}_2 &\leq -\hat{\Phi}_T(z_1) z_1 + \frac{\|\hat{\Phi}_d\|_\infty^2}{4d_1} + z_2 \Big(\hat{\Psi}_c(\hat{\phi}) + \hat{\Psi}_d(\xi) \\ &\quad + \frac{d_1}{4B^2} \left(-\hat{\Phi}_T(z_1) + \hat{\phi} \right) - \frac{d_1}{4B^2} \hat{\Phi}_d(\xi) - u \Big). \end{aligned} \tag{2.107}$$

Control law. To counteract the effect of the disturbances, a damping factor d_2 must be included and u is chosen as

$$\begin{aligned} u &= c_2 z_2 - k_3 \left(\alpha^3 + 3\alpha z_2^2 \right) - k_2 \hat{\phi}^2 - k_1 \alpha \\ &\quad + \frac{d_1}{4B^2} \left(-\hat{\Phi}_T(z_1) + \hat{\phi} \right) + d_2 z_2 \left(1 + \frac{d_1^2}{4B^2} \right). \end{aligned} \tag{2.108}$$

The parameter c_2 is now chosen according to

$$c_2 > |k_1|. \tag{2.109}$$

Inserting (2.97) in (2.107) gives

$$\begin{aligned}\dot{V}_2 \quad \leq \quad & -(c_2+k_1)z_2^2 - k_3(z_2^4+3\alpha^2 z_2^2) - \hat{\Phi}_T(z_1)z_1 + \frac{\|\hat{\Phi}_d\|_\infty^2}{4d_1} \\ & -d_2 z_2^2 + |z_2|\|\hat{\Psi}_d\|_\infty + \frac{d_1}{4B^2}|z_2|\|\hat{\Phi}_d\|_\infty - \frac{d_1^2}{4B^2}d_2 z_2^2. \end{aligned} \tag{2.110}$$

Using Young's inequality twice gives

$$|z_2|\|\hat{\Psi}_d\|_\infty \quad \leq \quad d_2 z_2^2 + \frac{\|\hat{\Psi}_d\|_\infty^2}{4d_2} \tag{2.111}$$

$$\frac{d_1}{4B^2}|z_2|\|\hat{\Phi}_d\|_\infty \quad \leq \quad \frac{1}{4B^2}\left(d_1^2 d_2 z_2^2 + \frac{\|\hat{\Phi}_d\|_\infty^2}{4d_2}\right). \tag{2.112}$$

The final upper bound for V_2 can now be written as

$$\dot{V}_2 \leq -W(z_1,z_2) + \frac{1}{\nu_1}\|\hat{\Phi}_d\|_\infty^2 + \frac{1}{\nu_2}\|\hat{\Psi}_d\|_\infty^2 \tag{2.113}$$

where

$$\frac{1}{\nu_1} = \left(\frac{1}{4d_1} + \frac{1}{16B^2 d_2}\right), \ \frac{1}{\nu_2} = \frac{1}{4d_2} \tag{2.114}$$

and

$$W(z_1,z_2) = (c_2+k_1)z_2^2 + k_3(z_2^4+3\alpha^2 z_2^2) + \hat{\Phi}(z_1)z_1 \tag{2.115}$$

is radially unbounded and positive definite. This implies that $\dot{V}_2 < 0$ outside a set $\mathcal{R}_2$ in the $z_1 z_2$ plane. As in section 6.1, the functions $V_2(\boldsymbol{z})$ and $W(\boldsymbol{z})$ exhibit the properties in (2.70). Again, it can be shown that this implies that $\boldsymbol{z}(\xi)$ is globally uniformly bounded and that $\boldsymbol{z}(\xi)$ converges to the residual set

$$\mathcal{R}_2 = \left\{\boldsymbol{z} : |\boldsymbol{z}| \leq \beta_1^{-1} \circ \beta_2 \circ \beta_3^{-1}\left(\frac{\|\hat{\Psi}_d\|_\infty^2}{\nu_1} + \frac{\|\hat{\Phi}_d\|_\infty^2}{\nu_2}\right)\right\}. \tag{2.116}$$

□

Remark 2.4 *Notice that the control law (2.97), as opposed to (2.82), requires knowledge of the coefficients in the compressor characteristic, the throttle characteristic and the B-parameter.* □

Remark 2.5 *Once the bounds on the disturbances $\|\hat{\Phi}_d\|_\infty$ and $\|\hat{\Psi}_d\|_\infty$ are known, the size of the set $\mathcal{R}_2$ in the $z_1 z_2$ plane can be made arbitrary small by choosing the damping factors d_1 and d_2 sufficiently large. The same comment applies to the set $\mathcal{R}_1$ defined in (2.87).* □

Corollary 2.2 (Convergence to the origin)
If the assumptions on $\hat{\Psi}_d(\xi)$ in equations (2.117) and (2.118) hold, and the following assumption on $\hat{\Phi}_d(\xi)$ is made:

$$|\hat{\Phi}_d(\xi)| \leq \overline{\Phi}_d(\xi) \; \forall \xi \geq 0 \tag{2.117}$$

and

$$\lim_{\xi \to \infty} \overline{\Phi}_d(\xi) = 0, \tag{2.118}$$

where $\overline{\Phi}_d(\xi)$ is a monotonically decreasing non-negative function. Then, the states of the model (2.38) converge to the origin. □

Proof: By using the same arguments as in the proof of Corollary 2.1, but with two disturbance terms, it can be shown that

$$\begin{aligned} V_2(\boldsymbol{z}(\xi)) \quad \leq \quad & V_2(\boldsymbol{z}(0))e^{-c\xi} + \frac{1}{c\nu_1}\left(\overline{\Phi}_d{}^2(0)e^{-\frac{c\xi}{2}} + \overline{\Phi}_d{}^2(\xi/2)\right) \\ & + \frac{1}{c\nu_2}\left(\overline{\Psi}_d{}^2(0)e^{-\frac{c\xi}{2}} + \overline{\Psi}_d{}^2(\xi/2)\right). \end{aligned} \tag{2.119}$$

Now $\lim_{\xi\to\infty} \overline{\Psi}_d{}^2(\xi/2) = 0$ and $\lim_{\xi\to\infty} \overline{\Phi}_d{}^2(\xi/2) = 0$ implies that $\lim_{\xi\to\infty} V_2(\boldsymbol{z}(\xi)) = 0$ and by the positive definiteness of V_2 it follows that

$$\lim_{\xi \to \infty} \boldsymbol{z}(\xi) = 0. \tag{2.120}$$

Thus we have shown that under the assumptions (2.88), (2.89), (2.117) and (2.118) on the disturbance terms, $\boldsymbol{z}(\xi)$ converge to the origin. This also implies that $\hat{\phi}(\xi)$ and $\hat{\psi}(\xi)$ converges to the origin and that $\Phi(\xi)$ and $\Psi(\xi)$ converge to the point of intersection of the compressor and throttle characteristic. □

A simulation of the response of the control law (2.97) with both mass flow and pressure disturbances is presented in Chapter 3, where it is compared to a passivity based controller.

2.3.4 Adaption of Constant Disturbances

A constant or slow varying disturbance in mass flow can cause the equilibrium of the compression system to be moved into the unstable area of the compressor map. Therefore, the problem of being able to stabilize the system in this case is a very important one. In addition constant disturbances in pressure is considered simultaneously. Consider the following model

$$\begin{aligned} \dot{\hat{\psi}} \quad &= \quad \frac{1}{4B^2 l_c}\left(\hat{\phi} - \hat{\Phi}_T(\hat{\psi}) - d_\phi\right) \\ \dot{\hat{\phi}} \quad &= \quad \frac{1}{l_c}\left(\hat{\Psi}_c(\hat{\phi}) - \hat{\psi} + d_\psi - u\right), \end{aligned} \tag{2.121}$$

where d_ϕ and d_ψ are constant and unknown disturbances in mass flow and pressure, respectively. Godhavn (1997) used adaptive backstepping for adaption of constant or slow varying sea current disturbances in a surface ship model. The same approach will now be employed here to stabilize (2.121). Two adaption laws will be designed in order to estimate the unknown disturbances and allow them to be counteracted by the control.

Theorem 2.4 *The controller*

$$u = \frac{l_c}{\vartheta_1} z_1 + c_2 z_2 - k_3 \left(\overline{d}_\phi^3 + 3\overline{d}_\phi z_2^2 \right) - k_2 \hat{\phi}^2 - k_1 \overline{d}_\phi + \overline{d}_\psi, \tag{2.122}$$

where the estimates $\overline{d}_\phi$ and $\overline{d}_\psi$ are updated with

$$\dot{\overline{d}}_\phi = -\frac{1}{\vartheta_1} z_1 \tag{2.123}$$

$$\dot{\overline{d}}_\psi = -\frac{1}{\vartheta_2} z_2, \tag{2.124}$$

where $\frac{1}{\vartheta_1}$ and $\frac{1}{\vartheta_2}$ are adaption gains, makes the equilibrium of (2.121) globally asymptotically stable. The states of the model converge to their equilibrium values and the parameter error dynamics are GAS. asymptotically stable. □

Proof: Backstepping is used

Step 1. The error variables z_1 and z_2 are defined as $z_1 = \hat{\psi}$ and $z_2 = \hat{\phi} - \alpha$. The first clf, V_1, is chosen as

$$V_1 = 2B^2 l_c z_1^2 + \frac{\vartheta_1}{2} \tilde{d}_\phi^2, \tag{2.125}$$

where

$$\tilde{d}_\phi \triangleq d_\phi - \overline{d}_\phi, \tag{2.126}$$

is the parameter error and $\overline{d}_\phi$ is an estimate of d_ϕ. The time derivative of V_1 now is

$$\dot{V}_1 = z_1 \left(-\hat{\Phi}_T(z_1) + z_2 - d_\phi + \alpha \right) - \vartheta_1 \tilde{d}_\phi \dot{\overline{d}}_\phi, \tag{2.127}$$

where (2.121) is used. Let the virtual control α be chosen as

$$\alpha = \overline{d}_\phi, \tag{2.128}$$

and the estimate $\overline{d}_\phi$ be updated as

$$\dot{\overline{d}}_\phi = -\frac{1}{\vartheta_1} z_1. \tag{2.129}$$

Thus, the terms including $\tilde{d}_\phi$ in (2.127) are cancelled out, and $\dot{V}_1$ can now be written as

$$\dot{V}_1 = z_1 z_2 - \hat{\Phi}_T(z_1) z_1. \tag{2.130}$$

Step 2. The second clf is chosen as

$$V_2 = V_1 + \frac{l_c}{2}z_2^2 + \frac{\vartheta_2}{2}\tilde{d}_\psi^2 = \frac{1}{2}\boldsymbol{z}^{\mathrm{T}}\boldsymbol{P}\boldsymbol{z} + \frac{1}{2}\tilde{\boldsymbol{d}}^{\mathrm{T}}\boldsymbol{\Gamma}^{-1}\tilde{\boldsymbol{d}}, \tag{2.131}$$

where

$$\tilde{d}_\psi \triangleq d_\psi - \overline{d}_\psi, \tag{2.132}$$

is the parameter error, $\overline{d}_\psi$ is an estimate of d_ψ,

$$\tilde{\boldsymbol{d}} = (\tilde{d}_\phi \;\; \tilde{d}_\psi),\; \boldsymbol{P} = \begin{pmatrix} 4B^2 l_c & 0 \\ 0 & l_c \end{pmatrix}, \text{ and } \boldsymbol{\Gamma}^{-1} = \begin{pmatrix} \vartheta_1 & 0 \\ 0 & \vartheta_2 \end{pmatrix}. \tag{2.133}$$

Using (2.121), $\dot{V}_2$ is calculated as

$$\dot{V}_2 = -\hat{\Phi}(z_1)z_1 + z_2(\hat{\Psi}_c(\hat{\phi}) - u + \frac{l_c}{\vartheta_1}z_1 + d_\psi) - \vartheta_2\tilde{d}_\psi\dot{\overline{d}}_\psi. \tag{2.134}$$

Let the estimate $\overline{d}_\psi$ be updated as

$$\dot{\overline{d}}_\psi = \frac{1}{\vartheta_2}z_2, \tag{2.135}$$

and the control be chosen as

$$u = \frac{l_c}{\vartheta_1}z_1 + c_2 z_2 - k_3\left(\alpha^3 + 3\alpha\boldsymbol{z}_2^2\right) - k_2\hat{\phi}^2 - k_1\alpha + \overline{d}_\psi. \tag{2.136}$$

Using the calculations from the case of time varying disturbances it can be shown that $\dot{V}_2$ can be upper bounded as

$$\dot{V}_2 \leq -(c_2 + k_1)z_2^2 - k_3(z_2^4 + 3\alpha^2 z_2^2) - \hat{\Phi}_T(z_1)z_1 \tag{2.137}$$

By inserting the update laws (2.129) and (2.135) and the control (2.136) in equations (2.121), it can be shown that the error dynamics get the following form

$$\dot{\boldsymbol{z}} = \boldsymbol{P}^{-1}\left(\boldsymbol{A}_z(\boldsymbol{z}, \overline{\boldsymbol{d}}) + \boldsymbol{P}_z\boldsymbol{z} + \tilde{\boldsymbol{d}}\right) \tag{2.138}$$

$$\dot{\tilde{\boldsymbol{d}}} = -\boldsymbol{\Gamma}\boldsymbol{z}, \tag{2.139}$$

where

$$\boldsymbol{A}_z(\boldsymbol{z}, \overline{\boldsymbol{d}}) = \begin{pmatrix} -\hat{\Phi}_T(z_1) \\ -c_2 z_2 - k_3(z_2^3 + 3\alpha^2 z_2) \end{pmatrix} \text{ and } \boldsymbol{P}_z = \begin{pmatrix} 0 & 1 \\ -1 & 0 \end{pmatrix}. \tag{2.140}$$

The stability result follows from application of LaSalle's theorem. From (2.137) it is seen that

$$\dot{V}_2 \equiv 0 \Rightarrow \boldsymbol{z} \equiv 0 \Rightarrow \dot{\boldsymbol{z}} \equiv 0. \tag{2.141}$$

Inserting (2.141) into (2.138) we find that $\tilde{\boldsymbol{d}} \equiv 0$. Thus the origin of (2.138) is GAS. □

This result could also have been stated by using the more general Theorem 4.12 in Krstić *et al.* (1995*a*) or the results in Krstić (1996).

Remark 2.6 *The stability properties of the proposed scheme of two parameter update laws and control law, can also be established through passivity analysis of the error dynamics.*

The model (2.138)-(2.139) has some useful properties that will be taken advantage of in the stability proof: The vector $-\boldsymbol{A}_z$ consists of sector nonlinearities, the matrices $\boldsymbol{C}$ and $\boldsymbol{\Gamma}$ are both diagonal and positive definite, and the matrix $\boldsymbol{P}_z$ is skew symmetric. Consider the positive function

$$S(\boldsymbol{z}) = \frac{1}{2}\boldsymbol{z}^{\mathrm{T}}\boldsymbol{P}\boldsymbol{z} \tag{2.142}$$

and calculate the time derivative of (2.142) along solution trajectories of (2.138):

$$\begin{aligned}\frac{d}{dt}S(\boldsymbol{z}) &= \boldsymbol{z}^{\mathrm{T}}\boldsymbol{P}\dot{\boldsymbol{z}} \\ &= \boldsymbol{z}^{\mathrm{T}}\left(\boldsymbol{A}_z(\boldsymbol{z},\overline{\boldsymbol{d}}) + \boldsymbol{P}_z\boldsymbol{z} + \tilde{\boldsymbol{d}}\right) \\ &= \boldsymbol{z}^{\mathrm{T}}\boldsymbol{A}_z(\boldsymbol{z},\overline{\boldsymbol{d}}) + \boldsymbol{z}^{\mathrm{T}}\tilde{\boldsymbol{d}}. \end{aligned} \tag{2.143}$$

The last step follows from the fact that $\boldsymbol{P}_z$ is skew symmetric. As both elements in $\boldsymbol{A}_z(\boldsymbol{z},\overline{\boldsymbol{d}})$ are sector nonlinearities, the following inequality will always hold:

$$-\boldsymbol{z}^{\mathrm{T}}\boldsymbol{A}_z(\boldsymbol{z},\overline{\boldsymbol{d}}) > 0. \tag{2.144}$$

Integrating (2.143) from 0 to t and using (2.144) results in

$$\int_0^t \boldsymbol{z}^{\mathrm{T}}(\sigma)\tilde{\boldsymbol{d}}(\sigma)d\sigma = S(\boldsymbol{z}(\xi)) - S(\boldsymbol{z}(0)) + \int_0^t -\boldsymbol{z}^{\mathrm{T}}\boldsymbol{A}_z(\boldsymbol{z},\overline{\boldsymbol{d}})d\sigma. \tag{2.145}$$

From this dissipation inequality it is concluded that the mapping $\tilde{\boldsymbol{d}} \mapsto \boldsymbol{z}$ is strictly passive with $S(\boldsymbol{z}) = \boldsymbol{z}^{\mathrm{T}}\boldsymbol{P}\boldsymbol{z}$ as storage function and $-\boldsymbol{z}^{\mathrm{T}}\boldsymbol{A}_z(\boldsymbol{z},\overline{\boldsymbol{d}})$ as dissipation rate. Inspection of (2.139) reveals that the mapping $\boldsymbol{z} \mapsto -\tilde{\boldsymbol{d}}$ is a passive integrator, and thus the system (2.138)-(2.139) is a negative feedback interconnection of a strictly passive and a passive system. This implies that the equilibrium $(\boldsymbol{z},\tilde{\boldsymbol{d}}) = (\boldsymbol{0},\boldsymbol{0})$ is globally uniformly stable and that $\boldsymbol{z}(\xi)$ converges to the origin as $t \to \infty$. The structure of the system is shown in Figure 2.6. □

Remark 2.7 *The result of this section also holds if either of the two constant disturbances are set to zero. In the case of $d_\phi \equiv 0$ and $d_\psi \neq 0$, the controller (2.122) with parameter update law (2.124) is equivalent to an ordinary linear PI-control law in z_2:*

$$u = c_2 z_2 - \int_0^t \frac{1}{\vartheta_2} z_2(\sigma)d\sigma. \tag{2.146}$$

By the same arguments as in the above proof, $\boldsymbol{z} = 0$ is GAS and $\overline{d}_\psi = \int_0^t \frac{1}{\vartheta_2} z_2(\sigma)d\sigma$ converges to the true value of d_ψ. □

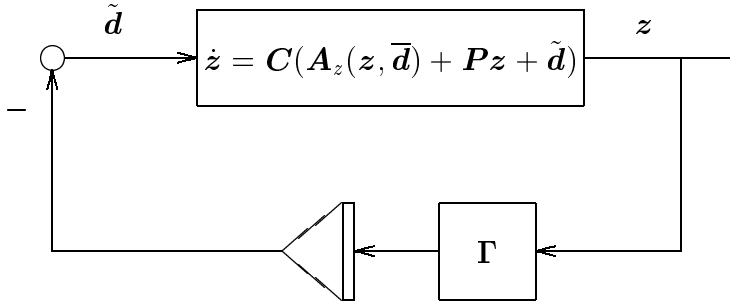

Figure 2.6: *Negative feedback interconnection of strictly passive system with passive system*

2.4 Control of Rotating Stall

In this section CCV controllers will be derived for the full Moore-Greitzer model (2.34). As in the section on surge control, two cases will be studied here as well. First, a stabilizing stall/surge controller is designed for the undisturbed model. Then, pressure disturbances are included in the model, and a second controller is derived. For use in the stability proofs of this section, the following lemma is needed:

Lemma 2.1 *The squared amplitude of rotating stall has an upper bound:*

$$\exists\, J_{\max} < \infty \text{ such that } J(\xi) < J_{\max}\ \forall\ \xi > 0 \tag{2.147}$$

□

Proof:
The proof is similar to that of section 2.4 in Krstić *et al.* (1995*a*):

$$\begin{aligned}
\dot{J} &= J\left(1 - \left(\frac{\Phi}{W} - 1\right)^2 - \frac{J}{4} - \frac{1}{\gamma^2}\frac{4W\Phi}{3H}\right)\varrho, \\
&= -\frac{J^2\varrho}{4} - \varrho J\left(\frac{\Phi^2}{W^2} - \frac{2\Phi}{W}\right) - \varrho J\frac{4W}{3H\gamma^2}\phi \\
&\leq -\frac{J^2\varrho}{4} + \frac{2\varrho}{W}J|\Phi| + \varrho J\frac{4W}{3H\gamma^2}|\Phi| \\
&\leq -\frac{J^2\varrho}{8} - \frac{\varrho J}{8}\left(J - \frac{16}{W}|\Phi| - \frac{32W}{3H\gamma^2}|\Phi|\right)
\end{aligned} \tag{2.148}$$

When $J(\xi) > 16|\Phi(\xi)|\left(\frac{1}{W} + \frac{2W}{3H\gamma^2}\right)$, $J(\xi)$ will decay faster than the solution $w(\xi)$ of the differential equation

$$\dot{w} = -\frac{w^2\varrho}{8}, \tag{2.149}$$

so that an upper bound of $J(\xi)$ is given by

$$J(\xi) < \frac{J(0)}{1+J(0)\frac{\varrho\xi}{8}} + 16 \sup_{0\le\tau<\xi} |\Phi(\tau)| \left(\frac{1}{W} + \frac{2W}{3H\gamma_{\min}^2}\right) \triangleq J_{\max}, \tag{2.150}$$

where $\gamma_{\min} > 0$ is a lower bound on the throttle gain. Equation (2.150) states that J is bounded if ϕ is bounded. An upper bound on ϕ is given by the choking of the mass flow:

$$\Phi \le \phi_{choke}, \tag{2.151}$$

so that a conservative value for $J_{\max}$ is

$$J_{\max} = \frac{J(0)}{1+J(0)\frac{\varrho\xi}{8}} + 16\phi_{choke} \left(\frac{1}{W} + \frac{2W}{3H\gamma_{\min}^2}\right). \tag{2.152}$$

□

The following assumption on the mass flow coefficient is also needed:

Assumption 2.1 *The lower bound on ϕ is given by the minimum value obtained during a deep surge cycle. This lower bound is negative, and is given by*

$$\exists\, \phi_m > 0 \text{ such that } \Phi(\xi) > -\phi_m \forall \xi > 0. \tag{2.153}$$

□

The assumption is not a conservative one. Compressors in general are not intended or designed for operation with reversed mass flow, so it is reasonable to assume that the lowest value of mass flow is reached during the extreme condition of deep surge, more precisely at the negative peak of a deep surge cycle.

2.4.1 Undisturbed Case

Theorem 2.5 *Consider the system (2.34) evolving in the set*

$$\mathcal{A} = \left\{\Psi, \Phi, J \mid \Psi \in I\!R,\ \Phi \in [-\phi_m, \phi_{choke}],\ J \in I\!R^+\right\} \tag{2.154}$$

with the controller

$$u = (c_2 + c_3)(\Phi - \phi_0), \tag{2.155}$$

where $c_2 > a_m$ and a_m is the maximum positive slope of the compressor characteristic, and $c_3 > 0$ is chosen according to

$$c_3^{\min} < c_3 < c_3^{\max}. \tag{2.156}$$

The origin of the closed loop system is then asymptotically stable with a region of attraction equal to $\mathcal{A}$. □

Proof:
The backstepping methodology of Krstić *et al.* (1995*a*) is now employed to design a controller for (2.34)

Step 1. Let the error variables z_1 and z_2 be chosen as

$$z_1 = \hat{\psi} \text{ and } z_2 = \hat{\phi} - \alpha, \tag{2.157}$$

and the CLF for this step be

$$V_1 = 2B^2 l_c z_1^2. \tag{2.158}$$

The time derivative of V_1 along solution trajectories is

$$\dot{V}_1 = z_1 \left(-\hat{\Phi}_T(z_1) + z_2 + \alpha \right). \tag{2.159}$$

As before, the throttle is assumed passive, such that $\hat{\psi}\hat{\Phi}(\hat{\psi}) \geq 0 \ \forall \hat{\psi}$. It follows that

$$\hat{\psi}\hat{\Phi}_T(\hat{\psi}) \geq 0 \ \Rightarrow \ -z_1\hat{\Phi}_T(z_1) \leq 0. \tag{2.160}$$

It is recognized that there is no need to cancel out terms in (2.159). Thus, the stabilizing function α is not needed and can be chosen as $\alpha = 0$, which in turn gives

$$\dot{V}_1 = -\hat{\Phi}_T(z_1)z_1 + z_1 z_2. \tag{2.161}$$

Although $\alpha = 0$ here, the notation of z_1 and z_2 is kept in the interest of consistency with section 2.4.2

Step 2. The derivative of z_2 is

$$\dot{z}_2 = \frac{1}{l_c}\left(-z_1 + \hat{\Psi}_c(z_2) - \frac{3H}{4} J \left(\frac{\Phi}{W} - 1 \right) - \frac{W^2 J}{2\gamma^2} - u \right). \tag{2.162}$$

The clf for this step is

$$V_2 = V_1 + \frac{l_c}{2} z_2^2 + \frac{1}{\varrho J_{\max}} J, \tag{2.163}$$

and $\dot{V}_2$ is calculated as

$$\begin{aligned} \dot{V}_2 \quad = \quad & -z_1\hat{\Phi}_T(z_1) + z_2(\hat{\Psi}_c(z_2) - u) + \frac{J}{J_{\max}} \left(1 - \left(\frac{\Phi}{W} - 1 \right)^2 \right. \\ & \left. - \frac{J}{4} - \frac{1}{\gamma^2}\frac{4W}{3H}\Phi \right) - \frac{3H}{4}\left(\frac{\Phi}{W} - 1 \right) z_2 J - \frac{W^2 J}{2\gamma^2} z_2. \end{aligned} \tag{2.164}$$

By choosing u according to

$$u = (c_2 + c_3) z_2, \tag{2.165}$$

where $c_2 > 0$ and $c_3 > 0$ are constants, $\dot{V}_2$ can be written

$$\dot{V}_2 = \sum_{i=1}^{4} \left(\dot{V}_2 \right)_i. \tag{2.166}$$

The four terms in (2.166) are

$$\left(\dot{V}_2\right)_1 = -z_1\hat{\Phi}_T(z_1), \tag{2.167}$$

$$\left(\dot{V}_2\right)_2 = z_2(\hat{\Psi}_c(z_2) - c_2 z_2), \tag{2.168}$$

$$\left(\dot{V}_2\right)_3 = \frac{J}{J_{\max}}\left(1 - \left(\frac{\Phi}{W} - 1\right)^2 - \frac{1}{\gamma^2}\frac{4W}{3H}\Phi\right), \tag{2.169}$$

$$\left(\dot{V}_2\right)_4 = -\begin{bmatrix} J & z_2 \end{bmatrix} \boldsymbol{P}(\Phi) \begin{bmatrix} J \\ z_2 \end{bmatrix}, \tag{2.170}$$

where

$$\boldsymbol{P}(\phi) = \begin{bmatrix} \frac{1}{4J_{\max}} & \frac{3H}{8}\left(\frac{\Phi}{W} - 1\right) + \frac{W^2}{4\gamma^2} \\ \frac{3H}{8}\left(\frac{\Phi}{W} - 1\right) + \frac{W^2}{4\gamma^2} & c_3 \end{bmatrix}. \tag{2.171}$$

Due to the passivity of the throttle, $\left(\dot{V}_2\right)_1 < 0$. As shown in section 2.3, if c_2 is chosen as

$$c_2 > a_m \geq a > \frac{k_2^2}{4k_3} - k_1, \tag{2.172}$$

where a_m is the maximum positive slope of the compressor characteristic, then $\left(\dot{V}_2\right)_2 < 0$.

By choosing the controller gains sufficiently large, $\left(\dot{V}_2\right)_3$ can be made negative for $\phi > 0$. As the proposed controller (2.165) is of the same form as (2.40), the expression (2.59) for γ, with gain $(c_2 + c_3)$, can be used. For $\left(\dot{V}_2\right)_3$ to be negative the following must be satisfied

$$1 - \left(\frac{\Phi}{W} - 1\right)^2 - \frac{4W}{3H}\frac{\Phi(c_2 + c_3)}{\Phi + \phi_0} < 0 \tag{2.173}$$

$$\Downarrow \quad \Phi > 0$$

$$c_2 + c_3 > \frac{3H}{4W}\frac{\Phi + \phi_0}{\Phi}\left(-\left(\frac{\Phi}{W} - 1\right)^2 + 1\right) \tag{2.174}$$

$$c_2 + c_3 > \frac{3H}{4W}(\Phi + \phi_0)\left(\frac{2}{W} - \frac{\Phi}{W^2}\right) \triangleq G_1(\Phi) \tag{2.175}$$

Simple calculations shows that the maximum of $G_1(\Phi)$ is reached for $\Phi = W - \frac{\phi_0}{2}$. The maximum is given by

$$\max_{\Phi > 0} G_1(\Phi) = \frac{3H}{4W^2}\left(\frac{\phi_0^2}{4W} + W + \phi_0\right). \tag{2.176}$$

By choosing

$$c_2 + c_3 > \frac{3H}{4W^2}\left(\frac{\phi_0^2}{4W} + W + \phi_0\right), \tag{2.177}$$

which implies

$$c_3 > \frac{3H}{4W^2}\left(\frac{\phi_0^2}{4W} + W + \phi_0\right) - c_2 \triangleq \underline{\mathcal{C}}_1(c_2), \tag{2.178}$$

it follows that $\left(\dot{V}_2\right)_3$ is made negative for $\phi > 0$.

For $\phi < 0$ the sum $\left(\dot{V}_2\right)_3 + \left(\dot{V}_2\right)_2$ can be made negative for $\phi > -\phi_m$, that is

$$z_2(\hat{\Psi}_c(z_2) - c_2 z_2) < -\frac{J}{J_{\max}}\left(1 - \left(\frac{\Phi}{W} - 1\right)^2 - \frac{1}{\gamma^2}\frac{4W}{3H}\Phi\right) \tag{2.179}$$

Using (2.59) and $\frac{J}{J_{\max}} < 1$, and rearranging (2.179) gives

$$\frac{c_3}{\Phi + \phi_0}\Phi > G_2(\Phi, c_2), \tag{2.180}$$

where

$$G_2(\Phi, c_2) \triangleq \frac{4W}{3H}\left(z_2\hat{\Psi}_c(z_2) - c_2 z_2^2 + 1 - \left(\frac{\Phi}{W} - 1\right)^2\right) - \frac{c_2}{\Phi + \phi_0}\Phi. \tag{2.181}$$

It can be shown that it is sufficient that (2.180) is satisfied at the end points of the interval:

$$G_2(-\phi_m, c_2) < \frac{\phi_m}{\phi_m - \phi_0}c_3 \tag{2.182}$$

$$G_2(0, c_2) < 0. \tag{2.183}$$

By inspection of (2.181) it is easily shown that (2.183) is always satisfied. It is assumed that $\phi_0 > \phi_m$, so that the condition in (2.182) can be rewritten as

$$c_3 < \frac{\phi_m - \phi_0}{\phi_m}G_2(-\phi_m, c_2) \triangleq \overline{\mathcal{C}}_2(c_2, \phi_m). \tag{2.184}$$

Plots of $\left(\dot{V}_2\right)_2$, $\left(\dot{V}_2\right)_3$ and their sum are shown in Figure 2.7.

Finally, c_3 must be chosen so that $\boldsymbol{P}$ is positive definite for $-\phi_m < \phi < \phi_{choke}$. The determinant of $\boldsymbol{P}$ is given by

$$\det \boldsymbol{P} = \frac{c_3}{4J_{\max}} - \left(\frac{3H}{8}\left(\frac{\Phi}{W} - 1\right) + \frac{W^2}{4\gamma^2}\right)^2 > 0. \tag{2.185}$$

A plot of $\det \boldsymbol{P}$ is shown in the lower part of Figure 2.7. Again, a sufficient condition for $\det \boldsymbol{P} > 0$ for $-\phi_m < \Phi < \phi_{choke}$ is that $\det \boldsymbol{P}(\phi_{choke}) > 0$ and $\det \boldsymbol{P}(-\phi_m) > 0$. As shown in Appendix E, this leads to the following conditions on c_3:

$$\max\left\{\underline{\mathcal{C}}_3(c_2, \phi_{choke}), \underline{\mathcal{C}}_4(c_2, \phi_m)\right\} < c_3 < \min\left\{\overline{\mathcal{C}}_3(c_2, \phi_{choke}), \overline{\mathcal{C}}_4(c_2, \phi_m)\right\} \tag{2.186}$$

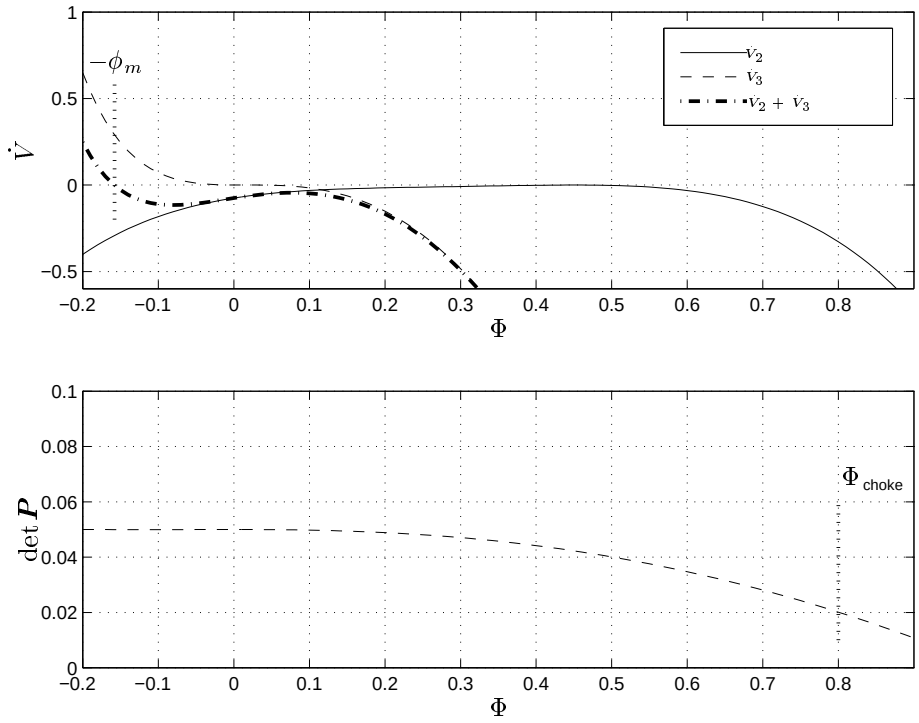

Figure 2.7: *Upper plot illustrates that* $\dot{V}_2 + \dot{V}_3 < 0$ *for* $\Phi > -\phi_m$. *Lower plot illustrates that* $\det \boldsymbol{P} > 0$ *for* $\Phi < \phi_{choke}$.

Choosing c_3 according to (2.186) ensures that

$$\left(\dot{V}_2\right)_4 < 0, \quad -\phi_m < \Phi < \phi_{choke}. \tag{2.187}$$

The requirements (2.172), (2.178), (2.184) and (2.186) are summarized as

$$c_2 > a_m \geq a > \frac{k_2^2}{4k_3} - k_1, \tag{2.188}$$

and

$$c_3 > \max\left\{\underline{\mathcal{C}}_1(c_2),\ \underline{\mathcal{C}}_3(c_2, \phi_{choke}),\ \underline{\mathcal{C}}_4(c_2, \phi_m)\right\} \triangleq c_3^{\min} \tag{2.189}$$

$$c_3 < \min\left\{\overline{\mathcal{C}}_2(c_2, \phi_m),\ \overline{\mathcal{C}}_3(c_2, \phi_{choke}),\ \overline{\mathcal{C}}_4(c_2, \phi_m)\right\} \triangleq c_3^{\max} \tag{2.190}$$

Provided c_2 and c_3 are chosen according to (2.188) to (2.190), $\dot{V}_2$ is upper bounded as

$$\dot{V}_2 \leq -U(z_1, z_2, J). \tag{2.191}$$

As $V_2 : \mathcal{A} \to \mathbb{R}$, $V_2(\mathbf{0}) = 0$, V_2 is positive definite and continuously differentiable on $\mathcal{A}$, and $\dot{V}(\boldsymbol{z}) < 0$ for $\boldsymbol{z} \in \mathcal{A} - \{\mathbf{0}\}$, the origin of the system is asymptotically stable with region of attraction equal to $\mathcal{A}$. □

By doing the same calculations as in Remark 2.1, the control law for the CCV gain is found to be:

$$\gamma = \sqrt{\frac{\Phi + \phi_0}{(c_2 + c_3)}}. \tag{2.192}$$

Notice that this control law requires sensing of mass flow ϕ only. The analysis leading to this control law was conservative, resulting in a large value of the parameter c_3, that is c_3 has to be chosen as $c_3 > c_3^{\min}$. As was the case in Krstić *et al.* (1995*b*), the controller should be implemented with a lower gain than dictated by the Lyapunov analysis. Consider the closed loop Jacobian of the model (2.34) with control law (2.155):

$$\boldsymbol{A}_{cl} = \begin{pmatrix} -\frac{1}{4B^2 l_c} a_\Phi & \frac{1}{4B^2 l_c} & 0 \\ -\frac{1}{l_c} - \frac{3H}{4 l_c W} & \frac{1}{l_c} a_\Psi - \frac{c_2 + c_3}{l_c} & 0 \\ 0 & 0 & \varrho\left(-\frac{\phi_0^2}{W^2} + \frac{2\phi_0}{W}\right) - \frac{4W\varrho(c_2+c_3)}{6H} \end{pmatrix}, \tag{2.193}$$

where

$$a_\Psi = \left.\frac{\partial \hat{\Phi}_T(z_1)}{\partial z_1}\right|_{z_1=0} \quad \text{and} \quad a_\Phi = \left.\frac{\partial \hat{\Psi}_c(z_2)}{\partial z_2}\right|_{z_2=0}. \tag{2.194}$$

It can be shown that if $\boldsymbol{A}_{cl}$ is Hurwitz for $c_3 > c_3^{\min}$, $\boldsymbol{A}_{cl}$ is also Hurwitz for $c_3 = 0$. The closed loop system is therefore locally stable with $c_3 = 0$.

2.4.2 Disturbed Case

The backstepping procedure is now used to design a controller that ensures boundedness of the states in the presence of pressure disturbances.

Theorem 2.6 *Consider the model (2.37) with time varying pressure disturbances only, that is $\hat{\Psi}_d(\xi) \neq 0$ and $\hat{\Phi}_d(\xi) \equiv 0$, evolving on the set $\mathcal{A}$. Let the controller u be defined as*

$$u = (c_2 + c_3) z_2 + d_2 z_2 \tag{2.195}$$

where $d_2 > 0$, c_2 satisfies

$$c_2 > a_m, \tag{2.196}$$

where a_m is an upper bound on the positive slope of the compressor characteristic, and c_3 satisfies

$$c_3^{\min} < c_3 < c_3^{\max} \tag{2.197}$$

where $c_3^{\min}$ and $c_3^{\max}$ are defined in (2.189) and (2.190). Then (2.195) makes the states of the model (2.37) uniformly ultimately bounded and ensures convergence to a set. □

Proof:
This result follows by combining the proofs of Theorem 2.3 and Theorem 2.5. The Lyapunov function

$$V_2 = V_1 + \frac{l_c}{2} z_2^2 + \frac{1}{J_{\max} \varrho} J \tag{2.198}$$

will have an upper bound on its time derivative given by

$$\dot{V}_2 \leq -U(z_1, z_2, J) + \frac{\hat{\Psi}_d^2(\xi)}{4d_2} \tag{2.199}$$

where

$$U(z_1, z_2, J) = \sum_{i=1}^{4} \left(\dot{V}_2 \right)_i . \tag{2.200}$$

and the four terms $\left(\dot{V}_2 \right)_i$ are given by (2.167)-(2.170) provided the control is chosen as (2.195).

Provided c_2 is chosen according to (2.188) and c_3 satisfies (2.189) and (2.190), then $\dot{V}_2 < 0$ outside a set $\mathcal{R}_3$. According to Krstić *et al.* (1995*a*), the fact that $V_2(z_1, z_2, J)$ is positive definite, radially unbounded and smooth, and $U(z_1, z_2, J)$ is positive definite for $-\phi_m < \Phi < \phi_{choke}$ implies that there exists class-$\mathcal{K}_\infty$ functions β_1, β_2 and a class-$\mathcal{K}$ function β_3 such that

$$\left.\begin{array}{l} \beta_1(|\boldsymbol{z}|) \leq V_2(\boldsymbol{z}) \leq \beta_2(|\boldsymbol{z}|) \\ \beta_3(|\boldsymbol{z}|) \leq U(\boldsymbol{z}) \end{array}\right\} \tag{2.201}$$

where $\boldsymbol{z} = (z_1,\ z_2,\ J)^{\mathrm{T}}$. This implies that $\boldsymbol{z}(\xi)$ is uniformly ultimately bounded and that $\boldsymbol{z}(\xi)$ converges to the set

$$\mathcal{R}_3 = \left\{ \boldsymbol{z} : |\boldsymbol{z}| \leq \beta_1^{-1} \circ \beta_2 \circ \beta_3^{-1} \left(\frac{\|\hat{\Psi}_d\|_\infty^2}{\kappa_1} \right) \right\}. \tag{2.202}$$

□

Remark 2.5 is also applicable to this case.

Remark 2.8 *The case of stabilizing rotating stall in the case of disturbances in mass flow as well as pressure rise, can be studied by combining Theorem 2.3 and Theorem 2.5. It is straightforward to extend the results on convergence to the origin and adaption of constant mass flow disturbances and pressure disturbances from Section 2.3 to the control design in this section.* □

2.5 Simulations

In this section, the proposed controllers of this chapter are simulated. Results form both surge and stall control, with and without disturbances, will be shown.

The compressor characteristic

$$\Psi_c(\phi) = \psi_{c0} + H\left(1 + \frac{3}{2}\left(\frac{\Phi}{W} - 1\right) - \frac{1}{2}\left(\frac{\Phi}{W} - 1\right)^3\right), \tag{2.203}$$

of Moore and Greitzer (1986) is used in all simulations. The throttle will be set so that the intersection of the throttle line and the compressor characteristic is located on the part of the characteristic that has positive slope, resulting in an unstable equilibrium. After some time, the controllers will be switched on, demonstrating that the system is stabilized.

2.5.1 Surge Control

Surge control will now be demonstrated. A Greitzer parameter of $B = 1.8$ is used in the simulations. The throttle gain is set to $\gamma = 0.61$ and thus the equilibrium is unstable. The initial conditions of the systems were chosen as

$$(\phi_0,\ \psi_0) = (0.6,\ 0.6). \tag{2.204}$$

In Figure 2.8, it is shown how the controller (2.40) with $c_2 = 1$ stabilizes the system.

In Figure 2.9 noise has been added, and the system is stabilized by the controller (2.97) with $c_2 = 1$, $d_1 = 0.3$ and $d_2 = 3$.

A simulation of surge induced by a constant disturbance is showed in Figure 2.10. The compression system is initially operating stably with a throttle setting of $\gamma = 0.65$ yielding a stable equilibrium. At $\xi = 200$ the constant disturbances $d_\phi = -0.1$ and $d_\psi = 0.05$ are introduced into the system, resulting in the state of the system being pushed over the surge line. Consequently, surge oscillations emerge. At $\xi = 420$ the adaptive controller (2.122) with update laws (2.123), and as can be seen, the surge oscillations are brought to rest. The parameters of the controller were $c_2 = 1.1$, $\vartheta_1 = 9$ and $\vartheta_2 = 20$. The disturbances are unknown to the controller, but as guaranteed by Theorem 2.4 their estimates converges to the true values.

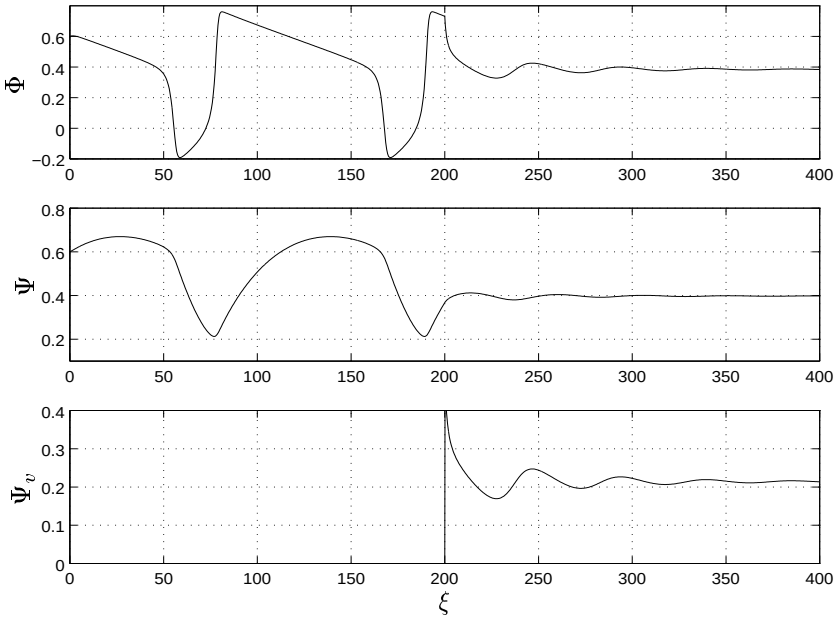

Figure 2.8: *The throttle gain is set to* $\gamma = 0.61$*, and the compressor is surging. The controllers are switched on at* $\xi = 200$*.*

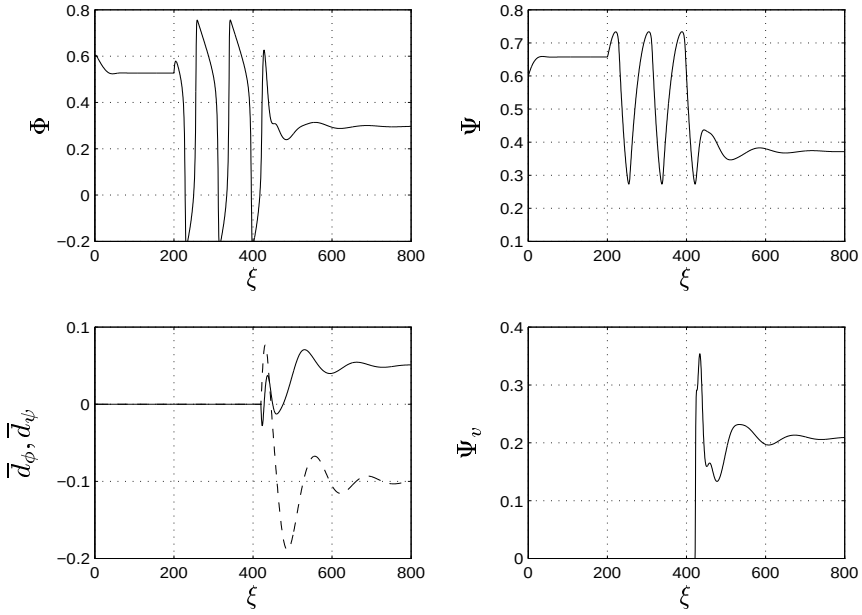

Figure 2.10: *Disturbance induced surge stabilized by the adaptive controller (2.122).*

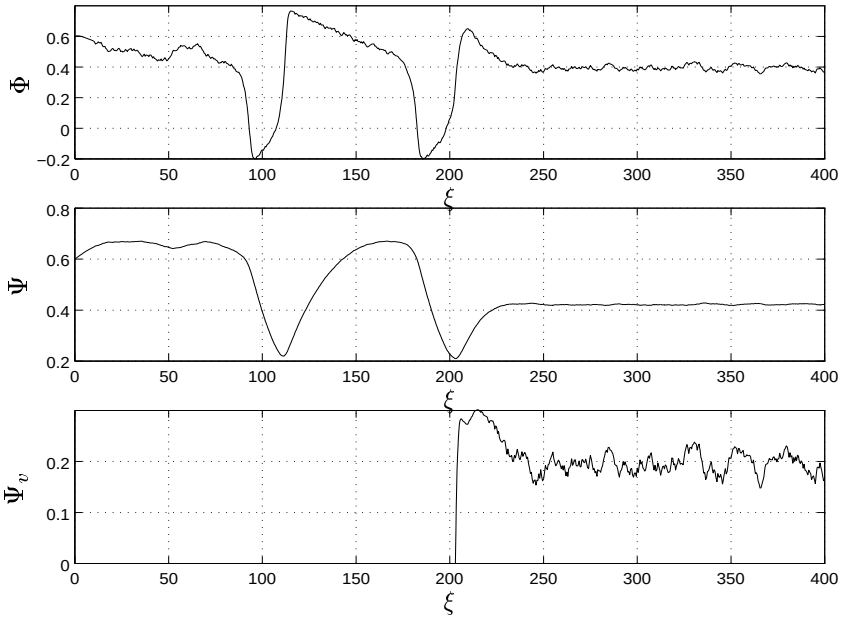

Figure 2.9: *Same situation as in Figure 2.8. However, here disturbances are taken into account. The pressure and the mass flow disturbances are both white noise varying between* ± 0.05.

2.5.2 Rotating Stall Control

In this section some simulation results of the proposed controllers for rotating stall are presented. In Figure 2.11 the response of system (2.34) with controller (2.165) is shown. The throttle gain is set at $\gamma_T = 0.61$, resulting in an unstable equilibrium for the unactuated system. The initial conditions of the systems were chosen as

$$(\phi_0\,;\psi_0,\ J_0) = (0.6,\ 0.6,\ 0.05). \tag{2.205}$$

The B-parameter is set to $B = 0.5$ for all the rotating stall simulations. Thus, the compressor enter rotating stall, and J increases until J_e is reached. At $\xi = 100$ the controller is switched on, and J decreases until $J = 0$ is reached. As discussed at the end of Section 2.4.1, the controller gains are chosen as $c_3 = 0$ and $c_2 = 1$. The simulation results are also plotted together with the compressor characteristic and the in-stall characteristic in Figure 2.12. As the compressor is stabilized it is seen that the pressure loss associated with the CCV is slightly less than that associated with operating in rotating stall, which would have been the case if e.g. the throttle control scheme of Krstić *et al.* (1995*b*) had been used.

The effect of pressure disturbances is shown in Figure 2.13. The B-parameter is $B = 0.5$ and the compressor stalls. The pressure disturbance is white noise of amplitude 0.1. Throttle setting and initial conditions were left unchanged. The control law (2.195) with parameters $c_2 = 1$ and $d_2 = 0.1$ is switched on at $\xi = 100$, bringing the compressor out of rotating stall, and damping the disturbances.

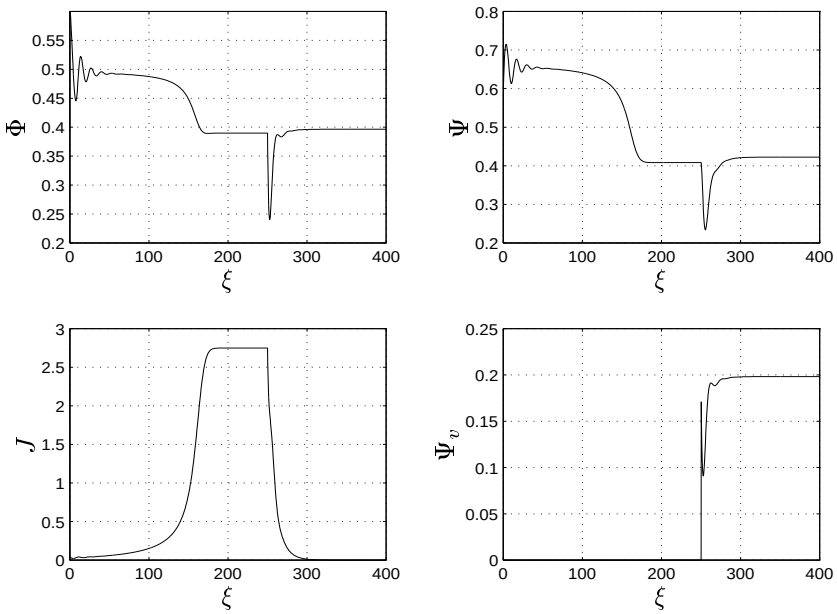

Figure 2.11: *Stabilization of rotating stall*

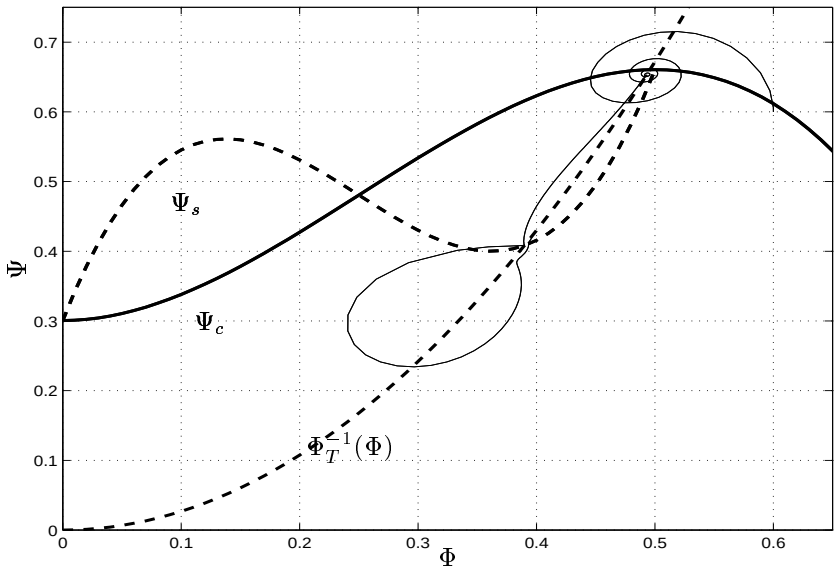

Figure 2.12: *Same simulation as in Figure 2.11, superimposed on the compressor characteristic and in-stall characteristic*

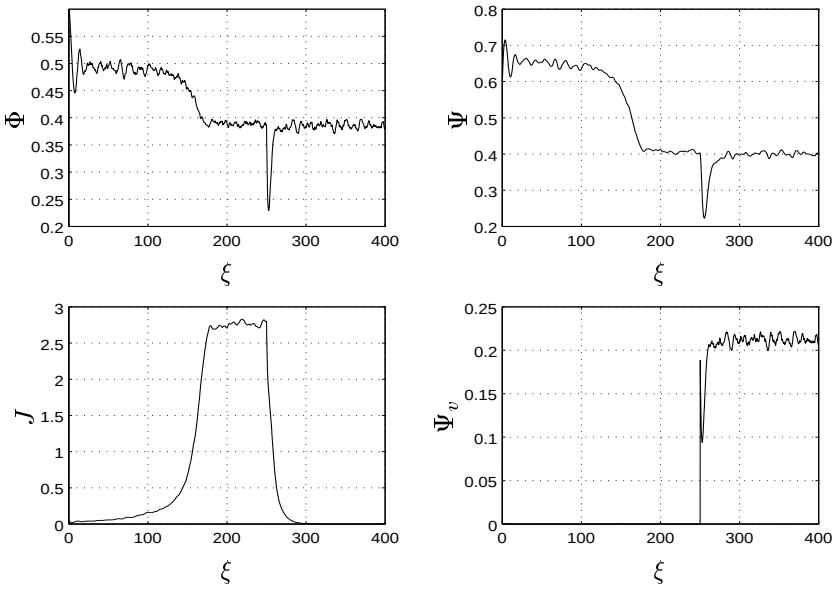

Figure 2.13: *Stabilization of rotating stall with pressure disturbances*

2.6 Conclusion

In this chapter, anti surge and stall controllers for a close-coupled valve in series with a compressor have been developed. First, surge was studied, and by the application of the backstepping methodology, a control law which uses feedback from mass flow only was derived. Global asymptotic stability was proven. Only an upper bound on the slope of the compressor characteristic was required to implement this controller. The controller was used both in the case of no disturbances and in the presence of pressure disturbances.

A more complicated surge control law was derived for the case of both pressure disturbances and mass flow disturbances. In order to implement this controller, the compressor characteristic and the B-parameter must be known. Global uniform boundedness and convergence to a set was proven. By assuming the disturbances upper bounded by a monotonically decreasing non-negative function, convergence to the origin was proven. In order to stabilize the compression system in the presence of constant disturbances, or biases, in mass flow and pressure, an adaptive version of the surge controller was derived. This controller ensures global asymptotic stability.

Then, controllers for rotating stall were considered. The close coupled valve was incooperated into the Moore-Greitzer model, and controllers were derived that enables stabilization of rotating stall beyond the surge line. Without disturbances, an asymptotically stable equilibrium is ensured, and in the presence of pressure disturbances uniform boundedness was proven.

Chapter 3

Passivity Based Surge Control

3.1 Introduction

In this chapter passivity will be used to derive a surge controller for a compression system when time varying disturbances are considered in both pressure as well as mass flow.

Passivity and input/output methods have been used in many control applications such as mechanical systems in general, electrical machines, marine vehicles and so on. To the authors best knowledge this is the first attempt to apply this method to the compressor surge control problem.

3.1.1 Motivation

In the previous chapter, backstepping was employed to derive a stabilizing control law when time varying disturbances were taken into account. The control law resulting from this approach was

$$\begin{aligned} u &= c_2 z_2 - k_3\left(\alpha^3 + 3\alpha z_2^2\right) - k_2\hat{\phi}^2 - k_1\alpha \\ &\quad + \frac{d_1}{4B^2}\left(-\hat{\Phi}_T(z_1) + \hat{\phi}\right) + d_2 z_2\left(1 + \frac{d_1^2}{4B^2}\right). \end{aligned} \tag{3.1}$$

Of particular interest here, will be the use of input/output methods to design controllers with disturbance rejection capabilities. This is motivated by the fact that the surge controller (3.1) seems unnecessary complicated.

3.1.2 Notation

A brief introduction to passivity and $\mathcal{L}_2$ is given here. For a comprehensive treatment of these concepts, consult van der Schaft (1996), from which the notation is taken. The signal space $\mathcal{L}_2$ consists, somewhat simplified, of all functions $f : \mathbb{R}_+ \to \mathbb{R}$ that satisfy

$$\int_0^\infty |f(\xi)|^2 d\xi < \infty. \tag{3.2}$$

The truncation of f to $[0, T]$ is defined as

$$f_T(\xi) = \begin{cases} f(\xi) & , \quad 0 \leq \xi < T \\ 0 & , \quad \xi \geq T \end{cases}, \tag{3.3}$$

and the set $\mathcal{L}_{2e}$, the extension of $\mathcal{L}_2$, consists of all functions f such that $f_T \in \mathcal{L}_2$. A mapping $\mathcal{G} : u \mapsto y$ with input $u \in \mathcal{L}_{2e}$ and output $y \in \mathcal{L}_{2e}$ is said to be passive if there exists a constant β so that

$$\int_0^T u(\xi) y(\xi) d\xi \geq \beta \tag{3.4}$$

for all $u \in L_{2e}$ and all $T \geq 0$. The inner product on $\mathcal{L}_{2e}$ is

$$\langle u, y \rangle_T = \int_0^T u(\xi) y(\xi) d\xi, \tag{3.5}$$

and the truncated norm is

$$\|u\|_T^2 = \langle u, u \rangle_T . \tag{3.6}$$

A concept that will be used in this chapter is that of strict output passivity. The mapping $\mathcal{G} : u \mapsto y$ is strict output passive if $\exists\, \kappa > 0$ and $\exists\, \beta$ such that

$$\langle y, u \rangle = \langle \mathcal{G}u, u \rangle \geq \kappa \|\mathcal{G}u\|_T^2 + \beta \;\; \forall u \in \mathcal{L}_{2e}, \;\; \forall T \geq 0. \tag{3.7}$$

3.2 Model

A compression system consisting of a compressor, axial or centrifugal, in series with a close-coupled valve, a plenum volume and a throttle is studied, consult figure 2.3. The system is presented in section 2.2.4, and repeated here for convenience:

$$\begin{aligned} \dot{\hat{\psi}} &= \frac{1}{4B^2 l_c}(\hat{\phi} - \hat{\Phi}_T(\hat{\psi})) \\ \dot{\hat{\phi}} &= \frac{1}{l_c}(\hat{\Psi}_c(\hat{\phi}) - u - \hat{\psi}), \end{aligned} \tag{3.8}$$

where $u = \hat{\Psi}_v$, and the equivalent compressor characteristic is $\hat{\Psi}_e = \hat{\Psi}_c - \hat{\Psi}_v$. The notation $\dot{x}$ is to be understood as differentiation with respect to nondimensional time $\xi = \frac{Ut}{R}$ as in the previous chapter.

Assumption 3.1 *The throttle is assumed to be a passive component, moreover the constant $\kappa_2 > 0$ can always be chosen sufficiently small so that the characteristic satisfies the sector condition:*

$$\forall\ \hat{\psi}\ \ \exists\, \kappa_2\ \text{ such that }\ \hat{\Phi}_T(\hat{\psi})\hat{\psi} \geq \kappa_2 \hat{\psi}^2, \tag{3.9}$$

Our aim will be to design a control law $u = \hat{\Psi}_v(\hat{\phi})$ for the valve such that the compressor also can be operated stably on the left side of the original surge line without going into surge.

3.3 Passivity

3.3.1 Passivity of Flow Dynamics

Consider the non-negative function

$$V_1(\hat{\phi}) = \frac{l_c}{2}\hat{\phi}^2 \tag{3.10}$$

The time derivative of (3.10) along solution trajectories of (3.8) is

$$\dot{V}_1 = -\hat{\psi}\hat{\phi} + \Psi_e(\hat{\phi})\hat{\phi}. \tag{3.11}$$

Then, it is evident that

$$\begin{aligned} \left\langle -\hat{\psi}, \hat{\phi} \right\rangle_T &= \left\langle -\hat{\Psi}_e(\hat{\phi}), \hat{\phi} \right\rangle_T + V_1(\xi) - V_1(0) \\ &\geq \left\langle -\hat{\Psi}_e(\hat{\phi}), \hat{\phi} \right\rangle_T - V_1(0) \end{aligned} \tag{3.12}$$

Hence, the flow dynamics

$$\mathcal{G}_1 : -\hat{\psi} \mapsto \hat{\phi}, \tag{3.13}$$

where $\mathcal{G}_1 : \mathcal{L}_{2e} \to \mathcal{L}_{2e}$ is an input-output mapping, can be given certain passivity properties if the equivalent compressor characteristic $\hat{\Psi}_e(\hat{\phi})$ can be shaped appropriately by selecting the valve control law $\hat{\Psi}_v(\hat{\phi})$.

3.3.2 Passivity of Pressure Dynamics

Proposition 3.1 *The pressure dynamics*

$$\mathcal{G}_2 : \hat{\phi} \mapsto \hat{\psi}, \tag{3.14}$$

where $\mathcal{G}_2 : \mathcal{L}_{2e} \to \mathcal{L}_{2e}$ is an input-output mapping, are strictly output passive. □

Proof : Consider the nonnegative function

$$V_2(\hat{\psi}) = 2B^2 l_c \hat{\psi}^2. \tag{3.15}$$

Differentiating V_2 along the solution trajectories of (3.8) gives

$$\dot{V}_2 = \hat{\psi}\hat{\phi} - \hat{\phi}(\hat{\psi})\hat{\psi}. \tag{3.16}$$

In view of Assumption 3.1 and (3.16) it follows that

$$\begin{aligned} \left\langle \hat{\psi}, \hat{\phi} \right\rangle_T &= \left\langle \hat{\phi}(\hat{\psi}), \hat{\psi} \right\rangle_T + \int_0^T \dot{V}_2 d\xi \\ &= \int_0^T \hat{\Phi}_T(\hat{\psi})\hat{\psi} d\xi + \int_0^T \dot{V}_2 d\xi \\ &\geq \kappa_2 \int_0^T \psi^2(\xi) d\xi + V_2(\xi) - V_2(0) \\ &\geq \kappa_2 \|\hat{\psi}\|_T^2 - V_2(0). \end{aligned} \tag{3.17}$$

Hence,

$$\left\langle \mathcal{G}_2\hat{\phi}, \hat{\phi} \right\rangle_T \geq \kappa_2 \|\mathcal{G}_2\hat{\phi}\|_T^2 - V_2(0), \tag{3.18}$$

and $\mathcal{G}_2$ is strictly output passive according to Definition 2.2.1 in van der Schaft (1996). □

Remark 3.1 *In Simon and Valavani (1991), the incremental energy*

$$V = \frac{l_c}{2}\hat{\psi}^2 + 2B^2 l_c \hat{\phi}^2, \tag{3.19}$$

with different coefficients due to the choice of nondimensional time, was used as a Lyapunov function candidate. The selection of the functions V_1 and V_2 used here is obviously inspired by this function. □

3.3.3 Control Law

The following simple control law is proposed:

Proposition 3.2 *Let the control law be given by*

$$\hat{\Psi}_v = c\hat{\phi} \tag{3.20}$$

where $c > \frac{k_2^2}{4k_3} - k_1 + \kappa_1$ and $\kappa_1 > 0$ is a design parameter. Then the equivalent compressor characteristic $-\hat{\Psi}_e(\hat{\phi})$ will satisfy the sector condition

$$\left\langle -\hat{\Psi}_e(\hat{\phi}), \hat{\phi} \right\rangle_T \geq \int_0^T \kappa_1 \hat{\phi}^2(\xi) d\xi = \kappa_1 \|\hat{\phi}\|_T^2 \tag{3.21}$$

□

Proof :
The compressor characteristic is defined in equation (2.24). The equivalent compressor characteristic $\hat{\Psi}_e(\hat{\phi})$ is then given by

$$\hat{\Psi}_e(\hat{\phi}) = -k_3\hat{\phi}^3(\xi) - k_2\hat{\phi}^2(\xi) - (k_1+c)\hat{\phi}(\xi) \tag{3.22}$$

Consider the inner product

$$\begin{aligned}\left\langle -\hat{\Psi}_e(\hat{\phi}), \hat{\phi} \right\rangle_T &= \int_0^T \hat{\phi}(\xi)\left(k_3\hat{\phi}^3(\xi) + k_2\hat{\phi}^2(\xi) + (k_1+c)\hat{\phi}(\xi)\right) d\xi \\ &= \int_0^T \hat{\phi}^2(\xi)\left(k_3\hat{\phi}^2(\xi) + k_2\hat{\phi}(\xi) + (k_1+c)\right) d\xi. \end{aligned} \tag{3.23}$$

It is noted that $K(\hat{\phi}) \stackrel{\triangle}{=} k_3\hat{\phi}^2 + k_2\hat{\phi} + (k_1+c)$ has a minimum value for $\hat{\phi} = -\frac{k_2}{2k_3}$. This minimum is calculated to be

$$K(\hat{\phi}) = k_3\hat{\phi}^2 + k_2\hat{\phi} + (k_1+c) \geq -\frac{k_2^2}{4k_3} + k_1. \tag{3.24}$$

With the choice

$$c \geq \frac{k_2^2}{4k_3} - k_1 + \kappa_1 \tag{3.25}$$

it it follows from (3.22) that

$$k_3\hat{\phi}^2(\xi) + k_2\hat{\phi}(\xi) + (k_1+c) \geq \kappa_1. \tag{3.26}$$

By inserting (3.26) into (3.23) we get

$$\left\langle -\hat{\Psi}_e(\hat{\phi}), \hat{\phi} \right\rangle_T \geq \int_0^T \kappa_1\hat{\phi}^2(\xi)d\xi = \kappa_1\|\hat{\phi}\|_T^2, \tag{3.27}$$

□

Provided $u = \hat{\Psi}_v$ is chosen as (3.20), it follows that also the flow dynamics are made strictly output passive, that is

$$\left\langle \mathcal{G}_1(-\hat{\psi}), -\hat{\psi} \right\rangle_T \geq \kappa_1\|\mathcal{G}_1(-\hat{\psi})\|_T^2 - V_1(0), \tag{3.28}$$

We now state a stability reslult for the closed loop system $\Sigma_{\mathcal{G}_1,\mathcal{G}_2}$, shown in figure 3.1.

Theorem 3.1 *The closed loop system $\Sigma_{\mathcal{G}_1,\mathcal{G}_2}$ consisting of the model (2.36) and control law (3.1) is $\mathcal{L}_2$-stable.* □

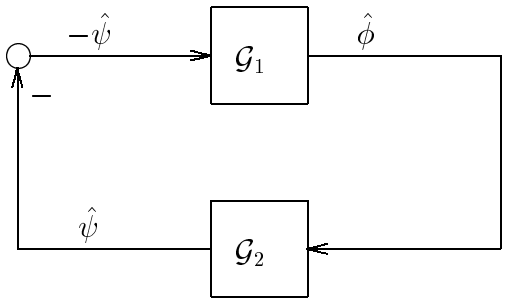

Figure 3.1: *The closed loop system* $\Sigma_{\mathcal{G}_1,\mathcal{G}_2}$

Proof :
The closed loop system $\Sigma_{\mathcal{G}_1,\mathcal{G}_2}$, shown in figure 3.1, is a feedback interconnection of the two systems $\mathcal{G}_1 : -\hat{\psi} \mapsto \hat{\phi}$ and $\mathcal{G}_2 : \hat{\phi} \mapsto \hat{\psi}$. As stated in (3.18) and (3.28), the two mappings satisfy

$$\left\langle -\hat{\psi}, \mathcal{G}_1(-\hat{\psi}) \right\rangle \geq \kappa_1 \|\mathcal{G}_1(-\hat{\psi})\|_T^2 - V_1(0) \tag{3.29}$$

$$\left\langle \hat{\phi}, \mathcal{G}_2\hat{\phi} \right\rangle \geq \kappa_2 \|\mathcal{G}_2\hat{\phi}\|_T^2 - V_2(0) \tag{3.30}$$

for all $T \geq 0$ and all $\hat{\phi}, \hat{\psi} \in \mathcal{L}_{2e}$. According to the *passivity theorem*, Theorem 2.2.6 in van der Schaft (1996), $\Sigma_{\mathcal{G}_1,\mathcal{G}_2}$ is $\mathcal{L}_2$-stable. □

3.4 Disturbances

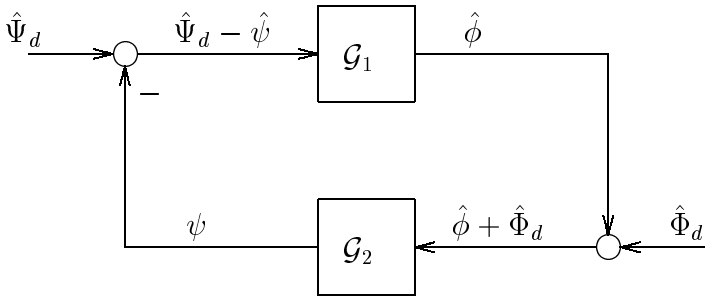

Figure 3.2: *The closed loop system* $\Sigma_{\mathcal{G}_1,\mathcal{G}_2}$ *with disturbances*

Consider the case when the compression system is subject to disturbances $\hat{\Phi}_d(\xi)$ in mass flow and $\hat{\Psi}_d(\xi)$ in pressure rise as in Section 2.2.5. The model is repeated

here for convenience:

$$\begin{aligned} \dot{\hat{\psi}} &= \frac{1}{4B^2 l_c}(\hat{\phi} + \hat{\Phi}_d(\xi) - \hat{\Phi}_T(\hat{\psi})) \\ \dot{\hat{\phi}} &= \frac{1}{l_c}(\hat{\Psi}_c(\hat{\phi}) - u - \hat{\psi} - \hat{\Psi}_d(\xi)) \end{aligned} \tag{3.31}$$

It is assumed that $\hat{\Psi}_d(\xi), \hat{\Phi}_d(\xi) \in \mathcal{L}_{2e}$. A stability result for the closed loop system shown in figure 3.2 is now stated:

Theorem 3.2 *The system (3.31) under control (3.20) is $\mathcal{L}_2$-stable if the disturbances $\hat{\Phi}_d(\xi)$ in mass flow and $\hat{\Psi}_d(\xi)$ in pressure rise are taken into account.* □

Proof :
Redefine $\mathcal{G}_1$ as $\mathcal{G}_1 : -(\hat{\psi} - \hat{\Psi}_d) \mapsto \hat{\phi}$ and $\mathcal{G}_2$ as $\mathcal{G}_2 : \hat{\phi} + \hat{\Phi}_d \mapsto \hat{\psi}$. The result follows by repeating the analysis in the preceding sections and replacing $-\hat{\psi}$ with $-\hat{\psi} + \hat{\Psi}_d$ when establishing the strict output passivity of $\mathcal{G}_1$, and replacing $\hat{\phi}$ with $\hat{\phi} + \hat{\Phi}_d$ when establishing the strict output passivity of $\mathcal{G}_2$. □

The structure of the closed loop system is shown in figure 3.2. Disturbance rejection of $\mathcal{L}_2$-disturbances in the Moore Greitzer model is also studied by Haddad *et al.* (1997), where throttle control of both surge and rotating stall is considered. While achieving global results and disturbance rejection for disturbances in both mass flow and rotating stall amplitude, the controller found by Haddad *et al.* (1997) is of high order, requires detailed knowledge of the compression system parameters and also needs full state feedback.

3.5 Simulations

Now the system (3.31) with control law (3.20) is simulated. The result is given in figure 3.3. The controller gain was set to $c = 1.1$, and the controller was switched on at $\xi = 400$. The disturbances were

$$\begin{aligned} \hat{\Phi}_d(\xi) &= 0.15e^{-0.015\xi}\cos(0.2\xi) \\ \hat{\Psi}_d(\xi) &= 0.1e^{-0.005\xi}\sin(0.3\xi), \end{aligned} \tag{3.32}$$

which has the same structure as the $\mathcal{L}_2$-disturbances considered in Haddad *et al.* (1997).

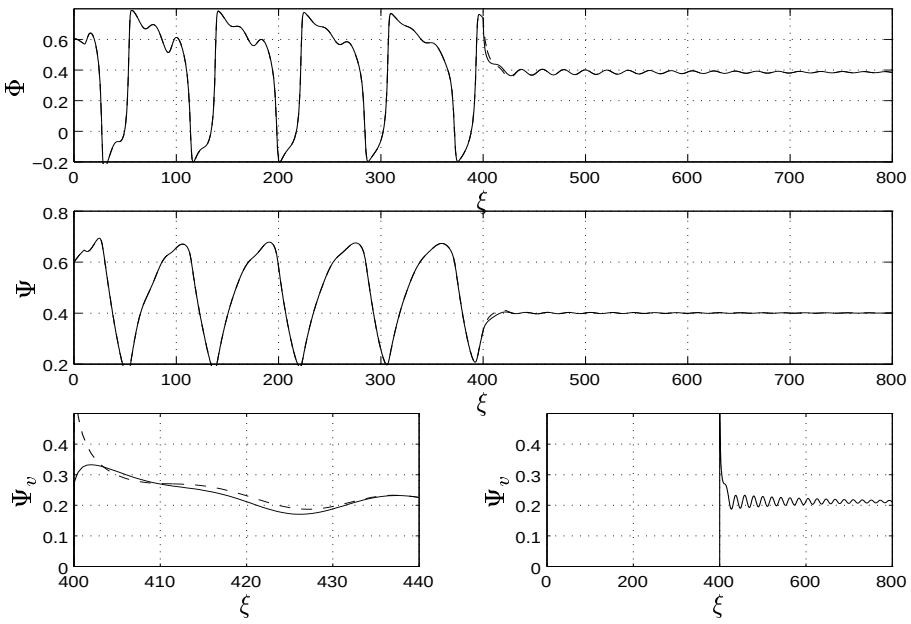

Figure 3.3: *Comparison of closed loop response with passivity based (solid lines) and backstepping based (dashed lines) controllers. The controllers were switched on at* $\xi = 400$.

Also plotted in Figure 3.3 is the response of the controller (3.1), simulated with the same disturbances. The parameters for (3.1) were chosen as $c_2 = 1$, $d_1 = 0.3$, $d_2 = 0.1$. The two set of responses are almost indistinguishable, but in the lower left plot there is a blown up plot of the CCV pressure drop, and as can be seen there is a small difference. Figure 3.3 also illustrates the result of Corollary 2.2, where the controller (3.1) guarantees convergence to the equilibrium in the presence of disturbances upper bounded by a monotonically decreasing non-negative function. The small difference in control action is due to the low damping (d_i) chosen for (3.1), but with the current disturbances that is all that was needed.

One advantage of the backstepping controller (3.1) compared to the passivity based (3.20) is that (3.1) ensures convergence to a set when the disturbances are *not* in $\mathcal{L}_2$, whereas the approach in this chapter demands that they are in $\mathcal{L}_2$.

3.6 Concluding Remarks

In this chapter the passivity properties of the Greitzer model was used to derive a surge control law for a close coupled valve. The results in this chapter, when not taking disturbances into account, are similar to the results in section 2.3.1. However, using input/output theory and passivity it was possible to show that the proportional controller $u = c\hat{\phi}$ yielded an $\mathcal{L}_2$-stable system in the presence of

both mass flow disturbances as well as pressure disturbances. Compared to the more complicated controller (3.1) the advantages of the input/output approach over the Lyapunov based approach of backstepping, in this particular case, should be evident.

However, it is believed that the simple controller $u = c\hat{\phi}$ also could have been derived using backstepping, but with considerable more involved algebraic manipulations, and possibly a new choice of Lyapunov function candidate.

It is straightforward to show that the stability result is still valid if the control law (3.20) is changed as long as the sector condition (3.21) hold. Thus, a more sophisticated controller could be used in order to e.g. minimize the steady state pressure drop over the CCV or improve transient performance, and still stability could be shown.

When comparing with the results on rotating stall control in Haddad *et al.* (1997), the passivity based method used here shows promise for developing a simple, low order, partial state feedback controller when rotating stall is also taken into account, and still achieving disturbance rejection. This is an interesting open problem.

Chapter 4

A Moore-Greitzer Type Model for Axial Compressors with Non-constant Speed

4.1 Introduction

In this chapter we propose an extension to the Moore-Greitzer model. Non-constant rotational speed of the compressor is taken into account. The consequence of this is that the new model includes the B-parameter as a state. Higher harmonics of rotating stall will also be included in the model.

In the original work of Moore and Greitzer, the compressor speed is assumed constant. Greitzer and Moore (1986) concluded that low values of Greitzer's B-parameter B lead to rotating stall, while high value of B leads to surge. High and low in this context is dependent on the design parameters of the compressor at hand, as Day (1994) points out. There exists a $B_{critical}$ for which higher B-values will lead to surge and lower B-values will lead to rotating stall. However this $B_{critical}$ is different for each compressor. As B is proportional to the angular speed of the machine, it is of major concern for stall/surge controller design to include the spool dynamics in a stall/surge-model, in order to investigate the influence of time varying speed on the stall/surge transients.

A model for centrifugal compressors with non-constant speed was presented by Fink *et al.* (1992). In Gravdahl and Egeland (1997*g*) a similar model was derived, and surge and speed control was investigated. However, both the models of Fink *et al.* (1992) and Gravdahl and Egeland (1997*g*) were developed for centrifugal machines, and do not include rotating stall as a state.

The model of Moore and Greitzer (1986) is based on a first harmonics approximation of rotating stall, using a Galerkin procedure. A fundamental shortcoming of the low order three state More Greitzer model is the one mode approximation. Mansoux *et al.* (1994) found that higher order modes interact with the first harmonic during stall inception. Relaxation of the one mode approximation has been presented by Adomatis and Abed (1993), Mansoux *et al.* (1994), Gu *et al.* (1996) and Leonessa *et al.* (1997*a*), and control designs for such models have been reported by several authors, see Table 4.1 below. Also, Banaszuk *et al.* (1997) reports of design of stall/surge controllers without using a Galerkin approximation, that is for the full PDE model. Leonessa *et al.* (1997*a*) highlights the importance of including higher order modes of rotating stall in the model, and demonstrates that the control law proposed by Krstić *et al.* (1995*a*), which was based on a one mode model, fails when applied to a higher order model.

In Table 4.1, the development in stall/surge modeling and control is outlined. Hansen *et al.* (1981) demonstrated that the model of Greitzer (1976*a*) also applies to centrifugal compressors. It seems that the modeling and control of an axial compression system including both rotating stall and spool speed is an open problem. The problem of non-constant speed is also listed among topics for further research in Greitzer and Moore (1986).

Reference(s)	states	A/C	M/C/S
Greitzer (1976*a*)	Φ, Ψ	A	M
Hansen *et al.* (1981)	Φ, Ψ	C	M
several, see de Jager (1995), incl. Gravdahl and Egeland (1997*c*)	Φ, Ψ	A/C	C
Fink *et al.* (1992)	Φ, Ψ, B	C	M
Gravdahl and Egeland (1997*g*)	Φ, Ψ, B	C	MCS
Moore and Greitzer (1986)	Φ, Ψ, J	A	M
Eveker and Nett (1991)	Φ, Ψ, B	A	MC
several, see de Jager (1995), incl. Gravdahl and Egeland (1997*d*)	Φ, Ψ, J	A	C
Mansoux *et al.* (1994)	Φ, Ψ, J_i	A	M
Leonessa *et al.* (1997*a*)	Φ, Ψ, J_i	A	MC
Adomatis and Abed (1993) Hendrickson and Sparks (1997) Humbert and Krener (1997)	Φ, Ψ, J_i	A	C
Gravdahl and Egeland (1997*a*)	Φ, Ψ, J, B	A	MS
Gravdahl and Egeland (1997*e*)	Φ, Ψ, J_i, B	A	MS

Table 4.1: *Outline of the development in compressor stall/surge modeling and control. A=Axial, C=Centrifugal, M=Modeling, C=stall/surge control, S=Speed control. The model of Eveker and Nett (1991) actually uses states with dimensions.*

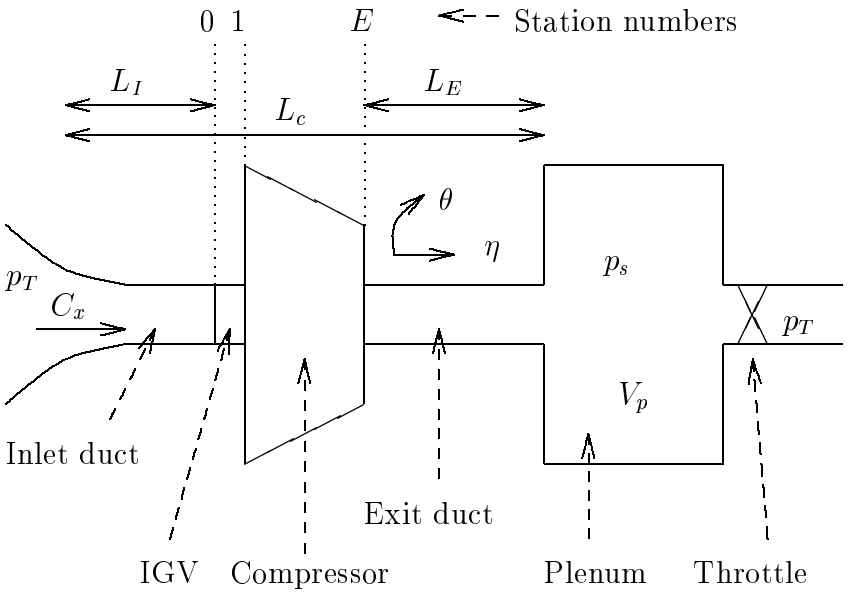

Figure 4.1: *Principal drawing of the compression system of (Moore and Greitzer 1986). The station numbers are used as subscripts in the following.*

4.2 Preliminaries

The compression system is essentially the same as in Chapter 2, and consists of an inlet duct, inlet guide vanes (IGV), axial compressor, exit duct, plenum volume and a throttle. The differences compared to Chapter 2 is that the compressor speed is non-constant, and a CCV is not included. The system is shown in Figure 4.1. Our aim is to develop a model for this system in the form

$$\dot{\boldsymbol{z}} = \boldsymbol{f}(\boldsymbol{z}), \tag{4.1}$$

where $\boldsymbol{z} = (\Phi,\ \Psi,\ J_i,\ B)^{\mathrm{T}} \in \mathbb{R}^q$ and

- Φ is the circumferentially averaged flow coefficient
- Ψ is the total-to-static pressure rise coefficient
- J_i is the squared amplitude mode i of angular variation (rotating stall)
- B is Greitzer's B-parameter which is proportional to the speed of the compressor.
- $i = 1 \ldots N$ is the rotating stall mode number. N is the maximum number of stall modes determined by the gas viscosity.
- The dimension of the state space is $q = N + 3$.

The modeling of the compression system relies heavily on the modeling in Moore and Greitzer (1986). However, the assumption of constant speed U, and thus constant B, is relaxed and a momentum balance for the spool is included. The gas viscosity as introduced by Adomatis and Abed (1993) is also taken into account, and N modes are included in the model as opposed to the work of Moore and Greitzer (1986) where a first harmonic approximation was used.

Moore and Greitzer (1986) define nondimensional time as

$$\xi_{MG} = \frac{Ut}{R}, \tag{4.2}$$

where U is the rotor tangential velocity at mean radius, R is the mean compressor radius and t is actual time in seconds. As we here consider time varying U, this normalization will not be used. Instead we propose to use

$$\xi = \frac{U_d t}{R}, \tag{4.3}$$

where U_d is the *desired* constant velocity of the wheel. Note that if $U_d = U = const$, we have that $\xi = \xi_{MG}$. All distances are nondimensionalized with respect to R, that is the nondimensional duct lengths, see Figure 4.1, are defined as

$$l_I = \frac{L_I}{R} \text{ and } l_E = \frac{L_E}{R}. \tag{4.4}$$

The axial coordinate is denoted η and the circumferential coordinate is the wheel angle θ. Greitzer's B-parameter is defined as

$$B \triangleq \frac{U}{2a_s}\sqrt{\frac{V_p}{A_c L_c}}, \tag{4.5}$$

where a_s is the speed of sound, V_p is the plenum volume, A_c is the compressor duct flow area and L_c is the total length of compressor and ducts. B and U are related as

$$U = bB, \tag{4.6}$$

where

$$b \triangleq 2a_s\sqrt{\frac{A_c L_c}{V_p}} \tag{4.7}$$

is a constant.

4.3 Modeling

4.3.1 Spool Dynamics

The momentum balance of the spool can be written

$$I\frac{d\omega}{dt} = \tau_t - \tau_c, \tag{4.8}$$

where ω is the angular speed, I is the spool moment of inertia, and τ_t and τ_c are the drive (turbine) torque and compressor torque respectively. Using $\omega = U/R$, (4.3) and (4.5), the spool dynamics (4.8) can be written

$$\frac{2a_s I U_d}{R^2}\sqrt{\frac{A_c L_c}{V_p}}\frac{dB}{d\xi} = \tau_t - \tau_c. \tag{4.9}$$

As in Fink *et al.* (1992), torques are nondimensionalized according to

$$\Gamma = \Gamma_t - \Gamma_c = \frac{\tau_t - \tau_c}{\rho A_c R U^2}, \tag{4.10}$$

where ρ is the constant inlet density. Now, (4.9) can be written

$$\frac{dB}{d\xi} = \Lambda_1 B^2(\Gamma_t - \Gamma_c), \tag{4.11}$$

where the constant Λ_1 is defined as

$$\Lambda_1 \triangleq \frac{\rho R^3 A_c}{I U_d} b. \tag{4.12}$$

As the compressor torque equals the change of angular momentum of the fluid, see for instance Mattingly (1996), the compressor torque can be written

$$\tau_c = m_c R(C_{\theta 2} - C_{\theta 1}) \tag{4.13}$$

where $C_{\theta 1}$ and $C_{\theta 2}$ are the tangential fluid velocity at the rotor entrance and exit respectively. Assuming that C_x, the flow velocity in the axial direction, is the same at entrance and exit,

$$\tau_c = m_c R C_x(\tan\beta_1 - \tan\beta_2) \tag{4.14}$$

where β_1 and β_2 fluid angles at the rotor entrance and exit respectively. The fluid angles are time varying. However, Cohen *et al.* (1996) show that

$$\tan\beta_{1b} - \tan\beta_{2b} = \tan\beta_1 - \tan\beta_2, \tag{4.15}$$

where β_{1b} and β_{b2} constant blade angles at the rotor entrance and exit respectively. The compressor mass flow is given by

$$m_c = \rho A_c U \Phi. \tag{4.16}$$

Combining (4.14), (4.15) and (4.16) gives

$$\tau_c = R\rho A_c \Phi^2 U^2(\tan\beta_{1b} - \tan\beta_{2b}) \tag{4.17}$$

and by (4.10) the nondimensional compressor torque is

$$\Gamma_c = \Phi^2(\tan\beta_{1b} - \tan\beta_{2b}). \tag{4.18}$$

In terms of the compressor speed U, the dynamics of the spool can be written

$$\frac{dU}{d\xi} = \frac{\Lambda_1}{b}\Gamma U^2. \tag{4.19}$$

4.3.2 Compressor

Moore (1984*a*) gives the pressure rise over a single blade row as

$$\frac{p_E - p_1}{\frac{1}{2}\rho U^2} = F(\phi) - \tau \frac{d\phi}{dt}, \tag{4.20}$$

where

$$\phi = \frac{C_x}{U} \tag{4.21}$$

is the local axial flow coefficient, $F(\phi)$ is the pressure rise coefficient in the blade passage, C_x is the velocity component along the x-axis, and τ is a coefficient of pressure rise lag. According to Moore and Greitzer (1986), $\frac{d\phi}{dt}$ can be calculated as

$$\frac{d\phi}{dt} = \left(\frac{\partial \phi}{\partial t}\right)_{rotor} + \left(\frac{\partial \phi}{\partial t}\right)_{stator}. \tag{4.22}$$

Using (4.3) it is seen that

$$\begin{aligned} \left(\frac{\partial \phi}{\partial t}\right)_{rotor} &= \frac{\partial \phi}{\partial \xi}\frac{\partial \xi}{\partial t} + \frac{\partial \phi}{\partial \theta}\frac{\partial \theta}{\partial t} \\ &= \frac{U_d}{R}\frac{\partial \phi}{\partial \xi} + \frac{\partial \phi}{\partial \theta}\frac{U(t)}{R} \qquad (4.23) \\ \left(\frac{\partial \phi}{\partial t}\right)_{stator} &= \frac{U_d}{R}\frac{\partial \phi}{\partial \xi}, \qquad (4.24) \end{aligned}$$

where the unsteadiness of the flow through the stator passage reflects the accelerations associated with transients effects. For the rotor there is also unsteadiness due to the rotor blades moving with velocity $U(t)$ through a circumferentially nonuniform flow. Considering a compressor of N_s stages, we get

$$\frac{p_E - p_1}{\frac{1}{2}\rho U^2} = N_s F(\phi) - \frac{1}{2a}\left(2\frac{\partial \phi}{\partial \xi} + \frac{U}{U_d}\frac{\partial \phi}{\partial \theta}\right), \tag{4.25}$$

where

$$a \triangleq \frac{R}{N_s \tau U_d} \tag{4.26}$$

is a constant. Note that if $U(\xi) = \text{const}$ and $U_d \equiv U$ such that $\xi = \xi_{MG}$, equation (4.25) is reduced to equation (5) in Moore and Greitzer (1986). It is noted that the flow coefficient ϕ can depend on both ξ and θ, even though the atmospheric stagnation pressure p_T is constant. The average of ϕ around the wheel is defined as

$$\frac{1}{2\pi}\int_0^{2\pi} \phi(\xi, \theta) d\theta \triangleq \Phi(\xi). \tag{4.27}$$

Further

$$\phi = \Phi(\xi) + g(\xi, \theta) \text{ and } h = h(\xi, \theta), \tag{4.28}$$

where h is a circumferential coefficient. As no circulation occurs in the entrance duct it is clear that the averages of g and h vanish:

$$\int_0^{2\pi} g(\xi, \theta) d\theta = \int_0^{2\pi} h(\xi, \theta) d\theta = 0. \tag{4.29}$$

4.3.3 Entrance Duct and Guide Vanes

The fact that the rotational speed of the wheel now is assumed time varying does not change the conditions upstream of the compressor. Therefore the equations stated in Moore and Greitzer (1986) are still valid, and will be presented here. The pressure difference over the IGVs, where the flow is axial, can be written

$$\frac{p_1 - p_0}{\rho U^2} = \frac{1}{2} K_G h^2, \tag{4.30}$$

where $0 < K_G \leq 1$ is the entrance recovery coefficient. If the IGVs are lossless $K_G = 1$. Upstream of the IGV irrotational flow is assumed so that a (unsteady) velocity potential $\tilde{\phi}$ exists. The gradient of $\tilde{\phi}$ gives axial and circumferential velocity coefficients everywhere in the entrance duct. At the IGV entrance point (denoted by subscript '0') we have

$$(\tilde{\phi}_\eta)_0 = \Phi(\xi) + g(\xi, \theta) \text{ and } (\tilde{\phi}_\theta)_0 = h(\xi, \theta), \tag{4.31}$$

where partial differentiation with respect to η and θ is denoted by subscripts. Bernoulli's equation for unsteady, frictionless and incompressible flow will be used to calculate the pressure drop in the entrance duct. As in Moore and Greitzer (1986) and White (1986), this can be written

$$\frac{p_T - p_0}{\rho U^2} = \frac{1}{2}(\phi^2 + h^2) + (\tilde{\phi}_\xi)_0, \tag{4.32}$$

where the term $(\tilde{\phi}_\xi)_0$ is due to unsteadiness in Φ and g. A straight inlet duct of nondimensional length l_I is considered, and the velocity potential can be written

$$\tilde{\phi} = (\eta + l_I)\Phi(\xi) + \tilde{\phi}'(\xi, \eta), \tag{4.33}$$

where $\tilde{\phi}'$ is a disturbance velocity potential such that

$$\tilde{\phi}'\Big|_{\eta=-l_I} = 0 \ , \ (\tilde{\phi}'_\eta)_0 = g(\xi, \theta) \text{ and } (\tilde{\phi}'_\theta)_0 = h(\xi, \theta). \tag{4.34}$$

Equation (4.32) can now be written

$$\frac{p_T - p_0}{\rho U^2} = \frac{1}{2}(\phi^2 + h^2) + l_I \frac{d\Phi}{d\xi} + (\tilde{\phi}'_\xi)_0. \tag{4.35}$$

4.3.4 Exit Duct and Guide Vanes

Downstream of the compressor the flow is complicated and rotational. As in Moore and Greitzer (1986), the pressure p in the exit duct is assumed to differ only slightly from the static plenum pressure $p_s(\xi)$, such that the pressure coefficient P satisfies Laplace's equation.

$$P \triangleq \frac{p_s(\xi) - p}{\rho U^2} \ , \ \nabla^2 P = 0. \tag{4.36}$$

The axial Euler equation, see for instance White (1986), is used to find the pressure drop across the exit duct. The Euler equation is the inviscid form of the differential equation of linear momentum. If integrated along a streamline of the flow, the Euler equation will yield the frictionless Bernoulli equation. The Euler equation in the x-coordinate, neglecting gravity, can be written as

$$-\frac{dp}{dx} = \rho \frac{dC_x}{dt}. \tag{4.37}$$

Employing the chosen nondimensionalization of time and distance,

$$\frac{d}{dt} = \frac{U_d}{R}\frac{d}{d\xi} \text{ and } \frac{d}{dx} = \frac{1}{R}\frac{d}{d\eta}, \tag{4.38}$$

we get

$$\frac{dp_E}{dx} = -\rho U^2 \frac{1}{R}(P_\eta)_E \tag{4.39}$$

$$\frac{dC_x}{dt} = \frac{U_d}{R}\frac{d}{d\xi}\left\{(\tilde{\phi}_\eta)_0 U\right\}. \tag{4.40}$$

Inserting (4.39) and (4.40) in (4.37) we get the following expression for the axial Euler equation, evaluated at E, where time varying U has been taken into account

$$\begin{aligned}(P_\eta)_E &= \frac{U_d}{U^2}\frac{d}{d\xi}\left\{(\tilde{\phi}_\eta)_0 U\right\} \\ &= \frac{U_d}{U^2}\left((\tilde{\phi}_{\eta\xi})_0 U + (\tilde{\phi}_\eta)_0 \frac{dU}{d\xi}\right).\end{aligned} \tag{4.41}$$

From (4.31) we have

$$(\tilde{\phi}_{\eta\xi})_0 = \Phi_\xi(\xi) + (\tilde{\phi}'_{\eta\xi})_0. \tag{4.42}$$

Inserting (4.31) and (4.42) into (4.41) we get

$$(P_\eta)_E = \frac{U_d}{U}\left(\frac{d\Phi}{d\xi} + (\tilde{\phi}'_{\eta\xi})_0\right) + \frac{U_d}{U^2}\frac{dU}{d\xi}\left(\Phi(\xi) + (\tilde{\phi}'_\eta)_0\right). \tag{4.43}$$

At the duct exit, $\eta = l_E$, we want that $p = p_s$, that is $P = 0$. Thus, when integrating (4.43), the constant of integration is chosen such that

$$P = \frac{U_d}{U(\xi)}\left((\eta - l_E)\frac{d\Phi}{d\xi} - \tilde{\phi}'_\xi\right) + \frac{U_d}{U^2}\frac{dU}{d\xi}\left((\eta - l_E)\Phi(\xi) - \tilde{\phi}'\right). \tag{4.44}$$

Finally, we get

$$\begin{aligned}\frac{p_s - p_E}{\rho U^2} &= (P)_E = \frac{U_d}{U(\xi)}\left(-l_E\frac{d\Phi}{d\xi} - (m-1)(\tilde{\phi}'_\xi)_0\right) \\ &\quad + \frac{U_d}{U^2}\frac{dU}{d\xi}\left(-l_E\Phi(\xi) - (m-1)(\tilde{\phi}')_0\right),\end{aligned} \tag{4.45}$$

where, as in Moore (1984*b*) and Moore and Greitzer (1986), the compressor duct flow parameter[1] m has been included. It is noted that if $U(\xi)$ =const and $U_d \equiv U$ such that $\xi = \xi_{MG}$, equation (4.45) is reduced to equation (20) in Moore and Greitzer (1986).

[1] $m = 1$ for a very short exit duct, and $m = 2$ otherwise.

4.3.5 Overall Pressure Balance

Using the preceding calculations, we now want to calculate the net pressure rise from the upstream reservoir total pressure p_T to the plenum static pressure p_s at the discharge of the exit duct. This is done by combining equations (4.25), (4.30), (4.35) and (4.45) according to

$$\begin{aligned}\frac{p_s - p_T}{\rho U^2} &= (NF(\phi) - \frac{1}{2}\phi^2) - (l_I + l_E\frac{U_d}{U} + \frac{1}{a})\frac{d\Phi}{d\xi} \\ &+ \left((1-m)\frac{U_d}{U} - 1\right)(\tilde{\phi}'_\xi)_0 - \frac{1}{2}(1-K_G)h^2 \\ &+ \frac{U_d}{U^2}\frac{dU}{d\xi}\left(-l_E\Phi(\xi) - (m-1)(\tilde{\phi}')_0\right) \\ &- \frac{1}{2a}\left(2(\tilde{\phi}'_{\xi\eta})_0 + \frac{U}{U_d}(\tilde{\phi}'_{\eta\theta})_0\right), \end{aligned} \tag{4.46}$$

where

$$\begin{aligned} 2\frac{\partial\phi}{\partial\xi} + \frac{\partial\phi}{\partial\theta} &= 2\frac{\partial\Phi}{\partial\xi} + 2\frac{\partial g}{\partial\xi} + \frac{\partial g}{\partial\theta} \\ &= 2\frac{\partial\Phi}{\partial\xi} + 2(\tilde{\phi}'_{\xi\eta})_0 + (\tilde{\phi}'_{\eta\theta})_0 \end{aligned} \tag{4.47}$$

has been used. By defining [2]

$$\begin{aligned} \Psi(\xi) &= \frac{p_s - p_T}{\rho U^2} \\ \Psi_c(\phi) &= NF(\phi) - \frac{1}{2}\phi^2 \\ l_c(U) &= l_I + l_E\frac{U_d}{U} + \frac{1}{a} \\ m_U(U) &= (1-m)\frac{U_d}{U} - 1, \end{aligned} \tag{4.48}$$

and assuming $K_G \equiv 1$, (4.46) can be written

$$\begin{aligned}\Psi(\xi) &= \Psi_c(\phi) - l_c(U)\frac{d\Phi}{d\xi} + m_U(U)(\tilde{\phi}'_\xi)_0 \\ &+ \frac{U_d}{U^2}\frac{dU}{d\xi}\left(-l_E\Phi(\xi) - (m-1)(\tilde{\phi}')_0\right) \\ &- \frac{1}{2a}\left(2(\tilde{\phi}'_{\xi\eta}) + \frac{U}{U_d}(\tilde{\phi}'_{\eta\theta}) - \mu(\tilde{\phi}'_{\eta\theta\theta})\right)_0, \end{aligned} \tag{4.49}$$

which, when assuming $U = U_d$ and $\mu = 0$, reduces to equation (26) in Moore and Greitzer (1986). In (4.49) the μ-term is included in order to account for viscous transportation of momentum in the compressor. Viscosity was first introduced

[2] Notice that $l_c \neq L_c R$. As in Fink *et al.* (1992) L_c, used in the definition of B, is a constant. See equation (4.5).

into the Moore-Greitzer model by Adomatis and Abed (1993), and included in the analysis of Gu *et al.* (1996) and Hendrickson and Sparks (1997). Adomatis and Abed (1993) concludes that the effect of viscous damping *must* be included in a multi mode Moore-Greitzer model. This to ensure that the large velocity gradients associated with higher modes will be damped out. Without viscosity, all the modes would have the same amplitude in fully developed rotating stall.

Equation (4.49) requires knowledge of the disturbance velocity potential $\tilde{\phi}'$ and its derivatives. As $\tilde{\phi}'$ satisfies Laplace's equation $\nabla^2\tilde{\phi}' = 0$ it has a Fourier series. This Fourier series has N terms, where the number N is dependent on μ. According to Adomatis and Abed (1993) and Gu *et al.* (1996),

$$N = \begin{cases} \infty & \text{for} \quad \mu = 0 \\ \text{finite} & \text{for} \quad \mu > 0 \end{cases} \tag{4.50}$$

By using (4.6), equation (4.49) can be written in terms of B, and by integration of (4.49) over one cycle with respect to θ, we get

$$\Psi(\xi) + l_c(B)\frac{d\Phi}{d\xi} + l_E\frac{U_d\Gamma\Lambda_1}{b}\Phi(\xi) = \frac{1}{2\pi}\int_0^{2\pi}\psi_c(\phi)d\theta, \tag{4.51}$$

which is the annulus averaged momentum balance.

4.3.6 Plenum Mass Balance

The mass balance in the plenum can be written

$$\frac{d}{d\xi}(\rho_p V_p) = m_c - m_t, \tag{4.52}$$

where ρ_p is the plenum density, m_c is the mass flow entering the plenum from the compressor, and m_t is the mass flow leaving through the throttle. Assuming the pressure variations in the plenum isentropic, we have

$$\frac{dp_p}{d\xi} = \frac{a_s^2}{V_p}(m_c - m_t), \tag{4.53}$$

which is shown in detail in Appendix B. By nondimensionalizing pressure with ρU^2, mass flow with $\rho U A_c$, transforming to nondimensional time ξ, and taking account for (4.5), (4.53) can be written

$$\frac{d\Psi}{d\xi} = \frac{\Lambda_2}{B}(\Phi - \Phi_T) - \frac{2}{B}\frac{dB}{d\xi}\Psi, \tag{4.54}$$

where the constant Λ_2 is defined as

$$\Lambda_2 \triangleq \frac{R}{L_c U_d}b. \tag{4.55}$$

Using (4.11) we get

$$\frac{d\Psi}{d\xi} = \frac{\Lambda_2}{B}(\Phi - \Phi_T) - 2\Lambda_1\Gamma B\Psi. \tag{4.56}$$

The model of the compression system now consists of the torque balance for the spool (4.11), the local momentum balance (4.49), the annulus averaged momentum balance (4.51) and the mass balance of the plenum (4.56).

The compression systems characteristics are taken from Moore and Greitzer (1986). The usual third order polynomial steady state compressor characteristic presented in Chapter 2 is used, and repeated here for convenience:

$$\Psi_c(\phi) = \psi_{c0} + H\left(1 + \frac{3}{2}(\frac{\phi}{W} - 1) - \frac{1}{2}(\frac{\phi}{W} - 1)^3\right), \tag{4.57}$$

where the parameters ψ_{c0}, H and W are defined in Chapter 2.

The throttle characteristics is again taken to be

$$\Phi_T(\Psi) = \gamma_T\sqrt{\Psi}. \tag{4.58}$$

4.3.7 Galerkin Procedure

In order to transform the PDE (4.49) into a set of ODEs, a Galerkin approximation is employed. The disturbance velocity potential $\tilde{\phi}'$ is represented by the function $(\tilde{\phi}')^*$:

$$(\tilde{\phi}')^* = \sum_{n=1}^{N}(\mu)\frac{W}{n}e^{n\eta}A_n(\xi)\sin(n\theta - r_n(\xi)), \tag{4.59}$$

where $A_n(\xi)$ is the amplitude of mode number n of rotating stall and $r_n(\xi)$, $n = 1 \ldots N(\mu)$ are unknown phase angles. The residue R_n, for use in the Galerkin approximation, is defined as

$$R_n \triangleq (\tilde{\phi}'_\xi)^*_0 - (\tilde{\phi}'_\xi)_0, \tag{4.60}$$

and using (4.49) and (4.59), R_n can be calculated as

$$\begin{aligned} R_n \;=\; & \frac{W}{n}\left(\frac{dA_n}{d\xi}\sin\zeta_n - A_n\frac{dr_n}{d\xi}\cos\zeta_n\right) \\ & -\frac{1}{m_B(B)}\left\{\Psi(\xi) + l_c(B)\frac{d\Phi}{d\xi} + l_E\frac{U_d\Gamma\Lambda_1}{b}\Phi - \Psi_c\left(\Phi + WA_n(\xi)\sin\zeta_n\right)\right. \\ & +\frac{U_d\Gamma\Lambda_1(m-1)W}{bn}A_n(\xi)\sin\zeta_n + \frac{W}{2a}\left(2\left(\frac{dA_n}{d\xi}\sin\zeta_n - A_n\frac{dr_n}{d\xi}\cos\zeta_n\right)\right. \\ & \left.\left.+\frac{Un}{U_d}A_n(\xi)\cos\zeta_n + \mu n^2A_n(\xi)\sin\zeta_n\right)\right\}, \end{aligned} \tag{4.61}$$

where

$$\zeta_n \triangleq n\theta - r_n(\xi). \tag{4.62}$$

The Galerkin approximation is calculated using the weight functions

$$h_1 = 1,\ h_2 = \sin\zeta_n,\ h_3 = \cos\zeta_n \tag{4.63}$$

and the inner product

$$\langle R_n, h_i \rangle = \frac{1}{2\pi} \int_0^{2\pi} R_n(\zeta) h_i(\zeta) d\zeta. \tag{4.64}$$

Calculating the moments

$$M_i = \langle R_n, h_i \rangle \text{ for } i = 1, 2, 3 \tag{4.65}$$

results in

$$\begin{aligned}
M_1 &= \frac{1}{2\pi} \left(\Psi(\xi) + l_c(B) \frac{d\Phi}{d\xi} + l_E \frac{U_d \Gamma \Lambda_1}{b} \Phi(\xi) \right. \\
&\quad \left. + \int_0^{2\pi} \Psi_c \left(\Phi + W A_n(\xi) \sin \zeta_n \right) d\zeta_n \right) \\
M_2 &= \frac{1}{2\pi} \left(\frac{U_d \Gamma \Lambda_1 (m-1)}{bn} A_n(\xi) + \frac{\mu n^2}{2Wa} A_n(\xi) \right. \\
&\quad + \frac{dA_n}{d\xi} \left(\frac{1}{a} - \frac{m_B(B)}{n} \right) \\
&\quad \left. + \int_0^{2\pi} \Psi_c \left(\Phi + W A_n(\xi) \sin \zeta_n \right) \sin \zeta_n d\zeta_n \right) \\
M_3 &= \frac{1}{2\pi} \left(- \left(\frac{dr_n}{d\xi} \left(\frac{1}{a} - \frac{m_B(B)}{n} \right) - \frac{bBn}{2aU_d} \right) A(\xi) \right. \\
&\quad \left. + \int_0^{2\pi} \Psi_c \left(\Phi + W A_n(\xi) \sin \zeta_n \right) \cos \zeta_n d\zeta_n \right)
\end{aligned} \tag{4.66}$$

It is recognized that, due to $\Psi_c(\phi)$ being even in ϕ, the last term in M_3 vanishes. Demanding $M_3 = 0$ and assuming $A_n \neq 0$ the phase angles r_n must satisfy

$$\frac{dr_n}{d\xi} = \frac{\frac{n}{2} \frac{b}{U_d}}{1 - \frac{m_B(B) a}{n}} B = \frac{n^2 b}{2U_d (n - m_B(B) a)} B. \tag{4.67}$$

Notice that time varying B implies that the phase angles r_n are not constant, which was the case in the constant speed, first harmonic model of Moore and Greitzer (1986) and the constant speed, higher order models of Adomatis and Abed (1993) and Gu *et al.* (1996).

4.3.8 Final Model

By evaluating the integrals in (4.66) using (4.57), demanding $M_1 = M_2 = 0$, and using (4.11)and (4.56) the following model for the compression system is found:

$$\begin{aligned}
\frac{d\Phi}{d\xi} &= \frac{H}{l_c(B)}\left(-\frac{\Psi-\psi_{c0}}{H}+1+\frac{3}{2}(\frac{\Phi}{W}-1)(1-\frac{J}{2})\right.\\
&\quad \left.-\frac{1}{2}(\frac{\Phi}{W}-1)^3-\frac{l_E U_d \Gamma \Lambda_1}{bH}\Phi\right) \qquad (4.68)\\
\frac{d\Psi}{d\xi} &= \frac{\Lambda_2}{B}(\Phi-\Phi_T)-2\Lambda_1\Gamma B\Psi \qquad (4.69)\\
\frac{dJ_n}{d\xi} &= J_n\left(1-(\frac{\Phi}{W}-1)^2-\frac{J_n}{4}-\frac{\mu n^2 W}{3aH}\right.\\
&\quad \left.-\frac{2U_d\Gamma\Lambda_1(m-1)W}{3bHn}\right)\frac{3aHn}{(n-m_B(B)a)W} \qquad (4.70)\\
\frac{dB}{d\xi} &= \Lambda_1\Gamma B^2 \qquad (4.71)
\end{aligned}$$

where $n = 1 \ldots N(\mu)$, J_n is defined as the square of the stall amplitude A_n

$$J_n(\xi) \triangleq A_n^2(\xi). \qquad (4.72)$$

and

$$J(\xi) \triangleq \frac{1}{N(\mu)}\sum_{n=1}^{N}(\mu)J_n(\xi). \qquad (4.73)$$

The model (4.68)-(4.71) is in the desired form of (4.1).

In the case of pure rotating stall, $\frac{dJ_n}{d\xi} = 0$ and $\Gamma = 0$, the equilibrium values of J_n is found from (4.70) to be

$$J_{ne} = 4\left(1-\left(\frac{\Phi}{W}-1\right)^2-\mu\frac{n^2W}{3aH}\right), \qquad (4.74)$$

which corresponds to the result by Gu *et al.* (1996).

If the Galerkin approximation is carried out with only one term in the Fourier expansion of $\tilde{\phi}'$ and assuming $\mu = 0$, as was done in Gravdahl and Egeland (1997*a*), equation (4.70) is changed to

$$\frac{dJ_1}{d\xi} = J_1\left(1-(\frac{\Phi}{W}-1)^2-\frac{J_1}{4}-\frac{2U_d\Gamma\Lambda_1(m-1)W}{3bH}\right)\frac{3aH}{(1-m_B(B)a)W}. \qquad (4.75)$$

The rest of the model is left unchanged, and the model is similar to that of Moore and Greitzer except for time varying B.

It should be noted that the model developed in this chapter also can be reduced to other well known compression system models. This is summed up in table 4.2.

Changes made to (4.68)-(4.71)	Redefine nondim. time acc. to	Gives the model of
$U = U_d$, $\Gamma = 0$ $J \equiv 0$, $\frac{dB}{d\xi} = 0$ $N = 1$, $\mu = 0$	$\xi := \frac{Ut}{R}$	Greitzer (1976*a*)
$\Gamma = 0$ $\frac{dB}{d\xi} = 0$, $U = U_d$ $N = 1$, $\mu = 0$	$\xi := \frac{Ut}{R}$	Moore and Greitzer (1986)
$J \equiv 0$ $N = 1$, $\mu = 0$	$\xi := t\omega_H$	Fink *et al.* (1992) (Centrifugal)
$N = 1$, $\mu = 0$	–	Gravdahl and Egeland (1997*a*)
$U = U_d$, $\Gamma = 0$ $\frac{dB}{d\xi} = 0$ $m = \lambda tanh(nl_I)$	$\xi := \frac{Ut}{R}$	Gu *et al.* (1996)
$U = U_d$, $\Gamma = 0$ $\frac{dB}{d\xi} = 0$	$\xi := \frac{Ut}{R}$	Adomatis and Abed (1993)

Table 4.2: *In this table it is shown how the model derived in this chapter can be reduced to other known models form the literature.* ω_H *is the Helmholtz frequency defined as* $\omega_H = a_s \left(\frac{A_c}{L_c V_p}\right)^{\frac{1}{2}}$.

4.4 Simulations

Here some simulations of the model developed in this chapter will be presented. For speed control, a simple P-type controller of the form

$$\Gamma_t = c_{speed}(U_d - U), \tag{4.76}$$

will be used. The nondimensional drive torque Γ_t is used as the control, and feedback from compressor speed U is assumed. In Gravdahl and Egeland (1997*g*) compressor speed was controlled in a similar manner, and stability was proven using Lyapunov's theorem. The desired speed was set to $U_d = 215\text{m/s}$ in both the following simulations. Numerical values for the parameters in the model are given in Appendix D.

4.4.1 Unstable Equilibrium, $\gamma = 0.5$

In Figure 4.2 the response of the model (4.68)-(4.71) with speed control (4.76) and $c_{speed} = 1$ is shown. Only the first harmonic J_1 of rotating stall is included in this simulation. Initial values were chosen as

$$(\Phi,\ \Psi,\ J_1,\ B)_0 = (0.55,\ 0.65,\ 0.1,\ 0.1), \tag{4.77}$$

such that the (Φ, Ψ)-trajectory starts on the stable part of the compressor characteristic as can be seen in Figure 4.3.

The throttle gain was set at $\gamma = 0.5$ so that the equilibrium is to the left of the local maximum of the characteristic. As can be seen from Figure 4.2, the compressor goes into rotating stall as B (and thus compressor speed U) is low. Moreover, when the applied torque from the speed controller cause B to increase, the stall amplitude J falls off and the compressor goes into surge. This is what could be expected according to Greitzer and Moore (1986). The surge oscillations have a period of $\xi \approx 180$, which correspond to a surge frequency of about 10Hz. A desired speed of $U_d = 215m/s$ corresponds to a desired B-parameter of $B_d = U_d/b = 2.23$. After $\xi \approx 1500$ this value is reached. As the compressor torque Γ_c varies with ϕ, see equation (4.18), we would expect oscillations in speed U as the compressor is in surge. This is confirmed by the lower right plot in Figure 4.2. In the upper plot of Figure 4.3, the trajectory starts on the stable part of the characteristic, then rotating stall occurs and the trajectory approaches the intersection of the throttle and in-stall characteristics. As B increases the resulting surge oscillations are clearly visible.

Now, the model is simulated using $N = 3$, that is three harmonics. Initial values were chosen as

$$(\Phi,\ \Psi,\ B,\ J_1,\ J_2,\ J_3)_0 = (0.55,\ 0.65,\ 0.1,\ 0.1,\ 0.05,\ 0.01). \tag{4.78}$$

The upper plot in Figure 4.4 shows the response of the three first harmonics of the squared amplitude of rotating stall J_1, J_2 and J_3. The response is otherwise similar to that of Figure 4.2. The lower plot is a magnified version of the 200 first time units of the upper plot, and shows that during stall inception the second harmonic J_2 dominates the first harmonic J_1. This emphasizes the importance of using higher order approximations of the Moore-Greitzer model. This phenomenon was also observed by Mansoux *et al.* (1994) for constant speed compressors.

The previous simulations have both used a desired speed of $U_d = 215m/s$ resulting in a high B-parameter and driving the compressor into surge. Now, the desired speed is changed to $U_d = 75m/s$ which corresponds to a B-parameter of 0.78. This is sufficiently low for the compressor studied here to become stuck in rotating stall. The simulation is shown in Figure 4.5 using three harmonics of the squared amplitude of rotating stall. The first harmonic J_1 has the highest equilibrium value. This equilibrium value decreases with mode number n due to the effect of viscosity, as stated in equation (4.74).

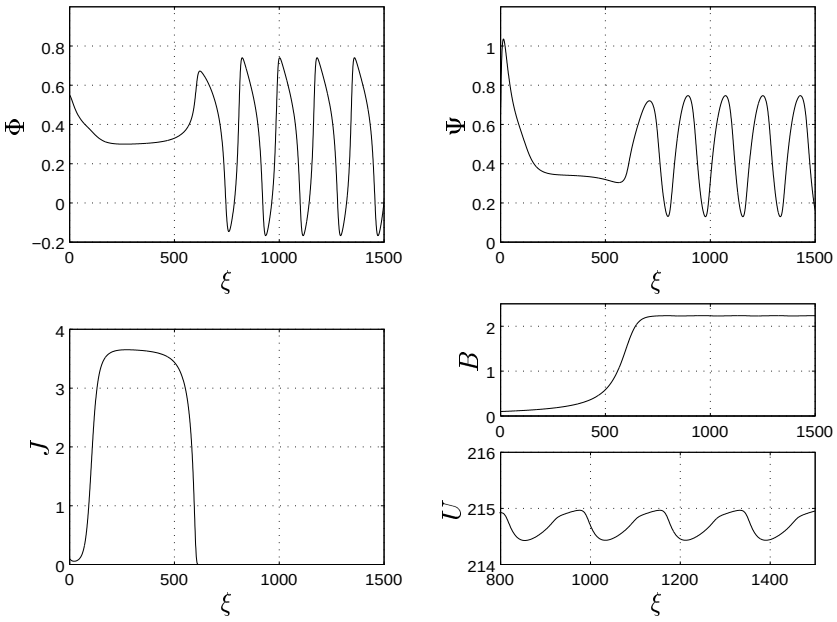

Figure 4.2: *Simulation of the system (4.68)-(4.71). Low B leads to rotating stall, and high B leads to surge.*

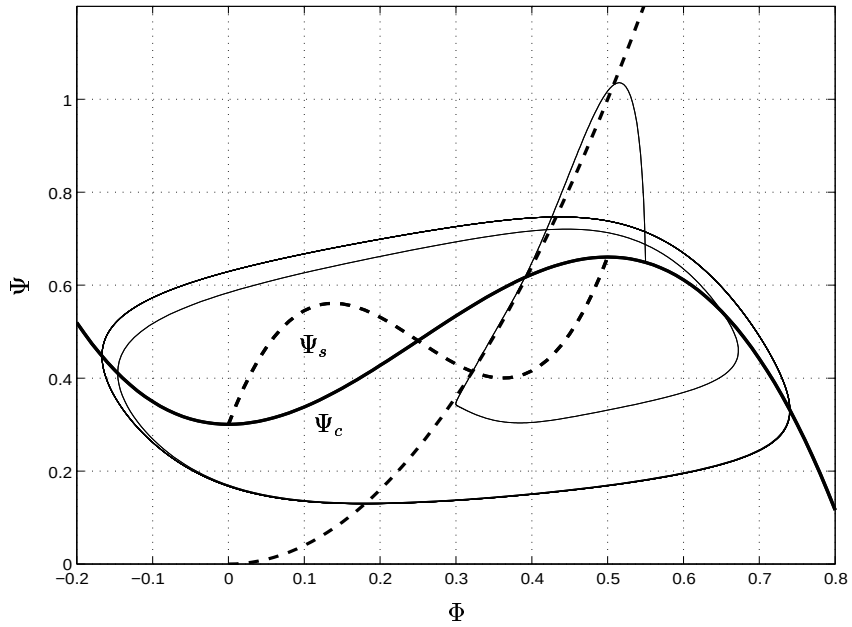

Figure 4.3: *Simulations result superimposed on the compression system characteristics. The compressor characteristic, the in-stall characteristic and the throttle characteristic are drawn with solid, dashed and dash-dot lines respectively.*

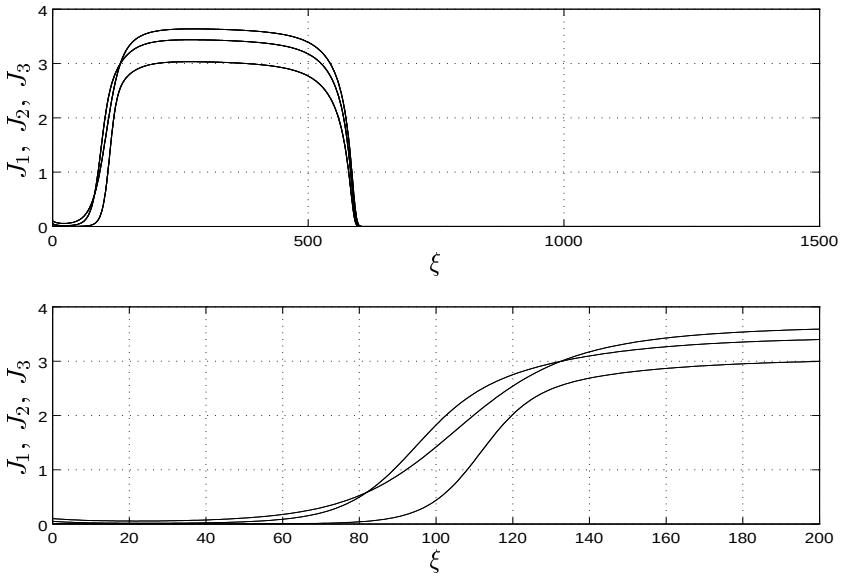

Figure 4.4: *The three first harmonics of rotating stall. The first harmonic J_1 has the highest maximum value. This maximum value decreases with mode number du to the effect of viscosity. The lower plot shows that J_2 dominates J_1 during stall inception.*

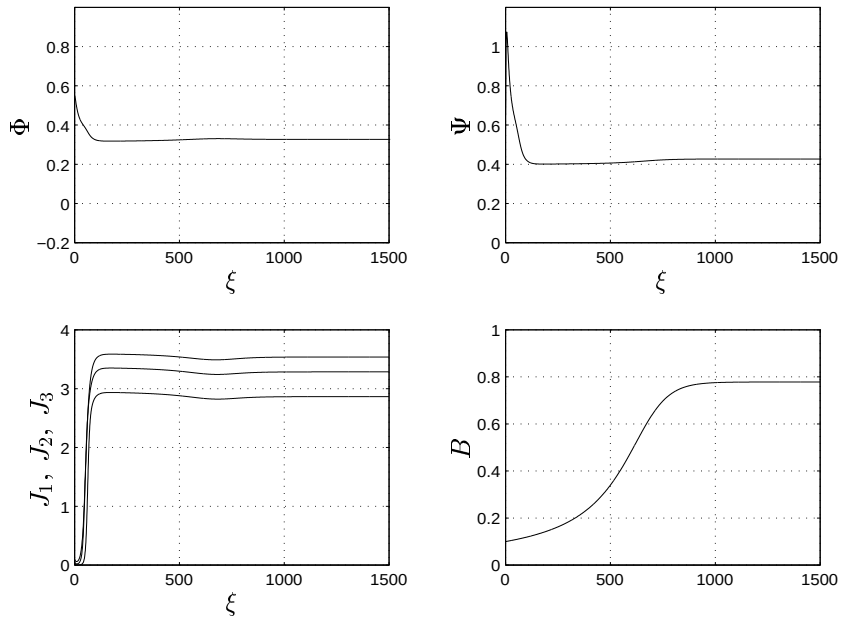

Figure 4.5: *System response with low U_d, resulting in the compressor being stuck in rotating stall.*

4.4.2 Stable Equilibrium $\gamma = 0.65$

In Figure 4.6, the impact of the spool dynamics on a stable equilibrium of the compression system is illustrated. Only J_1 is used in this simulation, and the initial values in (4.77) were used. Similar plots can be produced including higher harmonics. The throttle gain was set at $\gamma = 0.65$, giving a stable equilibrium, and the speed controller gain was again chosen as $c_{speed} = 1$. The solid trajectories show the system response to a speed change from $U = 0.05m/s$ to $U = 215m/s$. It can be seen that the acceleration of U affects the other states of the model. This is due to the couplings with speed U and torque Γ in the model. Of special interest here, is the stall amplitude. The initial value of $J(0) = 0.05$ grows to nearly fully developed rotating stall as the machine is accelerating, but is quickly damped out as desired speed is reached. Simulations show that this stalling can be avoided by accelerating the compressor at a lower rate, that is by using a smaller c_{speed}. This could possibly also be achieved with other, more advanced speed controllers, and is a topic for further research.

In contrast, the dashed trajectories in Figure 4.6 show the response without the spool dynamics. Now, the initial value $J(0) = 0.05$ is damped out very quickly, and Φ and Ψ converges to their equilibrium values. The transient effects observed are due to the initial conditions.

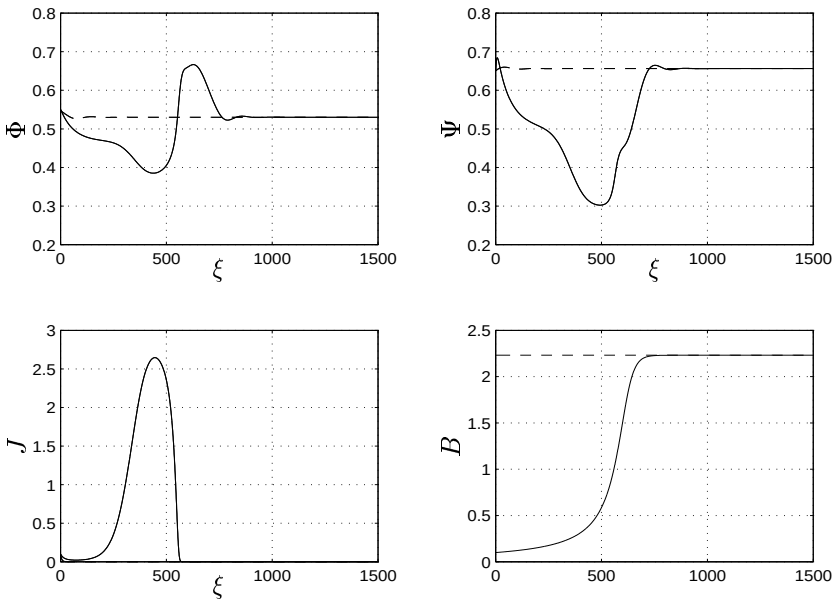

Figure 4.6: *Stable equilibrium with and without B-dynamics*

4.5 Concluding Remarks

In this chapter, a multi mode Moore-Greitzer axial compressor model with spool dynamics was derived. This resulted in a model with time varying B-parameter. Through simulations it was demonstrated that the model was capable of demonstrating both rotating stall and surge, and that the type of instability depended on the compressor speed. Compressor speed was controlled with a simple proportional control law. In the original Moore Greitzer model only the first mode of rotating stall is included. The simulations in this chapter show that during stall inception, higher order modes can dominate the first mode. This is in accordance with known results, and is shown here to be valid also for variable speed compressors.

Further work on this topic includes 1) Stability analysis and stall/surge control design for variable speed axial compressors and 2) The use of simultaneous speed control and stall/surge control to achieve rapid acceleration without stalling the compressor.

Chapter 5

Modelling and Control of Surge for a Centrifugal Compressor with Non-constant Speed

5.1 Introduction

In this chapter the compressor characteristic for a variable speed centrifugal compressor is investigated. This characteristic is incooperated in a model similar to that of Fink *et al.* (1992), and surge phenomena is studied in connection with varying compressor speed. Energy losses in the compressor components is used to derive the characteristic, making a departure from the usual cubic characteristic most commonly encountered in the surge control literature. Inspired by Ferguson (1963) and Watson and Janota (1982), fluid friction and incidence losses, as well as other losses, in the compressor components are modeled, and a variable speed compressor characteristic is developed based on this. Both annular and vaned diffusers are studied. Surge and speed controllers for variable speed centrifugal compressors are presented and analyzed. The speed is controlled with a PI-control law.

Axial and centrifugal compressors mostly show similar flow instabilities, but in centrifugal compressors, the matching between components, such as impeller and diffuser, influences the stability properties. According to Emmons *et al.* (1955), de Jager (1995) and others, rotating stall is believed to have little effect on centrifugal compressor performance. The modeling and analysis in this chapter is thus restricted to surge. Hansen *et al.* (1981) showed that the model of Greitzer (1976*a*) is also applicable to centrifugal compressors, and this model will also be used here.

Since compressors are variable speed machines, it is of interest to investigate the

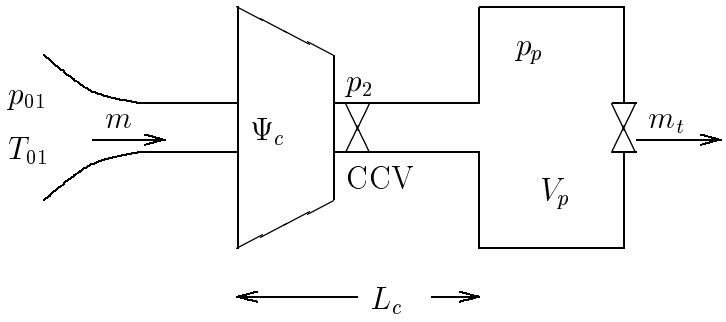

Figure 5.1: *Compression system with CCV.*

influence of speed transients on the surge dynamics. Models describing this interaction was developed in Eveker and Nett (1991) for axial compressors and in Fink *et al.* (1992) for centrifugal compressors. As surge can occur during acceleration of the compressor speed, it is of major concern to develop controllers that simultaneously can control both surge and compressor speed.

For surge control, the CCV is again employed. Semi-global exponential stability results for the proposed controllers are given using Lyapunovs method. The results are confirmed through simulations.

5.2 Model

We are considering a compression system consisting of a centrifugal compressor, close coupled valve, compressor duct, plenum volume and a throttle. The throttle can be regarded as a simplified model of a turbine. The system is showed in figure 5.1. The model to be used for controller design is in the form

$$\begin{aligned} \dot{p}_p &= \frac{a_{01}^2}{V_p}(m - m_t) \\ \dot{m} &= \frac{A_1}{L_c}(p_2 - p_p) \\ \dot{\omega} &= \frac{1}{I}(\tau_t - \tau_c), \end{aligned} \tag{5.1}$$

where m is the compressor mass flow, p_p is the plenum pressure, p_2 is the pressure downstream of the compressor, a_{01} is the inlet stagnation sonic velocity, L_c is the length of compressor and duct, A_1 is the area of the impeller eye (used as reference area), I is the spool moment of inertia, τ_t is the drive torque and τ_c is the compressor torque. The two first equations of (5.1) are equivalent to the model of Greitzer (1976*a*) which was also used in Chapter 2 and 3, whereas the whole model (5.1) is similar to the model of Fink *et al.* (1992). In addition to the assumptions used in the derivation of model of Greitzer (1976*a*), it is now

assumed that the gas angular momentum in the compressor passages is negligible compared to rotor angular momentum. Note that in the model used throughout this chapter, the states are *with* dimension, as opposed to the previous chapters, where nondimensional states were used.

The angular speed of the compressor ω is included as a state in addition to mass flow and pressure rise which are the states in Greitzer's surge model. The equation for $\dot{p}_p$ follows from the mass balance in the plenum, assuming the plenum process isentropic, the derivation is shown in Appendix B. The equation for $\dot{m}$ follows from the impulse balance in the duct. In the following, the model (5.1) will be developed in detail. In particular, expressions must be found for the terms p_2 and τ_c. It will also be shown that an expression for the compressor characteristic results from this derivation.

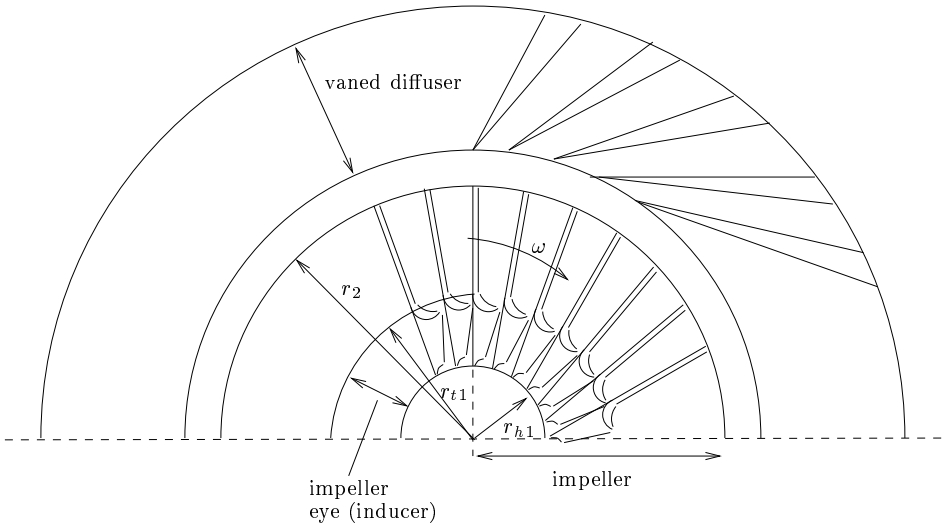

Figure 5.2: *Diagrammatic sketch of a radially vaned centrifugal compressor. Shown here with a vaned diffuser.*

The calculation of the compressor pressure rise will be based on energy transfer and energy losses in the various parts of the compressor. In the following sections, the different components of the centrifugal compressor will be studied. The centrifugal compressor consists essentially of a rotating impeller which imparts a high velocity to the gas, and a number of fixed diverging passages in which the gas is decelerated with a consequent rise in static pressure. A schematic drawing of a compressor is shown in Figure 5.2. The innermost part of the impeller is known as the inducer, or the impeller eye, where the gas is sucked into the compressor. The part of the compressor containing the diverging passages is known as the diffuser. The diffuser can be vaned, as in Figure 5.2, or vaneless. A vaneless diffuser (also known as an annular diffuser) is a simple annular channel with increasing area. The choice of diffuser type depends on the application of the compressor. After leaving the

diffuser, the gas may be collected in a volute (also known as a scroll), as shown in Figure 5.3.

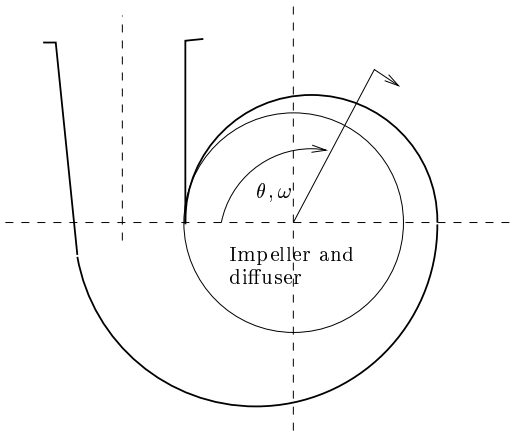

Figure 5.3: *Diagrammatic sketch of centrifugal compressor fitted with a volute.*

The energy transfer *to* the gas takes place in the impeller. In the ideal case, this energy is converted into a pressure rise. However, a number of losses occur in the compressor, the main ones being friction losses and incidence losses in the impeller and the diffuser. These losses shape the compressor characteristic, and the incidence losses are the cause of the positive slope of the characteristic, which in turn determines the area of the compressor characteristic where surge occurs. Therefore, these components will be studied in detail in the following. A number of other losses, e.g. losses in the volute, are taken into account as drops in efficiency.

5.2.1 Impeller

Incoming gas (air) enters the impeller eye (the inducer) of the compressor with velocity C_1, see Figure 5.4. The mass flow m and C_1 is given by

$$C_1 = \frac{1}{\rho_{01} A_1} m, \tag{5.2}$$

where ρ_{01} is the constant stagnation inlet density. The tangential velocity U_1, at diameter D_1, of the inducer is calculated as

$$U_1 = \frac{D_1}{2}\omega = D_1 \pi N, \tag{5.3}$$

where ω is the angular velocity of the impeller and N is the number of revolutions per second. The average diameter D_1 is defined according to

$$D_1^2 = \frac{1}{2}(D_{t1}^2 + D_{h_1}^2), \tag{5.4}$$

where D_{t1} and D_{h_1} are the diameters at inducer tip and hub casing respectively. The circle with diameter D_1 and area A_1 divides the inducer in two annuli of equal area.

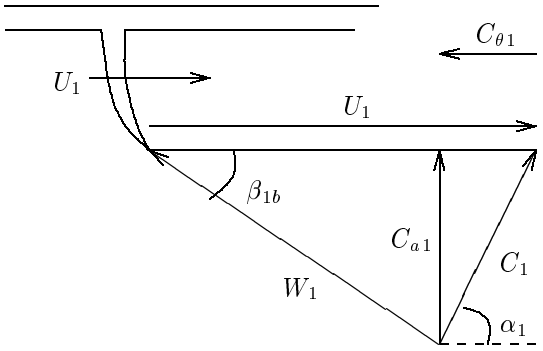

Figure 5.4: *Velocity triangle at inducer. Section through inducer at radius* $r_1 = D_1/2$.

From Figure 5.4 it is seen that the gas velocity W_1 relative to the impeller is

$$W_1^2 = C_1^2 + U_1^2 - 2U_1C_{\theta 1}. \tag{5.5}$$

The gas leaves the impeller at the impeller tip with velocity C_2 as shown in Figure 5.5. The diameter at the impeller tip is D_2 and the tangential tip velocity is U_2.

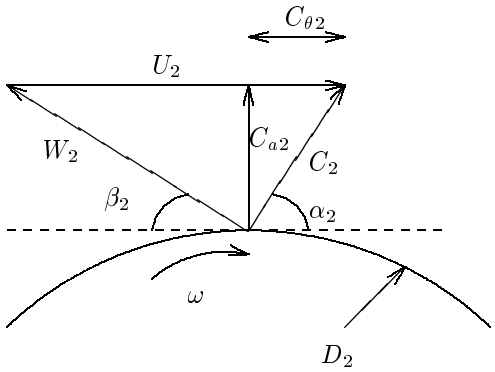

Figure 5.5: *Velocity triangle at impeller tip.*

5.2.2 Diffuser

Centrifugal compressors are usually fitted with either a vaneless (annular) or a vaned diffuser. The influence of the diffuser upon compressor performance cannot be over emphasized, as a considerable proportion of the fluid energy at the impeller tip is kinetic energy and its efficient transformation into static pressure is important Ferguson (1963).

Annular Diffuser

The annular diffuser is a simple annular channel in which the fluid loses velocity and gains static pressure. One disadvantage of the annular diffuser is its size, as its outlet radius must be twice its inlet radius if the velocity is to be halved in it Ferguson (1963). Its advantages are its price and wide range of operation.

Vaned Diffuser

In a vaned diffuser, vanes are used to guide the flow so that he overall rate of diffusion is higher than in an annular diffuser. This leads to a smaller size, but higher production costs. The vaned diffuser has a higher efficiency but less mass flow range than the annular diffuser. This is due to stalling of the diffuser vanes for low mass flows.

5.3 Energy Transfer, Compressor Torque and Efficiency

5.3.1 Ideal Energy Transfer

For turbomachines, applied torque equals the change in angular momentum of the fluid:

$$\tau_c = m(r_2 C_{\theta 2} - r_1 C_{\theta 1}), \tag{5.6}$$

where τ_c is the compressor torque, $r_1 = \frac{D_1}{2}$, $r_2 = \frac{D_2}{2}$ and $C_{\theta 2}$ is the tangential component of the gas velocity C_2. Power delivered to the fluid is

$$\begin{aligned} \dot{W}_c &= \omega \tau_c = \omega m(r_2 C_{\theta 2} - r_1 C_{\theta 1}) \\ &= m(U_2 C_{\theta 2} -_1 C_{\theta 1}) = m\Delta h_{0c,ideal} \end{aligned} \tag{5.7}$$

where $\Delta h_{0c,ideal}$ is the specific enthalpy delivered to the fluid without taking account for losses. Equation (5.7) is known as Euler's pump equation. For simplicity the following two assumptions are made:

1. A radially vaned (no backsweep) impeller is considered with $\beta_{2b} = 90°$, and
2. There is no pre-whirl, that is $\alpha_1 = 90° \Rightarrow C_{\theta 1} = 0$.

The slip factor is defined as

$$\sigma \triangleq \frac{C_{\theta 2}}{U_2} \approx 1 - \frac{2}{i}. \tag{5.8}$$

The approximation is known as Stanitz' formula where i is the number of compressor blades. From (5.7), and using (5.8), we have that the ideal specific enthalpy delivered to the fluid is

$$\Delta h_{0c,ideal} = \frac{\dot{W}_{c,ideal}}{m} = \sigma U_2^2. \tag{5.9}$$

Notice that $\Delta h_{0c,ideal}$ is independent of mass flow m, and ideally we would have the same energy transfer for all mass flows[1]. However, due to various losses, the energy transfer is not constant, and we now include this in the analysis. According to Watson and Janota (1982), Ferguson (1963), Nisenfeld (1982) and other authors, the two major losses, expressed as specific enthalpies, are:

1. Incidence losses in impeller and diffuser, Δh_{ii} and Δh_{id}
2. Fluid friction losses in impeller and diffuser, Δh_{fi} and Δh_{fd}

The incidence losses and fluid friction losses play an important role in determining the region of stable operation for the compressor. Other losses, such as back flow losses, clearance losses and losses in the volute will be taken into account when computing the efficiency of the compressor. There also exist other losses such as inlet casing losses, mixing losses and leakage losses, but these will be ignored in the following. For a further treatment on this topic, some references are Baljé (1952), Johnston and Dean, Jr. (1966), Whitfield and Wallace (1975) and Cumpsty (1989).

5.3.2 Compressor Torque

Using the assumption of no pre whirl and equation (5.6), the compressor torque is

$$\tau_c^+ = m r_2 C_{\theta 2} = m r_2 \sigma U_2, \; m > 0. \tag{5.10}$$

The torque calculated in (5.10) is for forward flow. However, the compressor may enter deep surge, that is reversal of flow, and there is need for an expression for the compressor torque at negative mass flow. According to Koff and Greitzer (1986), an axial compressor in reversed flow can be viewed as a throttling device. Here it is assumed that a centrifugal compressor in reversed flow can be approximated with a turbine. This allows for the use of Euler's turbine equation:

$$\tau_c^- = m(r_1 C_{\theta 1} - r_2 C_{\theta 2}) = -m r_2 \sigma U_2, \; m < 0. \tag{5.11}$$

Combination of (5.10) and (5.11) gives

$$\tau_c = |m| r_2 \sigma U_2, \; \forall m \tag{5.12}$$

which is in accordance with the compressor torque used by Fink *et al.* (1992).

[1] If backswept impeller blades, $\beta_{2b} < 90^\circ$, were considered, $\Delta h_{0c,ideal}$ would decrease with increasing m.

Disc Friction Torque

The torque set up by the rotation of the impeller in a fluid is modeled as rotation of a disc. When a disc is rotated in a fluid, a resistive torque is set up given by

$$\tau_{df} = 2\int_{r_1}^{r_2} \tau_{tan} 2\pi r^2 dr, \tag{5.13}$$

where r_1 is the radius of the shaft, r_2 is the radius of the disc and τ_{tan} is the tangential component of the shear stress between the disc and fluid. According to Ferguson (1963) the torque can be approximated by

$$\tau_{df} = \frac{C_m \rho r_2^5 \omega^2}{2} = \frac{2C_m \rho r_2^5}{D_1^2} U_1^2 \tag{5.14}$$

where C_m is a torque coefficient depending on the disc Reynolds number and the space between the disc and the casing, ρ is the density of the fluid and ω is the angular velocity of the disc. In (5.14) it has been assumed that $r_1 << r_2$.

5.3.3 Incidence Losses

The losses due to incidence onto the rotor and vaned diffuser play an important role in shaping the compressor characteristic. There exists several methods of modeling this loss, and a comparative study is given by Whitfield and Wallace (1973). The two most widely used approaches are:

(1) The so called "NASA shock loss theory" reported in Watson and Janota (1982) and Whitfield and Wallace (1973), which is based upon the tangential component of kinetic energy being destroyed.

(2) A constant pressure incidence model reported by Whitfield and Wallace (1973) where it is assumed that the flow just inside the blades has adapted to the blades via a constant pressure process.

Watson and Janota (1982) concludes that for centrifugal compressors, the differences between the two models are small. According to Whitfield and Wallace (1973), the main difference lies in the prediction of the incidence angle at which zero loss occurs. For model (1) zero loss is predicted when the flow angle at the inlet equals the blade angle. This is not the case for model (2). Based on this, and the simplicity of (1), the NASA shock loss theory is used here. As Ferguson (1963) points out, the term shock loss is misleading as nothing akin to shock occurs in practice, but the simple notion of shock is used to explain the shape of the compressor characteristic.

Depending on whether the mass flow is lower or higher than the design flow, positive or negative stall is said to occur. The use of model (2) leads to a loss varying with the square of the mass flow, symmetrical about the design flow. Ferguson (1963) states that the incidence loss in practice increase more rapidly

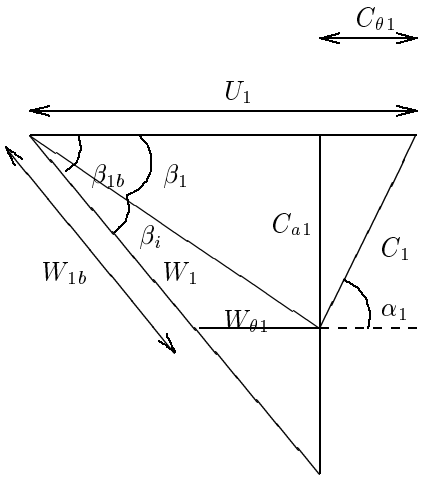

Figure 5.6: *Incidence angles at inducer.*

with reduction of flow below design flow, than with increase of flow above the design flow. This leads to a steeper compressor characteristic below the design point than above. According to Sepulchre and Kokotović (1996) and Wang and Krstić (1997*b*), such a characteristic is said to be right skew.

Impeller

The velocity of the incoming gas relative to the inducer is denoted W_1. In off-design operation there will be a mismatch between the *fixed* blade angle β_{1b} and the direction of the gas stream $\beta_1 = \beta_1(U_1, C_1)$, as shown in Figure 5.6. The angle of incidence is defined by

$$\beta_i \triangleq \beta_{1b} - \beta_1. \tag{5.15}$$

As the gas hits the inducer, its velocity instantaneously changes its direction to comply with the blade inlet angle β_{1b}. The direction is changed from β_1 to β_{1b}, and the kinetic energy associated with the tangential component $W_{\theta 1}$ of the velocity is lost. That is, the incidence loss can be expressed as

$$\Delta h_i = \frac{W_{\theta 1}^2}{2}. \tag{5.16}$$

From Figure 5.6 it is easily seen that

$$\cos\beta_1 = \frac{U_1 - C_{\theta 1}}{W_1} \quad \text{and} \quad \sin\beta_1 = \frac{C_{a1}}{W_1}. \tag{5.17}$$

Furthermore,

$$W_{\theta 1} = \frac{\sin(\beta_{1b} - \beta_1)}{\sin\beta_{1b}} W_1 = (\cos\beta_1 - \cot\beta_{1b}\sin\beta_1)\, W_1. \tag{5.18}$$

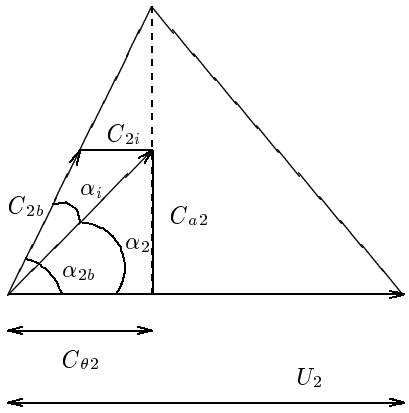

Figure 5.7: *Incidence angles at diffuser.*

Inserting (5.17) in (5.18) gives

$$W_{\theta 1} = U_1 - C_{\theta 1} - \cot \beta_{1b} C_{a1}. \tag{5.19}$$

and the incidence loss (5.16) can be written

$$\Delta h_i = \frac{1}{2} \left(U_1 - C_{\theta 1} - \cot \beta_{1b} C_{a1} \right)^2 = \frac{1}{2} \left(U_1 - \frac{\cot \beta_{1b} m}{\rho_{01} A_1} \right)^2 \tag{5.20}$$

where the second equality if found using (5.2). Similar results are presented in Chapter 5 in Ferguson (1963).

Diffuser

According to Watson and Janota (1982), the losses in the vaned diffuser can be modeled with friction/incidence losses in a similar manner as in the impeller. Similar to the inducer incidence loss, it is assumed that the velocity of the fluid entering the diffuser is instantaneously changed to comply with the fixed diffuser inlet angle α_{2b}. The direction is changed from α_2 to α_{2b}, and the kinetic energy associated with the tangential component C_{2i} of the velocity is lost, see Figure 5.7. That is, the incidence loss can be expressed as

$$\Delta h_{id} = \frac{C_{2i}^2}{2}. \tag{5.21}$$

Using Figure 5.7 it is seen that

$$\begin{aligned} \Delta h_{id} &= \frac{1}{2} \left(C_{\theta 2} - \cot \alpha_{2b} C_{a2} \right)^2 \\ &= \frac{1}{2} \left(\sigma U_2 - \cot \alpha_{2b} C_{a2} \right)^2. \end{aligned} \tag{5.22}$$

For simplicity the choice[2] $C_{a1} = C_{a2}$ is made. The diffuser inlet angle α_{2b}, is now designed such that there is minimum incidence loss in both impeller and diffuser for the same mass flow m. For $\beta_i = 0$, we have that

$$U_1 = C_{a1} \cot \beta_{1b} \quad \Rightarrow \quad C_{a2} = U_1 \tan \beta_{1b}. \tag{5.23}$$

From Figure 5.7 and (5.23), it follows that

$$\tan \alpha_{2b} = \frac{C_{a2}}{C_{\theta 2}} = \frac{U_1 \tan \beta_{1b}}{\sigma U_2} \tag{5.24}$$

and

$$\alpha_{2b} = \operatorname{atan}\left(\frac{D_1 \tan \beta_{1b}}{\sigma D_2}\right), \tag{5.25}$$

and consequently the diffuser incidence loss (5.22) can be written

$$\Delta h_{id} = \frac{1}{2}\left(\frac{\sigma D_2 U_1}{D_1} - \frac{m \cot \alpha_{2b}}{\rho_{01} A_1}\right). \tag{5.26}$$

5.3.4 Frictional Losses

Impeller

According to Ferguson (1963) loss due to friction can be calculated as

$$\Delta h_{fi} = C_h \frac{l}{D} \frac{W_{1b}^2}{2}, \tag{5.27}$$

where C_h is the surface friction loss coefficient[3] , l is the mean channel length and D is the mean hydraulic channel diameter. This friction loss is actually calculated for constant area pipes of circular cross section. The friction loss coefficient C_h is defined as in Watson and Janota (1982):

$$C_h = 4f, \tag{5.28}$$

where the friction factor f depends on the Reynolds number. Many different formulas for the friction factor have been published, see e.g. Ferguson (1963) or White (1986). Here we will use Blasius' formula:

$$f = 0.3164(Re)^{-0.25}. \tag{5.29}$$

According to White (1986), (5.29) was found empirically for turbulent flow in smooth pipes with Reynolds number Re below 100.000. The mean hydraulic channel diameter D is defined as

$$D = \frac{4A}{a}, \tag{5.30}$$

[2] This is a design choice, and other choices will lead to different expression for the diffuser angle α_{2b}

[3] The friction loss considered here is due to friction in the impeller. According to Watson and Janota (1982) diffusion losses in the impeller are small compared to impeller friction losses, but they may be included in the analysis by choosing C_h to suit.

where the cross section area A and perimeter a are mean values for the passage. The mean hydraulic diameter D corresponds to a circle with area A and perimeter a. Although the passages between the blades in the compressor are neither circular nor of constant area, Baljé (1952) reports of good agreement between theory and measurement using (5.29).

Using Figure 5.6, it is seen that

$$\frac{W_{1b}}{\sin\beta_1} = \frac{W_1}{\sin\beta_{1b}} \tag{5.31}$$

and using $\sin\beta_1 = \frac{C_{a1}}{W_1}$ we get

$$W_{1b} = \frac{C_1}{\sin\beta_{1b}}. \tag{5.32}$$

Inserting (5.2) and (5.32) in (5.27) gives

$$\Delta h_{fi} = \frac{C_h l}{2D\rho_1^2 A_1^2 \sin^2\beta_{1b}} m^2 = k_{fi} m^2. \tag{5.33}$$

As can be seen the friction losses are quadratic in mass flow and independent of wheel speed U. Equation (5.33) represents the loss due to friction of a mass flow m through a pipe of hydraulic diameter D.

Diffuser

The loss due to fluid friction in the diffuser can be modeled in a similar manner as in the impeller:

$$\Delta h_{fd} = k_{fd} m^2. \tag{5.34}$$

In the vaned diffuser a pipe friction loss is calculated for each diffuser passage.

5.3.5 Efficiency

The isentropic efficiency of the compressor is defined as, see e.g. Cumpsty (1989) or any other text on turbomachinery,

$$\eta_i(m, U_1) = \frac{\Delta h_{0c,ideal}}{\Delta h_{0c,ideal} + \Delta h_{loss}}. \tag{5.35}$$

where the Δh_{loss}-term is the sum of the friction and incidence losses from the previous sections. Furthermore, the efficiency will be corrected with losses in the volute and the additional losses arising from clearance and back-flow. The efficiency is also dependent on the diffusers ability to convert the kinetic energy of the flow into pressure. Collection the various losses, the isentropic efficiency from equation (5.36) is adjusted to

$$\eta_i(m, U_1) = \frac{\Delta h_{0c,ideal}}{\Delta h_{0c,ideal} + \Delta h_{loss}} - \Delta\eta_{bf} - \Delta\eta_c - \Delta\eta_v - \Delta\eta_d, \tag{5.36}$$

where

$$\Delta h_{loss} = \Delta h_{if} + \Delta h_{ii} + \Delta h_{df} + \Delta h_{di}. \tag{5.37}$$

The additional losses are discussed below. In Figure 5.8, the efficiency is plotted. In the upper plot, the compressor is equipped with a vaned diffuser and in the lower plot with an annular diffuser. As can be seen, the vaned diffuser offer a higher efficiency, but a narrower range of flow compared with the annular diffuser.

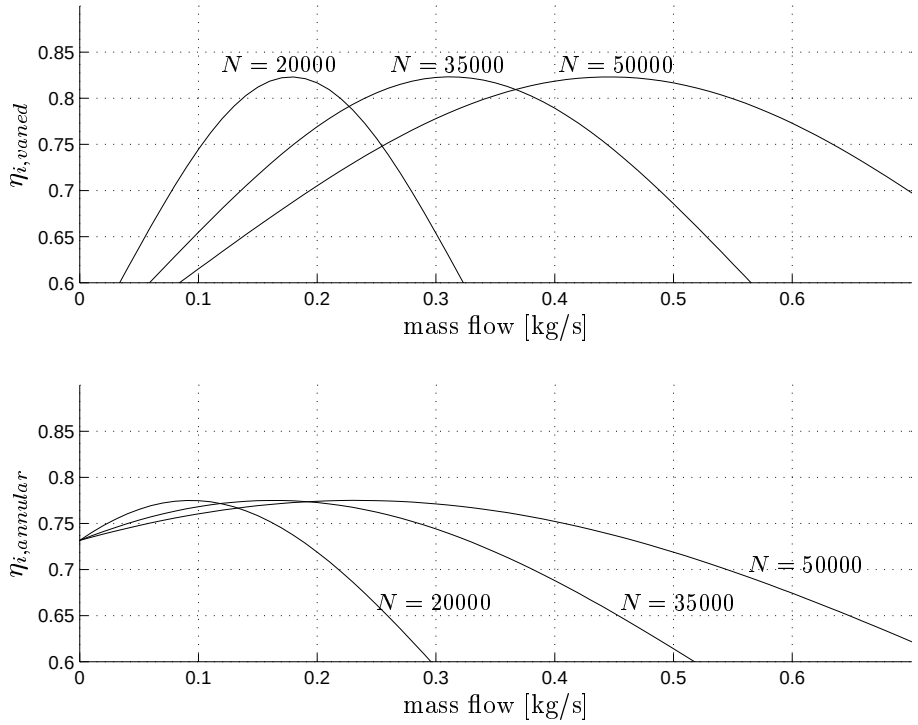

Figure 5.8: *Efficiencies for compressor with vaned (upper plot) and annular (lower plot) diffuser.*

Clearance

Pampreen (1973) found that the clearance loss of a centrifugal compressor can be approximated by

$$\Delta \eta_c = 0.3 \frac{l_{cl}}{b}, \tag{5.38}$$

where l_{cl} is the axial clearance and b is the impeller tip width.

Backflow

The back-flow loss occurs because the compressor has to reprocess the fluid that has been reinjected into the impeller due to pressure gradients existing in the

impeller tip region. Due to the lack of accurate modeling of this loss, Watson and Janota (1982) suggest a loss of 3 points of efficiency as typical:

$$\Delta\eta_{bf} = 0.03. \tag{5.39}$$

Volute

In the volute a loss will take place mainly due to the inability of the volute to use the radial kinetic energy out of the diffuser. Cumpsty (1989) assumes this loss to lie within 2-5 point of efficiency:

$$0.02 \leq \Delta\eta_v \leq 0.05. \tag{5.40}$$

This loss is likely to be higher for compressor with a vaned diffuser than with an annular diffuser, as a larger part of the total kinetic energy at the outlet of the vaned diffuser is in the radial direction. A more comprehensive treatment of loss in volutes can be found in Lorett and Gopalakrishnan (1986).

Diffusion

The purpose of the diffuser is decelerate the flow with high kinetic energy, and thus convert this into pressure. This can be achieved more or less efficient depending on the construction of the diffuser. Due to inadequate diffusion in the diffuser there will be a degradation $\Delta\eta_d$ in the efficiency η_i. The efficiency drop $\Delta\eta_d$ is dependent on the pressure recovery coefficient, see e.g. Cumpsty (1989) or Watson and Janota (1982), but for simplicity $\Delta\eta_d$ will be considered constant here. According to Watson and Janota (1982) vaned diffusers offer a 2 to 7 points increase in efficiency compared to annular diffusers.

5.4 Energy Transfer and Pressure Rise

Including the losses, the total specific energy transfer can be calculated by subtracting (5.33), (5.20), (5.26) and (5.34) from (5.9):

$$\Delta h_{0c}(U_1, m) = \Delta h_{0c,ideal} - \Delta h_{if} - \Delta h_{ii} - \Delta h_{df} - \Delta h_{di}. \tag{5.41}$$

Δh_{0c} is a second degree polynomial in m, and as opposed to the ideal case, we see that energy transfer to the fluid is varying with mass flow m. This is shown in Figure 5.9.

To find an expression for the pressure rise we now need a relation between pressure rise and energy transfer. The pressure rise is modeled as

$$p_2 = \left(1 + \frac{\eta_i(m, U_1)\Delta h_{0c,ideal}}{T_{01} c_p}\right)^{\frac{\kappa}{\kappa-1}} p_{01} = \Psi_c(U_1, m) p_{01}, \tag{5.42}$$

where the losses have been taken into account, and $\Psi_c(U_1, m)$ is the compressor characteristic. It is shown in Appendix B how to arrive at (5.42). We now have an expression for the pressure p_2 needed in the model (5.1). Notice that for each speed N, both the pressure rise (5.42) and the efficiency (5.36) reach maximum for the same value of mass flow m. Thus, the maximum efficiency is reached on the surge line, stressing the need for active control in order to be able to operate safely in the neighborhood of the surge line. The inlet stagnation temperature T_{01}, specific heat capacity c_p and κ are assumed constant. The ideal energy transfer and the losses are shown for a compressor with annular diffuser in figure 5.9. In the case of vaned diffuser, the curves look similar, but with a steeper slope due to the incidence losses at the diffuser. The curves are calculated for a compressor speed of $N = 35,000$rpm.

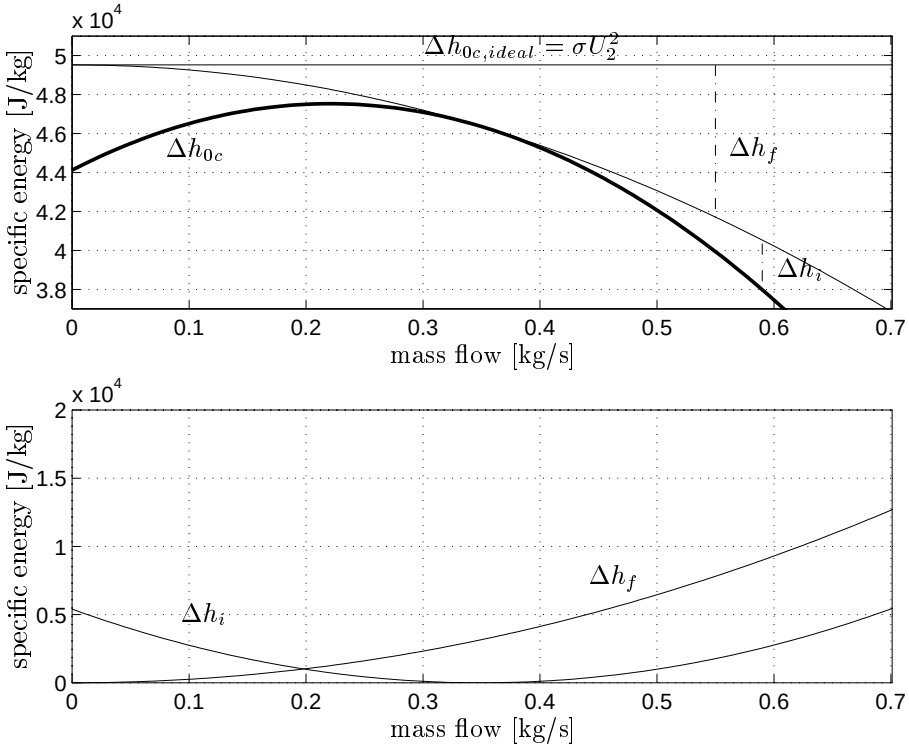

Figure 5.9: *Energy transfer for $N = 35,000$ rpm. Compressor with annular diffuser.*

The compressor pressure characteristic as calculated from equation (5.42) is showed in Figure 5.10.

In figures 5.9 and 5.10 the numerical values for the compressor parameters is taken from Fink *et al.* (1992). Comparing the compressor map in Figure 5.10 with

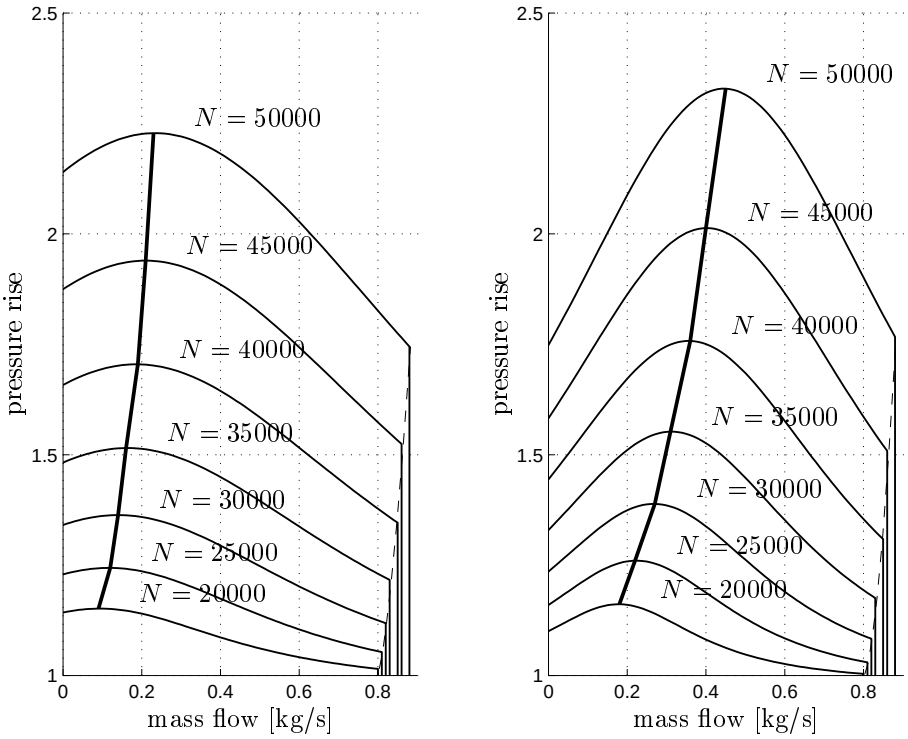

Figure 5.10: *Centrifugal compressor characteristic. The left plot is for an annular diffuser, and the right for a vaned diffuser. The dashed lines to the right are choke lines, also known as stone walls.*

Figure 3 in Fink *et al.* (1992), which is based on physical measurements, we see that they are almost similar.

The surge line is the line in the compressor map that divides the map into an area of stable compressor operation and unstable (surge) operation. The line passes through the local maxima of the constant speed lines in the map, and is drawn with a solid line in figure 5.12.

5.5 Choking

When the flow reaches sonic velocity at some cross-section of the compression system, the flow chokes. Assuming isentropic flow, Dixon (1978) calculated the choking flow for the components most likely to choke in centrifugal compressors, the impeller eye (the inducer) and at the entry of the diffuser.

The effect of choking can be seen in Figure 5.10, where a choke line, also known as a stone wall, has been drawn. In this paper, the effect of choking is treated in a approximate manner. Due to sonic effects, the pressure rise would fall off more

gradually when approaching the stone wall than shown in Figure 5.10. Dixon (1978) showed that the mass flows for which choking occurs are:

- **Choking in impeller**

$$m_{choke}(U_1) = A_1 \rho_{01} a_{01} \left[\frac{2 + (\kappa - 1)\left(\frac{U_1}{a_{01}}\right)^2}{\kappa + 1} \right]^{\frac{(\kappa+1)}{2(\kappa-1)}}, \tag{5.43}$$

where

$$\rho_{01} = \frac{p_{01}}{RT_{01}} \text{ and } a_{01} = \sqrt{\kappa R T_{01}} \tag{5.44}$$

is the inlet stagnation density and inlet stagnation sonic velocity, respectively. It is seen than the choking mass flow is dependent on blade speed U_1. Thus the impeller can accept a greater limiting mass flow rate at higher rotational speeds. By inserting $U_1 = 0$ in (5.43) the expression for choked flow through a nozzle is found. This is shown in Appendix B.

- **Choking in the diffuser entry**

$$m_{choke}(U_2) = A_4 \rho_{01} a_{01} \frac{1 + (\kappa - 1)\eta_{imp}\sigma\left(\frac{U_2}{a_{01}}\right)^2}{\sqrt{1 + (\kappa - 1)\sigma\left(\frac{U_2}{a_{01}}\right)^2}} \left(\frac{2}{\kappa + 1}\right)^{\frac{(\kappa+1)}{2(\kappa-1)}}, \tag{5.45}$$

where A_4 is the flow area of the diffuser entry, and η_{imp} is the impeller efficiency.

5.6 Dynamic Model

To complete the dynamic model (5.1), an expression for the throttle mass flow is needed. The mass flow m_t through the throttle is modeled as

$$m_t = k_t \sqrt{p_p - p_{01}}, \tag{5.46}$$

where k_t is the throttle gain proportional to throttle opening and p_p is the plenum pressure. The momentum balance of the spool is

$$I\dot{\omega} = \tau_t - \tau_c. \tag{5.47}$$

Using (5.3) it is seen that

$$\omega = \frac{2U_1}{D_1} \Rightarrow \dot{\omega} = \frac{2\dot{U}_1}{D_1}, \tag{5.48}$$

and thus we get a differential equation for U_1,

$$\dot{U}_1 = \frac{D_1}{2I}\left(\tau_t - \tau_c\right). \tag{5.49}$$

The drive torque τ_t may be delivered by a turbine, and will be used as a control variable for speed control. The compressor and spool can only rotate in one direction, and the speed is assumed upper bounded:

$$0 \leq U_1(t) < U_m. \tag{5.50}$$

Using (5.12) and (5.49), and inserting equations (5.42) and (5.46) in (5.1), we get the following dynamic model for the compression system

$$\begin{aligned} \dot{p}_p &= \frac{a_{01}^2}{V_p}(m - k_t\sqrt{p_p - p_{01}}) \\ \dot{m} &= \frac{A}{L}\left(\left(1 + \frac{\eta_i(m, U_1)\Delta h_{0c,ideal}}{T_{01}c_p}\right)^{\frac{\kappa}{\kappa-1}} p_{01} - p_p\right) \\ \dot{U}_1 &= \frac{D_1}{2I}\left(\tau_t - \tau_c\right). \end{aligned} \tag{5.51}$$

It is worth noticing that a time varying U is equivalent with a time varying B-parameter Fink *et al.* (1992). Greitzer's B-parameter as defined in Greitzer (1976*a*) is given by $B = \frac{U_1}{2a_{01}}\sqrt{\frac{V_p}{A_1 L_c}}$, where V_p is the plenum volume and L_c is the length of the compressor and duct. Using (5.49), a nonlinear differential equation for B can be found.

5.7 Surge Control Idea

The reason for equilibria to the left of the surge line being unstable, and causing the compressor to go into surge, is the positive slope of the characteristic in this area. From Figure 5.9 it is seen that the positive slope is due to the incidence losses at low mass flows. From the expression for the incidence loss, equation (5.20), it is clear that a variable blade angle β_{1b} would make it possible to minimize the incidence losses over a range of mass flows. Thus variable inducer blades might be used as a means of surge stabilization.

On the other hand, the maximum energy transfer and minimum incidence loss do not occur for the same mass flow. This is due to the friction losses. The friction shifts the point of maximum energy transfer, and consequently pressure rise, to the left of the point of minimum incidence loss. From this, we conclude that the friction losses in fact have a stabilizing effect, and introducing additional fluid friction would move the point of maximum energy transfer to the left. The result of this is that the surge line will be shifted to the left, and the area of stable compressor operation is expanded.

This motivates us to introduce a valve in series with compressor. The valve will introduce a pressure drop into the system, and the characteristic of the valve will have the same qualitative impact on the equivalent compressor characteristic as introducing more fluid friction. The pressure drop over this valve will serve as the control variable, and it will be used to introduce additional friction at low

mass flows in order to avoid surge. The use of a close coupled valve for constant speed centrifugal compressor surge control was studied by Dussourd *et al.* (1977), Jungowski *et al.* (1996) and Pinsley *et al.* (1991).

5.8 Controller Design and Stability Analysis

The equivalent compressor characteristic for compressor and close coupled valve is defined as

$$\Psi_e(m, U_1) = \Psi_c(m, U_1) - \Psi_v(m), \tag{5.52}$$

where $\Psi_v(m)p_{01}$ is the pressure drop across the CCV and

$$\Psi_c(m, U_1) = \left(1 + \frac{\eta_i(m, U_1)\Delta h_{0c,ideal}}{T_{01}c_p}\right)^{\frac{\kappa}{\kappa-1}}. \tag{5.53}$$

Assume p_0, m_0 to be the equilibrium values of pressure and mass flow as dictated by the intersection of the throttle and compressor characteristics, and U_d to be the desired spool speed. Define the following error variables

$$\hat{p} = p_p - p_0, \quad \hat{m} = m - m_0, \quad \hat{U} = U_1 - U_d. \tag{5.54}$$

The equations of motion (5.51) are now transformed so that the origin becomes the equilibrium under study. Notice that no assumptions are made about the numeric values of m_0 and p_0, so that the equilibrium can be on either side of the surge line. The equilibrium values is calculated using the same method as described in section 2.3.2. Define

$$\hat{m}_t(\hat{p}) = m_t(\hat{p} + p_0) - m_0 \tag{5.55}$$

$$\hat{\Psi}_c(\hat{m}, \hat{U}) = \Psi_c(\hat{m} + m_0, \hat{U} + U_d) - p_0 \tag{5.56}$$

$$\hat{\Psi}_v(\hat{m}, \hat{U}) = \Psi_v(\hat{m} + m_0, \hat{U} + U_d) - p_0 \tag{5.57}$$

By including the CCV (5.52), and using (5.55)-(5.57), the model (5.51) can be written in the form

$$\begin{aligned} \dot{\hat{p}} &= \frac{a^2}{V_p}\left(\hat{m} - \hat{m}_t(\hat{p})\right) \\ \dot{\hat{m}} &= \frac{A}{L}\left(\left(\hat{\Psi}_c(\hat{m}, \hat{U}) - \hat{\Psi}_v(\hat{m})\right)p_{01} - \hat{p}\right) \\ \dot{\hat{U}}_1 &= \frac{D_1}{2I}\left(\hat{\tau}_t - \hat{\tau}_c\right) \end{aligned} \tag{5.58}$$

where a hat denotes transformation to the new coordinates (5.54), and $(\hat{p}\ \hat{m}\ \hat{U})^{\mathrm{T}} = (0\ 0\ 0)^{\mathrm{T}}$ is the equilibrium. The expressions for the characteristics $\hat{m}_t(\hat{p})$, $\hat{\Psi}_c(\hat{m}, \hat{U})$ and $\hat{\Psi}_v(\hat{m})$ are found in a similar manner as in Chapter 2. From (5.12) it is known that

$$\tau_c = \frac{D_2^2\sigma}{2D_1}|m|U_1 = \frac{D_2^2\sigma}{2D_1}\mathrm{sgn}(m)mU_1. \tag{5.59}$$

As in Nicklasson (1996), a scaled hyperbolic tangent function will be used to mimic the signum function in the analysis in order to avoid additional difficulties regarding continuity:

$$\tau_c = \frac{D_2^2\sigma}{2D_1}\tanh(\frac{m}{\varsigma})mU_1, \tag{5.60}$$

where $\varsigma > 0$ is a sufficiently large constant. The torque $\hat{\tau}_c$ is defined as

$$\hat{\tau}_c = \tau_c - \tau_{co} \tag{5.61}$$

and calculated as

$$\begin{aligned}\tau_c &= \frac{D_2^2\sigma}{2D_1}\tanh(\frac{m}{\varsigma})(\hat{m}+m_0)(\hat{U}+U_d)\\ &= \underbrace{\frac{D_2^2\sigma}{2D_1}\tanh(\frac{m}{\varsigma})(\hat{m}+m_0)(\hat{m}\hat{U}+\hat{m}U_d+m_0\hat{U})}_{\hat{\tau}_c}\\ &\quad + \underbrace{\frac{D_2^2\sigma}{2D_1}\tanh(\frac{m}{\varsigma})m_0U_d}_{\tau_{c0}}.\end{aligned} \tag{5.62}$$

By choosing

$$\hat{\tau}_t = \tau_t - \tau_{co}, \tag{5.63}$$

the last equation in (5.58) follows from the last equation in (5.51).

Theorem 5.1 *The surge control law*

$$\hat{\Psi}_v = k_v\hat{m}, \tag{5.64}$$

and the speed control law

$$\begin{aligned}\hat{\tau}_t &= -k_p\hat{U} - k_i\hat{I},\\ \dot{\hat{I}} &= \hat{U},\end{aligned} \tag{5.65}$$

where

$$k_p > 0\,,\ \ k_i > 0 \ \text{ and } \ k_v > \sup_{\hat{U},\hat{m}}\left\{\frac{\partial\hat{\Psi}_c(\hat{m},\hat{U})}{\partial\hat{m}}\right\} + \delta_1, \tag{5.66}$$

and $\delta_1 > 0$, makes the origin of (5.58) semi-global exponentially stable. That is, desired compressor speed U_d is achieved whether the equilibrium is to the right or to the left of the original surge line. The integral term in (5.65) is added in order to robustify the controller with respect to unmodeled disturbance torques. □

Proof:
Define

$$\boldsymbol{z} \triangleq \begin{pmatrix}\hat{U}\\ \hat{I}\end{pmatrix} \ \text{ and } \ \boldsymbol{P} \triangleq \begin{pmatrix}\frac{2I}{D_1} & \lambda\\ \lambda & k_i\end{pmatrix}, \tag{5.67}$$

where $\lambda > 0$ and $k_i > 0$ are design parameters. Consider the following Lyapunov function candidate

$$V(\hat{p}, \hat{m}, \hat{U}, \hat{I}) = \frac{1}{2}\left(V_{\hat{p}} + V_{\hat{m}} + V_{spool}\right), \tag{5.68}$$

where

$$V_{\hat{p}} = \frac{V_p}{a_{01}^2 \rho_{01}} \hat{p}^2 \ , \ \ V_{\hat{m}} = \frac{L}{A_1 \rho_{01}} \hat{m}^2 \text{ and } V_{spool} = \boldsymbol{z}^{\mathrm{T}} \boldsymbol{P} \boldsymbol{z}. \tag{5.69}$$

As all coefficients in (5.68) are constant it follows that V is positive definite and radially unbounded, provided that λ is chosen such that $\boldsymbol{P} > 0$, that is

$$\lambda < \sqrt{\frac{2Ik_i}{D_1}}. \tag{5.70}$$

Calculating the time derivative of (5.68) along the solutions of (5.58) and accounting for (5.65) gives

$$\begin{aligned} \dot{V} &= \hat{m}\left(\hat{\Psi}_c(\hat{m}, \hat{U}) - \hat{\Psi}_v(\hat{m})\right) \frac{p_{01}}{\rho_{01}} - \frac{1}{\rho_{01}} \hat{p} \hat{m}_t(\hat{p}) - k_p \hat{U}^2 \\ &\quad + \lambda \hat{U}^2 - \frac{\lambda k_i D_1}{2I} \hat{I}^2 - \frac{\lambda k_p D_1}{2I} \hat{U}\hat{I} - \hat{U}\hat{\tau}_c - \frac{\lambda D_1}{2I} \hat{I}\hat{\tau}_c. \end{aligned} \tag{5.71}$$

The last term in (5.71) can be upper bounded as

$$\begin{aligned} -\frac{\lambda D_1}{2I} \hat{I}\hat{\tau}_c &= -\frac{\lambda D_2^2 \sigma}{4I} \left(\tanh(\frac{m}{\varsigma}) \hat{m} U + m_0 \hat{U}\right) \hat{I} \\ &\leq \frac{\lambda D_2^2 \sigma}{4I} \left(\frac{U_m}{2} \left(\frac{\hat{m}^2}{\eta_1} + \eta_1 \hat{I}^2\right) + m_0 \hat{U}\hat{I}\right) \end{aligned} \tag{5.72}$$

using (5.12), (5.50) and Young's inequality. The parameter $\eta_1 > 0$ can be chosen freely. The $\hat{U}\hat{\tau}_c$-term can be upper bounded as

$$\begin{aligned} -\hat{U}\hat{\tau}_c &= -\frac{D_2^2 \sigma}{2D_1} \tanh(\frac{m}{\varsigma}) \left((\hat{m} + m_0)\hat{U} + \hat{m} U_d\right) \hat{U} \\ &\leq -\frac{D_2^2 \sigma}{2D_1} \tanh(\frac{m}{\varsigma}) m \hat{U}^2 + \frac{D_2^2 \sigma}{4D_1} \left(\frac{\hat{m}^2}{\eta_2} + \eta_2 (U_d \hat{U})^2\right). \end{aligned} \tag{5.73}$$

Now, (5.71) can be upper bounded as

$$\begin{aligned} \dot{V} &\leq \hat{m}\left(\hat{\Psi}_c(\hat{m}, \hat{U}) - \hat{\Psi}_v(\hat{m})\right) \frac{p_{01}}{\rho_{01}} - \frac{D_2^2 \sigma}{2D_1} \tanh(\frac{m}{\varsigma}) m \hat{U}^2 \\ &\quad + \left(\frac{\sigma \lambda D_2^2 U_m}{8I\eta_1} + \frac{D_2^2 \sigma}{4D_1 \eta_2}\right) \hat{m}^2 - \frac{1}{\rho_{01}} \hat{p} \hat{m}_t(\hat{p}) - \boldsymbol{z}^{\mathrm{T}} \boldsymbol{R} \boldsymbol{z}, \end{aligned} \tag{5.74}$$

where

$$\boldsymbol{R} = \begin{pmatrix} k_p - \lambda - \frac{D_2^2 \sigma U_d^2 \eta_2}{4D_1} & \frac{\lambda}{4I}\left(D_1 k_p - \frac{\sigma D_2^2 m_0}{2}\right) \\ \frac{\lambda}{4I}\left(D_1 k_p - \frac{\sigma D_2^2 m_0}{2}\right) & \frac{\lambda}{2I}\left(k_i D_1 - \frac{\sigma D_2^2 U_m \eta_1}{4}\right) \end{pmatrix}. \tag{5.75}$$

Demanding $\boldsymbol{R} > 0$ gives the following conditions on k_p, η_1 and λ

$$k_p > \frac{D_2^2 \sigma U_d^2 \eta_2}{4D_1}, \tag{5.76}$$

$$\eta_1 < \frac{4k_i D_1}{\sigma D_2 U_m} \tag{5.77}$$

and

$$\lambda < \min\left\{\lambda_1, \lambda_2\right\}, \tag{5.78}$$

where

$$\lambda_1 = k_p - \frac{D_2^2 \sigma U_d^2 \eta_2}{4D_1} \tag{5.79}$$

and

$$\lambda_2 = \frac{\left(k_p - \frac{D_2^2 \sigma U_d^2 \eta_2}{4D_1}\right)\left(k_i D_1 - \frac{\sigma D_2 U_m \eta_1}{4}\right)}{k_i D_1 - \frac{\sigma D_2 U_m \eta_1}{4} + \frac{1}{8I}\left(D_1 k_p - \frac{\sigma D_2 m_0}{2}\right)^2}. \tag{5.80}$$

It is assumed that $\hat{m}_t$ satisfies the sector condition

$$\hat{p}\hat{m}_t(\hat{p}) > \delta_2 \hat{p}^2, \tag{5.81}$$

that is, the throttle is assumed passive as in Simon and Valavani (1991). As $\hat{p}\hat{m}_t(\hat{p})$ is of order $\frac{3}{2}$ in $\hat{p}$, (5.81) does not hold globally. However, for a given $\hat{p}_{max}$ such that

$$|\hat{p}(t)| \leq \hat{p}_{max} \; \forall \; t > 0 \tag{5.82}$$

it will always be possible to chose δ_2 small enough for (5.81) to hold for $|\hat{p}(t)| \leq \hat{p}_{max}$. This is the same assumption as made in Assumption 3.1. Now, the CCV pressure drop $\Psi_v(\hat{m})$ is to be chosen such that for the first term in (5.74), the condition

$$-\hat{m}\left(\hat{\Psi}_c(\hat{m}, \hat{U}) - \hat{\Psi}_v(\hat{m})\right)\frac{p_{01}}{\rho_{01}} > 0 \; \forall \hat{U} \tag{5.83}$$

is satisfied. Since $\frac{p_{01}}{\rho_{01}} > 0$, sufficient conditions for (5.83) to hold is

$$-\left(\hat{\Psi}_c(\hat{m}, \hat{U}) - \hat{\Psi}_v(\hat{m})\right)\Big|_{\hat{m}=0} = 0 \tag{5.84}$$

and

$$\frac{\partial}{\partial \hat{m}}\left(-\hat{\Psi}_c(\hat{m}, \hat{U}) + \hat{\Psi}_v(\hat{m})\right) > 0. \tag{5.85}$$

It can be recognized that

$$\hat{\Psi}_c(0, \hat{U}) = \Psi_c(m_0, U_d) - \Psi_c(m_0, U_d) = 0, \tag{5.86}$$

$$\hat{\Psi}_v(\hat{m}) = k_v \hat{m} \; \Rightarrow \; \hat{\Psi}_v(0) = 0, \tag{5.87}$$

and thus (5.84) is satisfied. From (5.85), we get

$$-\frac{\partial}{\partial \hat{m}}\hat{\Psi}_c(\hat{m}, \hat{U}) + k_v > 0, \tag{5.88}$$

and it follows that choosing k_v according to

$$k_v > \sup_{\hat{U},\hat{m}} \left\{ \frac{\partial \hat{\Psi}_c(\hat{m},\hat{U})}{\partial \hat{m}} \right\}, \tag{5.89}$$

guarantees that (5.85), and thereby (5.83) being satisfied. Moreover, if k_v is chosen as

$$k_v > \sup_{\hat{U},\hat{m}} \left\{ \frac{\partial \hat{\Psi}_c(\hat{m},\hat{U})}{\partial \hat{m}} \right\} + \delta_1, \tag{5.90}$$

where $\delta_1 > 0$, we get $\hat{m}\Psi_v(\hat{m}) > \delta_1 \hat{m}^2$, and (5.83) is modified to

$$-\hat{m}\left(\hat{\Psi}_c(\hat{m},\hat{U}) - \hat{\Psi}_v(\hat{m})\right)\frac{p_{01}}{\rho_{01}} > \frac{p_{01}}{\rho_{01}}\delta_1 \hat{m}^2 \ \forall \hat{U}. \tag{5.91}$$

Consequently, $\dot{V}$ can now be upper bounded as

$$\dot{V} \leq -\left(\frac{p_{01}}{\rho_{01}}\delta_1 - \frac{\sigma\lambda D_2^2 U_m}{8I\eta_1} - \frac{D_2^2\sigma}{4D_1\eta_2}\right)\hat{m}^2 - \delta_2\hat{p}^2 - \frac{1}{2}\boldsymbol{z}^{\mathrm{T}}\boldsymbol{R}\boldsymbol{z} \quad \forall \ \hat{m},\hat{p},\boldsymbol{z} \tag{5.92}$$

We now set out to compare the coefficients of V and $\dot{V}$. The cross terms in $\hat{U}$ and $\hat{I}$ are upper bounded using Young's inequality,

$$\lambda\hat{U}\hat{I} \leq \frac{\lambda}{2}\left(\frac{\hat{U}^2}{\eta_3} + \eta_3\hat{I}^2\right) \tag{5.93}$$

$$-\frac{\lambda(4D_1k_p - \sigma D_2^2 m_0)}{2I}\hat{U}\hat{I} \leq \frac{\lambda(4D_1k_p - \sigma D_2^2 m_0)}{4I} \times \left(\hat{U}^2/\eta_4 + \eta_4\hat{I}^2\right), \tag{5.94}$$

where $\eta_3 > 0$ and $\eta_4 > 0$ are constants that can be chosen freely. Using (5.93) and (5.94) and comparing the coefficients in (5.68) and (5.92), it can be recognized that if the following inequalities are satisfied for some constant $\varpi > 0$:

$$\delta_1 - \frac{\sigma\lambda D_2^2 U_m \rho_{01}}{8I\eta_1 p_{01}} - \frac{D_2^2\sigma\rho_{01}}{4D_1\eta_2 p_{01}} > \varpi\frac{L}{A\rho_{01}} \tag{5.95}$$

$$\delta_2 > \varpi\frac{V_p}{a_{01}^2\rho_{01}}, \tag{5.96}$$

$$k_p - \lambda - \frac{\lambda(4D_1k_p - \sigma D_2^2 m_0)}{4I\eta_4} > \varpi\left(\frac{I}{D_1} + \frac{\lambda}{2\eta_3}\right), \tag{5.97}$$

$$\lambda k_i - \frac{\lambda(4D_1k_p - \sigma D_2^2 m_0)}{4I}\eta_4 > \varpi\left(\frac{k_i}{D_1} + \frac{\varpi\eta_3}{2}\right), \tag{5.98}$$

the following holds

$$\dot{V} \leq -\varpi V \ \Rightarrow \ V(t) \leq V(0)e^{-\varpi t}. \tag{5.99}$$

If η_1 is chosen according to (5.77), and δ_1 is chosen according to

$$\delta_1 > \frac{\sigma\lambda D_2^2 U_m \rho_{01}}{8I\eta_1 p_{01}} + \frac{D_2^2\sigma\rho_{01}}{4D_1\eta_2 p_{01}}, \tag{5.100}$$

and k_v is chosen so that $k_v > \sup_{\hat{U},\hat{m}} \left\{ \frac{\partial \hat{\Psi}_c(\hat{m},\hat{U})}{\partial \hat{m}} \right\} + \delta_1$, and λ is chosen according to (5.70) and (5.78), then the inequalities (5.95)-(5.98) are satisfied for some $\varpi > 0$. By (5.99) the origin of (5.58) is exponentially stable. Due to assumption (5.82), the stability result holds whenever $|\hat{p}(0)| \leq \hat{p}_{max}$, and thus the origin is semi globally exponentially stable. □

Notice that the parameter ϖ can be used to calculate a lower bound on the convergence rate of the system.

Providing the parameters k_i and λ with appropriate units, V is a energy-like function of unit $[J]$. The term

$$V_{\hat{U}} = \frac{1}{2} z_1 P_{11} z_1 = \frac{I}{2D_1^2} \hat{U}^2 \tag{5.101}$$

is recognized as the kinetic energy, expressed in the new coordinates, of the rotating spool.

5.9 Simulations

In order to model the compressor pressure rise for negative mass flow (deep surge) it is assumed that the pressure rise is proportional to the square of the mass flow for $m < 0$, that is,

$$\Psi_c(U_1, m) = \begin{cases} c_n m^2 + \psi_{c0}(U_1) & , \quad m \leq 0, \\ \left(1 + \frac{\eta_i(m,U_1)\Delta h_{0c,ideal}}{T_{01} c_p}\right)^{\frac{\kappa}{\kappa-1}} & , \quad m > 0 \end{cases}, \tag{5.102}$$

where the choice

$$\psi_{c0}(U_1) = \left(1 + \frac{\eta_i(m,U_1)\Delta h_{0c,ideal}}{T_{01} c_p}\right)^{\frac{\kappa}{\kappa-1}} \Bigg|_{m=0}, \tag{5.103}$$

of the shut off value ψ_{c0} ensures that $\Psi_c(U_1, m)$ is continuous in m. According to Willems (1996) and Day (1994), the back-flow characteristic defines the resistance which the rotating blades offer to flow in reversed direction. Day (1994) states that, in reversed flow the compressor can be regarded as a throttling device with a positive pressure bias.

A quadratic characteristic for reversed flow is also proposed by Hansen *et al.* (1981) for centrifugal compressors, and by Mansoux *et al.* (1994), Willems (1996) and Day (1994) for axial compressors. It is widely accepted in the literature (see e.g. Greitzer (1981)) that the compressor characteristic has a negative slope for negative mass flow. This slope depends on the choice of the constant c_n.

The two cases of annular and vaned diffuser are now simulated with and without surge control.

Annular Diffuser

In Figure 5.11 the response (solid lines) of the compression system during surge is showed. The set point for compressor speed was $U_d = 150\text{m/s} \Rightarrow N \approx 50.000\text{rpm}$ and the speed control law (5.65) parameters were set to $k_p = 0.1$ and $k_i = 0.07$. The throttle gain was set to $k_t = 0.0003$ which gives an unstable equilibrium to the left of the surge line. Notice the oscillation in speed U_1. These variations in spool speed during surge was first described by Eveker and Nett (1991) for an axial compressor. This simulation is also shown in Figure 5.12, where the pressure rise has been plotted versus the mass flow in the compressor characteristic. As can be seen, the compressor undergoes severe (deep) surge oscillations, and the compressor speed oscillates around the desired value.

Now, the surge controller (5.64) is used with $k_v = 0.5$. The speed set point, speed controller parameters and throttle gain are as before. The results are shown in Figure 5.11 (dashed lines). The desired speed is reached and the surge oscillations are eliminated. As previously mentioned there is a loss associated with the CCV control approach. The pressure drop over the valve is shown in the lower right corner of Figure 5.11. At equilibrium the pressure drop for this particular case is at ca. 5kPa. Compared to the pressure rise over the compressor at this equilibrium, well over 200kPa this seems little when taken into account that the compressor now is operating in an area of the compressor map previously not possible. The CCV loss is dependent on the controller gain k_v. In this simulation the gain was set to $k_v = 0.5$ to dominate the maximum positive slope of the compressor characteristic.

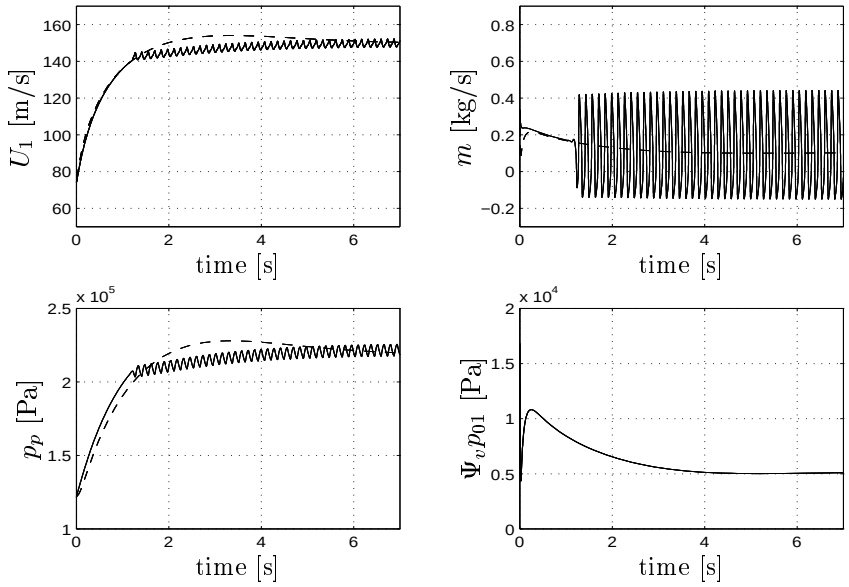

Figure 5.11: *Transient response of centrifugal compression system with annular diffuser. Without surge control, the compressor goes into surge, shown with solid lines. The system response with the surge controller is shown with dashed lines.*

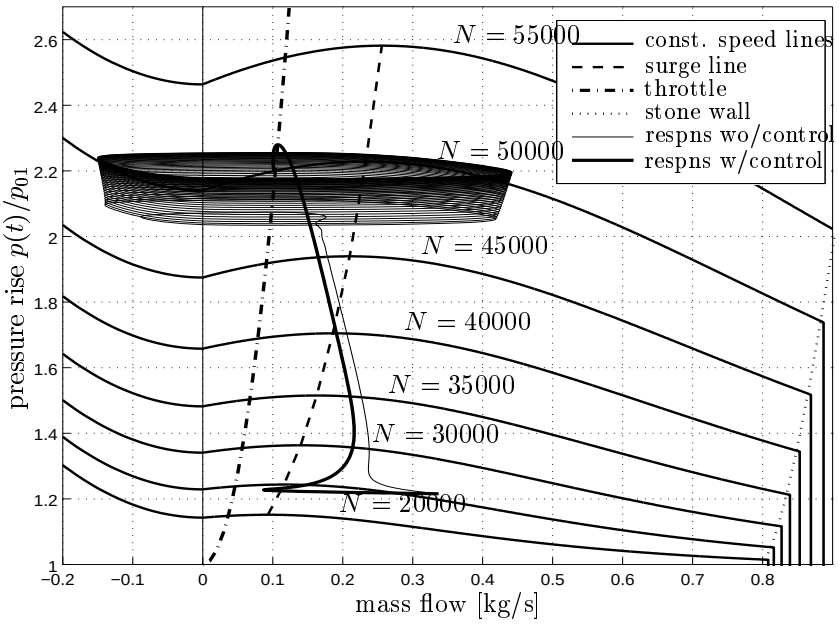

Figure 5.12: $(m(t), p(t)/p_{01})$-*trajectories plotted together with the compressor characteristic.* N *is the compressor speed in rpm. In the case of no surge control, the surge cycle is clearly visible, but with surge control the state converges to the intersection of the throttle and the compressor characteristic.*

Vaned Diffuser

The response of the compression system with speed control only is shown in Figure 5.13 (solid lines). The speed control parameters were set to $k_p = 0.1$ and $k_i = 0.07$, and the throttle gain was set at $k_T = 0.00075$. As the vaned diffuser gives a steeper and more narrow characteristic, the amplitude of the pressure oscillations is larger than for the annular diffuser. This is also the case for the speed and mass flow oscillations.

When the surge control is in use, we get the response plotted with dashed lines in Figure 5.13, and as can be seen the oscillations are avoided at the cost of a pressure loss over the CCV. Since the positive slope of the compressor characteristic is larger in this case compared to the annular diffuser, this pressure drop is also larger. However, a pressure drop of 35kPa over the valve is still less than the pressure rise of 180kPa over the compressor.

By comparing the in-surge response of the two cases, it is seen that the frequency of the surge oscillations is lower for the vaned diffuser (3Hz), than for the annular diffuser (7Hz). This is in accordance with Greitzer (1981) and Willems (1996) where it is shown that the surge frequency depends on the slope of the compressor characteristic in such a way that a steeper slope leads to lower frequency, and a less steep slope leads to higher frequency.

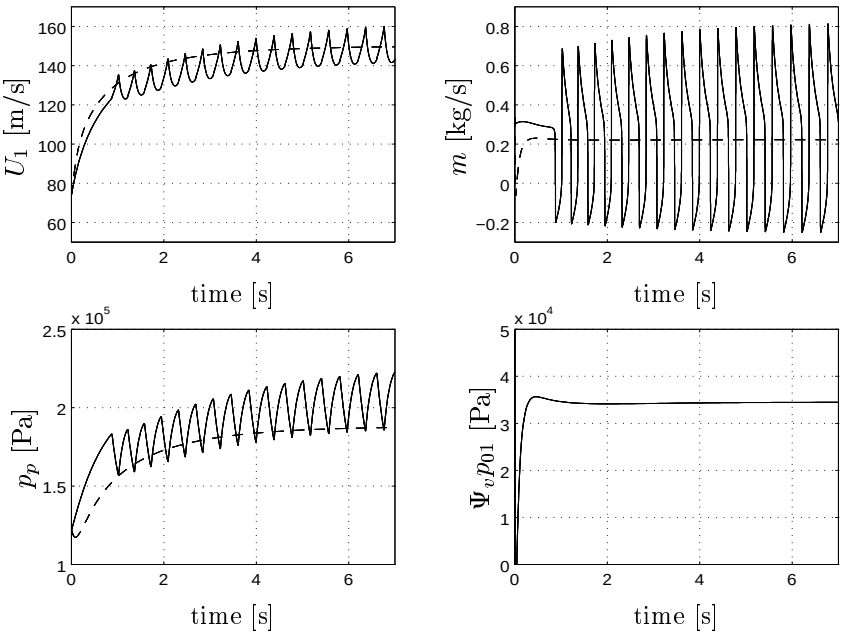

Figure 5.13: *Transient response of centrifugal compression system with vaned diffuser. Without surge control, the compressor goes into surge. This is plotted with a solid line. The dashed lines is the system response when the CCV surge controller is in use.*

5.10 Conclusion

In this chapter, a dynamic model of a centrifugal compression system with non-constant compressor speed was presented. The compressor characteristic was derived by calculating the energy transfer end losses in the components of the compressor. Incidence and friction losses in the impeller and the diffuser were considered in addition to other losses. Both vaned and annular diffusers were considered.

Control laws for surge and speed of the centrifugal compression system were developed. A close coupled valve was chosen as an actuator for the control of surge. Using Lyapunov's method, the systems equilibrium was showed to be semi-global exponentially stable. Through simulations it was confirmed that the compressor can operate stable

and reach desired speed in the previous unstable area to the right of the surge line in the compressor map.

From a surge control point of view, the main difference between the annular and vaned diffusers are the steeper slope of the compressor characteristic when a vaned diffuser is used. A consequence of this is that if a close coupled valve is used to

control surge, a greater pressure drop must be accepted over the valve in the case of a vaned diffuser than in the case of an annular diffuser.

Chapter 6

Conclusions

In this thesis modeling and control of surge and rotating stall in axial and centrifugal compressors have been studied.

First, surge and stall controllers for a close coupled valve in series with a compressor were developed. Using backstepping, a surge control law for the close coupled valve was derived. Global asymptotic stability was proven. A more complicated surge control law was derived for the case of both pressure disturbances and mass flow disturbances. Global uniform boundedness and convergence was proven. In order to stabilize the compression system in the presence of constant disturbances, or biases, in mass flow and pressure, an adaptive version of the surge controller was derived. This controller ensures global asymptotic stability. Then, controllers for rotating stall were considered. The close coupled valve was incooperated into the Moore-Greitzer model, and controllers were derived that enables stabilization of rotating stall beyond the surge line. Without disturbances, an asymptotically stable equilibrium is ensured, and in the presence of pressure disturbances uniform boundedness was proven.

Then, the passivity properties of the Greitzer model was used to derive a surge control law for a close coupled valve. This resulted in a simple proportional control law, that was capable of stabilizing the compression system in the presence of both mass flow disturbances as well as pressure disturbances.

A multi mode Moore-Greitzer axial compressor model with spool dynamics was derived. This resulted in a model with time varying B-parameter. Through simulations it was demonstrated that the model was capable of demonstrating both rotating stall and surge, and that the type of instability depended on the compressor speed. In the original Moore Greitzer model only the first mode of rotating stall is included. The simulations in this chapter show that during stall inception, higher order modes can dominate the first mode. This is in accordance with known results, and is shown here to be valid also for variable speed compressors.

A dynamic model of a centrifugal compression system with non-constant compressor speed was presented. The compressor characteristic was derived by calculating

the energy transfer and losses in the components of the compressor. Incidence and friction losses in the impeller and the diffuser were considered in addition to other losses. Both vaned and annular diffusers were considered. Control laws for surge and speed of the centrifugal compression system were developed. A close coupled valve was chosen as an actuator for the control of surge. Using Lyapunov's method, the systems equilibrium was showed to be semi-global exponentially stable. Through simulations it was confirmed that the compressor can operate stable and reach desired speed in the previous unstable area to the right of the surge line in the compressor map.

Bibliography

Abed, E.H., P.K. Houpt and W.M. Hosny (1993). Bifurcation analysis of surge and rotating stall in axial flow compressors. *Journal of Turbomachinery* **115**, 817–824.

Adomatis, R.A. and E.H. Abed (1993). Local nonlinear control of stall inception in axial flow compressors. In: *Proceedings of the AIAA/SAE/ASME/ASEE Joint Propulsion Conference*. Monterey, CA.

Badmus, O.O., S. Chowdhury and C.N. Nett (1996). Nonlinear control of surge in axial compression systems. *Automatica* **32**(1), 59–70.

Badmus, O.O., S. Chowdhury, K.M. Eveker and C.N. Nett (1995). Control-oriented high-frequency turbomachinery modelling: Single-stage compression system one-dimensional modell. *Journal of Turbomachinery* **117**, 47–61.

Balchen, J.G and K.I. Mummé (1988). *Process control : Structures and applications*. Van Nostrand Reinhold Company. New York.

Baljé, O.E. (1952). A contribution to the problem of designing radial turbomachines. *Transactions of the ASME* **74**, 451–472.

Banaszuk, A., H.A. Hauksson and I. Mezić (1997). A backstepping controller for a partial differential equation model of compression system instabilities. In: *Proceedings of the 36th Conference on Decision and Control*. San Diego, CA. pp. 1050–1055.

Bazanella, A.S., P.V. Kokotović and A.S. e Silva (1997). On the control of dynamic systems with unknown operating point. In: *Proceedings of the 1997 European Control Conference*. Brussels, Belgium.

Behnken, R.L. and R.M. Murray (1997). Combined air injection control of rotating stall and bleed valve control of surge. In: *Proceedings of the 1997 American Control Conference*. Albuquerque, NM.

Brown, D., L. Rachul and K. Williams (1997). NASA Researching Engine Airflow Controls to Improve Performance, Fuel Efficiency. NASA press release, downloaded from Usenet newsgroup `sci.space.news`. Release: 97-183.

Cohen, H., G.F.C. Rogers and H.I.H Saravanamuttoo (1996). *Gas turbine theory*. 4th ed.. Longman. Essex.

Covert, E.E. (1995). Evolution of the commercial airliner. *Scientific American* **273**(3), 82–85.

Cumpsty, N.A. (1989). *Compressor Aerodynamics*. Longman.

Day, I.J. (1993). Active suppression of rotating stall and surge in axial compressors. *Journal of Turbomachinery* **115**, 40–47.

Day, I.J. (1994). Axial compressor performance during surge. *Journal of propulsion and power* **10**(3), 329–336.

de Jager, B. (1995). Rotating stall and surge control : A survey. In: *Proceedings of the 35th Conference on Decision and Control*. New Orleans, LA. pp. 1857–1862.

DeLaat, J.C., R.D. Southwick and G.W. Gallops (1996). High stability engine control (HISTEC). In: *Proceedings of AIAA/SAE/ASME/ASEE 32nd Joint Propulsion Conference*. Lake Buena Vista, FL. NASA TM 107272, AIAA-96-2586.

Dixon, S.L. (1978). *Thermodynamics of turbomachinery*. 3rd ed.. Pergamon Press.

Dussourd, J.L., G.W. Pfannebecker and S.K. Singhania (1976). Considerations for the control of surge in dynamic compressors using close coupled resistances. In: *Centrifugal compressor and pump stability, stall and surge* (P.C. Tramm and R.C. Dean, Jr., Eds.). pp. 1–28. ASME. New Orleans, Louisiana. Presented at the 1976 Joint gas turbine and fluids engineering divisions' Conference.

Dussourd, J.L., G.W. Pfannebecker and S.K. Singhania (1977). An experimental investigation of the control of surge in radial compressors using close coupled resistances. *Journal of Fluids Engineering* **99**, 64–76.

Eastop, T.D. and A.McConkey (1986). *Applied thermodynamics for engineering technologists*. 4th ed.. Longman. New York.

Emmons, H.W., C.E. Pearson and H.P. Grant (1955). Compressor surge and stall propagation. *Transactions of the ASME* **77**, 455–469.

Epstein, A.H., J.E. Ffowcs Williams and E.M. Greitzer (1989). Active suppression of aerodynamic instabilities in turbomachines. *Journal of Propulsion and Power* **5**(2), 204–211.

Erskine, J.B. and N. Hensman (1975). Vibration induced by pump instability and surging. In: *Vibrations and noise in pump, fan, and compressor installations*. The Institution of Mechanical Engineers. Mechanical Engineering Publications limited. Southamton, UK. pp. 87–98.

Eveker, K.M. and C.N. Nett (1991). Model development for active surge control rotating stall avoidance in aircraft gas turbine engines. In: *Proceedings of the 1991 American Control Conference*. pp. 3166–3172.

Ferguson, T.B. (1963). *The centrifugal compressor stage*. Butterworths. London.

Ffowcs Williams, J.E. and X.Y. Huang (1989). Active stabilization of compressor surge. *Journal of Fluid Mech.* **204**, 245–262.

Ffowcs Williams, J.E., M.F.L. Harper and D.J. Allwright (1993). Active stabilization of compressor instability and surge in a working engine. *Journal of Turbomachinery* **115**, 68–75.

Fink, D.A., N.A. Cumpsty and E.M. Greitzer (1992). Surge dynamics in a free-spool centrifugal compressor system. *Journal of Turbomachinery* **114**, 321–332.

Godhavn, J.-M. (1997). Topics in nonlinear motion control: nonholonomic, underactuated and hybrid systems. PhD thesis. Norwegian University of Science and Technology. Dept of Engineering Cybernetics.

Gravdahl, J.T. (1998). *Modeling and Close Coupled Valve Control of Compressor Surge and Rotating Stall*. Advances in Industrial Control. Springer-Verlag. London. Accepted for publication, to appear.

Gravdahl, J.T. and O. Egeland (1997*a*). A Moore-Greitzer axial compressor model with spool dynamics. In: *Proceedings of the 36th IEEE Conference on Decision and Control*. San Diego, CA. pp. 4714–4719.

Gravdahl, J.T. and O. Egeland (1997*b*). Centrifugal compressor surge and speed control. *Submitted to IEEE Transactions on Control Systems Technology*.

Gravdahl, J.T. and O. Egeland (1997*c*). Compressor surge control using a close-coupled valve and backstepping. In: *Proceedings of the 1997 American Control Conference*. Albuquerque, NM.

Gravdahl, J.T. and O. Egeland (1997*d*). Control of the three-state Moore-Greitzer compressor model using a close-coupled valve. In: *Proceedings of the 1997 European Control Conference*. Brussels, Belgium.

Gravdahl, J.T. and O. Egeland (1997*e*). Modeling of rotating stall and surge in a free spool axial compression system. *Submitted to Journal of Turbomachinery*.

Gravdahl, J.T. and O. Egeland (1997*f*). Passivity based compressor surge control using a close-coupled valve. In: *Proceedings of the 1997 COSY Workshop on Control of Nonlinear and Uncertain Systems* (A. Isidori and F. Allgöwer, Eds.). Zurich, Switzerland. pp. 139–143.

Gravdahl, J.T. and O. Egeland (1997*g*). Speed and surge control for a low order centrifugal compressor model. In: *Proceedings of the 1997 International Conference on Control Applications*. Hartford, CT. pp. 344–349.

Gravdahl, J.T. and O. Egeland (1998*a*). Close Coupled Valve control of surge and rotating stall in compressors. *Submitted to Automatica*.

Gravdahl, J.T. and O. Egeland (1998*b*). Speed and surge control for a low order centrifugal compressor model. *Modeling, Identification and Control* **19**(1), 13–29.

Gravdahl, J.T. and O. Egeland (1998*c*). Two results on compressor surge control with disturbance rejection. Submitted to the 37th IEEE Conference on Decision and Control.

Greitzer, E.M. (1976*a*). Surge and Rotating stall in axial flow compressors, Part I: Theoretical compression system model. *Journal of Engineering for Power* **98**, 190–198.

Greitzer, E.M. (1976*b*). Surge and rotating stall in axial flow compressors, Part II: Experimental results and comparison with theory. *Journal of Engineering for Power* **98**, 199–217.

Greitzer, E.M. (1977). Coupled compressor-diffuser flow instability. *Journal of aircraft* **14**(3), 233–238.

Greitzer, E.M. (1980). REVIEW–Axial compressor stall phenomena. *Journal of Fluids Engineering* **102**, 134–151.

Greitzer, E.M. (1981). The stability of pumping systems – The 1980 Freeman scholar lecture. *Journal of Fluids Engineering* **103**, 193–242.

Greitzer, E.M. and F.K. Moore (1986). A theory of post-stall transients in a axial compressor systems: Part II–Application. *Journal of Engineering for Gas Turbines and Power* **108**, 231–239.

Greitzer, E.M. and H.R. Griswold (1976). Compressor-diffuser interaction with circumferential flow distortion. *The journal of mechanical engineering science* **18**(1), 25–43.

Gu, G., S. Banda and A. Sparks (1996). An overview of rotating stall and surge control for axial flow compressors. In: *Proceedings of the 35th Conference on Decision and Control*. Kobe, Japan.

Gysling, D.L., J. Dugundji, E.M. Greitzer and A.H. Epstein (1991). Dynamic control of centrifugal compressors surge using tailored structures. *Journal of Turbomachinery* **113**, 710–722.

Haddad, W.M., J.L. Fausz, V.-S. Chellaboina and A. Leonessa (1997). Nonlinear robust disturbance rejection controllers for rotating stall and surge in axial flow compressors. In: *Proceedings of the 1997 International Conference on Control Applications*. Hartford, CT. pp. 767–772.

Hansen, K.E., P. Jørgensen and P.S. Larsen (1981). Experimental and theoretical study of surge in a small centrifugal compressor. *Journal of Fluids Engineering* **103**, 391–394.

Hendricks, G.J. and D.L. Gysling (1994). Theoretical study of sensor-actuator schemes for rotating stall control. *Journal of Propulsion and Power* **10**(1), 101–109.

Hendrickson, E.S. and A.G. Sparks (1997). On the suitability of bifurcation stabilization control laws for high order Moore-Greitzer compressor models. In: *Proceedings of the 1997 American Control Conference*. Albuquerque, NM.

Horlock, J.H. (1958). *Axial flow compressors: Fluid mechanics and Thermodynamics*. Butterworths scientific publications. London.

Humbert, J.S. and A.J. Krener (1997). Analysis of higher order Moore-Greitzer compressor models. In: *Proceedings of the 1997 International Conference on Control Applications*. Hartford, CT. pp. 651–656.

Hynes, J.M., G.J. Hendricks and A.H. Epstein (1994). Active stabilization of rotating stall in a three-stage axial compressor. *Journal of Turbomachinery* **116**, 226–239.

Hynes, T.P. and E.M. Greitzer (1987). A method for assessing effects of circumferential flow distortion on compressor stability. *Journal of Turbomachinery* **109**, 371–379.

Johnston, J.P. and R.C. Dean, Jr. (1966). Losses in vaneless diffusers of centrifugal compressors and pumps. Analysis, experiment and design. *Journal of Engineering for Power* pp. 49–62.

Jungowski, W.M., M.H. Weiss and G.R. Price (1996). Pressure oscillations occurring in a centrifugal compressor system with and without passive and active surge control. *Journal of Turbomachinery* **118**, 29–40.

Koff, S.G. and E.M. Greitzer (1986). Axisymmetrically stalled flow performance for multistage axial compressors. *Journal of Turbomachinery* **108**, 216–249.

Krstić, M. (1996). Invariant manifolds and asymptotic properties of adaptive nonlinear stabilizers. *IEEE Transactions on automatic control* **41**(6), 817–829.

Krstić, M. and P.V. Kokotović (1995). Lean backstepping designs for jet engine compressor model. In: *Proceedings of the 4th IEEE Conference on Control Applications*. pp. 1047–1052.

Krstić, M., I. Kanellakopoulos and P.V. Kokotović (1995*a*). *Nonlinear and Adaptive Control Design*. John Wiley & Sons Inc.

Krstić, M., J.M. Protz, J.D. Paduano and P.V. Kokotović (1995*b*). Backstepping designs for jet engine stall and surge control. In: *Proceedings of the 35th Conference on Decision and Control*. New Orleans, LA. pp. 3049–3055.

Leonessa, A., V.-S. Chellaboina and W.M. Haddad (1997*a*). Globally stabilizing controllers for multi-mode axial flow compressor models via equilibria-dependent lyapunov functions. In: *Proceedings of the 1997 International Conference on Control Applications*. Hartford, CT. pp. 63–68.

Leonessa, A., V.-S. Chellaboina and W.M. Haddad (1997*b*). Robust stabilization of axial flow compressors with uncertain pressure-flow maps. In: *Proceedings of the 1997 International Conference on Control Applications*. Hartford, CT. pp. 671–676.

Liaw, D.-C. and E.H. Abed (1992). Stability analysis and control of rotating stall. In: *Proceedings of NOLCOS'92: Nonlinear Control System Design Symposium* (M. Fliess, Ed.). Bourdaux, France. pp. 88–93.

Liaw, D.-C. and E.H. Abed (1996). Active control of compressor stall inception: a bifurcation-theoretic approach. *Automatica* **32**(1), 109–115.

Lorett, J.A. and S. Gopalakrishnan (1986). Interaction between impeller and volute of pumps at off-design conditions. *Journal of fluids engineering* **108**, 12–18.

Mansoux, C.A., D.L. Gysling, J.D. Setiawan and J.D. Paduano (1994). Distributed nonlinear modeling and stability analysis of axial compressor stall and surge. In: *Proceedings of the 1994 American Control Conference*. Baltimore, Maryland. pp. 2305–2316.

Mattingly, J.D. (1996). *Elements of gas turbine propulsion*. McGraw-Hill series in aeronautical and aerospace engineering. McGraw-Hill.

McCaughan, F.E. (1989). Application of Bifurcation theory to axial flow compressor instability. *Journal of Turbomachinery* **111**, 426–433.

Moore, F.K. (1984*a*). A theory of rotating stall of multistage axial compressors: Part I–Small disturbances. *Journal of Engineering for Gas Turbines and Power* **106**, 313–320.

Moore, F.K. (1984*b*). A theory of rotating stall of multistage axial compressors: Parts I,II,III. *J. of Engineering for Gas Turbines and Power* **106**, 313–336.

Moore, F.K. and E.M. Greitzer (1986). A theory of post-stall transients in a axial compressor systems: Part I–Development of equations. *Journal of Engineering for Gas Turbines and Power* **108**, 68–76.

Murray, S. Yeung R.M. (1997). Reduction of bleed valve rate requirements for control of rotating stall using continuous air injection. In: *Proceedings of the 1997 International Conference on Control Applications*. Hartford, CT. pp. 683–690.

Nicklasson, P.J. (1996). Passivity-based control of electric machines. PhD thesis. Norwegian Institute of Technology. Dept of Engineering Cybernetics.

Nisenfeld, A.E. (1982). *Centrifugal compressors: principles of operation and control*. Instrument society of America.

Osborn, W.M. and J.M. Wagner (1970). Effect of simulated downstream flow blockage doors on the performance of an axial-flow fan rotor. Technical Report TN D-6071. NASA.

Paduano, J.D., A.H. Epstein, L. Valavani, J.P. Longley, E.M. Greitzer and G.R. Guenette (1993). Active control of rotating stall in a low-speed axial compressor. *Journal of Turbomachinery* **115**, 48–56.

Paduano, J.D., A.H. Epstein, L. Valavani, J.P. Longley, E.M. Greitzer and G.R. Guenette (1995). Modelling for control of rotating stall. *Automatica* **30**(9), 1357–1373.

Pampreen, R.C. (1973). Small turbomachinery compressor and fan aerodynamics. *Journal of engineering for power* **95**, 251–256.

Perko, L. (1991). *Differential equations and dynamical systems.* Vol. 7 of *Texts in Applied Mathematics.* Springer-Verlag.

Pinsley, J.E., G.R. Guenette, A.H. Epstein and E.M. Greitzer (1991). Active stabilization of centrifugal compressor surge. *Journal of Turbomachinery* **113**, 723–732.

Protz, J.M. and J.D. Paduano (1997). Rotating stall and surge: Alternate modeling and control concepts. In: *Proceedings of the 1997 International Conference on Control Applications.* Hartford, CT. pp. 866–873.

Ruffles, P.C (1996). Innovation in aero engines. *The Aeronautical Journal* **100**(1000), 473–484.

Sepulchre, R. and P. Kokotović (1996). Shape signifiers for throttle control of a low-order compressor model.

Simon, J.S. and L. Valavani (1991). A Lyapunov based nonlinear control scheme for stabilizing a basic compression system using a close-coupled control valve. In: *Proceedings of the 1991 American Control Conference.* pp. 2398–2406.

Simon, J.S., L. Valavani, A.H. Epstein and E.M. Greitzer (1993). Evaluation of approaches to active compressor surge stabilization. *Journal of Turbomachinery* **115**, 57–67.

Simon, S. (1993). Feedback stabilization of compression systems. PhD thesis. MIT.

Stenning, A.H. (1980). Rotating stall and surge. *Journal of fluids engineering* **102**, 14–21.

van de Wal, M. and F. Willems (1996). Selection of actuators and sensors for compressor control. Technical Report WFW 96.155. Eindhoven University of Technology.

van de Wal, M., F. Willems and B. de Jager (1997). Selection of actuators and sensors for active surge control. In: *Proceedings of the 1997 International Conference on Control Applications.* Hartford, CT. pp. 121–127.

van der Schaft, A.J. (1996). *L_2-gain and passivity techniques in nonlinear control.* Vol. 218 of *Lecture notes in Control and Information Sciences.* Springer-Verlag. Heidelberg.

Wang, H.-H. and M. Krstić (1997*a*). Control of Deep-Hysteresis aeroengine compressors–Part I : A Moore-Greitzer type model. In: *Proceedings of the 1997 American Control Conference.* Albuquerque, NM.

Wang, H.-H. and M. Krstić (1997*b*). Control of deep hysteresis compressors under limited actuator bandwidth. In: *Proceedings of the 1997 International Conference on Control Applications*. Hartford, CT. pp. 657–662.

Watson, N. and M.S. Janota (1982). *Turbocharging the internal combustion engine*. MacMillan.

Weigl, H.J. and J.D. Paduano (1997). Application of $\mathcal{H}_\infty$ control with eigenvalue perturbations to stabilize a transonic compressor. In: *Proceedings of the 1997 International Conference on Control Applications*. Hartford, CT. pp. 691–698.

White, F.M. (1986). *Fluid mechanics*. 2nd ed.. McGraw-Hill. New York.

Whitfield, A. and F.J. Wallace (1973). Study of incidence loss models in radial and mixed-flow turbomachinery. In: *Proceedings of the conference on heat and fluid flow in steam and gas turbine plant*. The instn. of Mech. Engnrs.. U. of Warwick, Coventry. pp. 122–128.

Whitfield, A. and F.J. Wallace (1975). Performance prediction for automotive turbocharger compressors. *Proceedings of the institution of mechanical engineers* **189**(12), 59–67.

Willems, F. (1996). Modeling and control of compressor flow instabilities. Technical Report WFW 96.151. Eindhoven University of Technology.

Appendix A

Nomenclature

A.1 Acronyms

CCV	Close Coupled Valve
CLF	Control Lyapunov Function
IGV	Inlet Guide vanes
ODE	Ordinary Differential Equation
PDE	Partial Differential Equation
PDF	Positive Definite Function
GAS	Globally Asymptotically Stable
GES	Globally Exponentially Stable
MG	Moore-Greitzer

A.2 Subscripts

0	Equilibrium value
c	Compressor
d	Disturbance or desired value
x, a	Axial
p	Plenum
η, θ, ξ	Partial derivative with respect to η, θ or ξ

A.3 Superscripts

$\prime$	$\hat{\phi}'$ is a disturbance velocity potential
$*$	$(\hat{\phi}')^*$ is an approximation of $\hat{\phi}'$

A.4 Mathematical Symbols and Definitions

$\dot{(\cdot)}$	Total time derivative, $\frac{d}{dt}$ or $\frac{d}{d\xi}$
$\frac{\partial}{\partial x}$	Partial derivative with respect to variable x
$(\cdot)^{-1}$	Inverse operator
$\hat{(\cdot)}$	Deviation from equilibrium, transformed coordinates
$\|\cdot\|_\infty$	The $\mathcal{L}_\infty$-norm of the function $f : \mathbb{R}^+ \to \mathbb{R}$ is defined as $\|f\|_\infty = \sup_{t\geq 0} \|f(t)\|$
$\|\cdot\|$	Magnitude of vector
$(\cdot)^{\mathrm{T}}$	Transpose operator
$\forall$	For all
$\exists$	Exists
$\mathbb{R}$	Real numbers
$\mathbb{R}^+$	Nonnegative real numbers $\{x \in \mathbb{R} \ : \ x \geq 0\}$
$\mathbb{R}^n$	Linear space of n-tuples in $\mathbb{R}$
∇	Divergence operator. $\nabla \cdot \boldsymbol{f}(x_1, x_2, \ldots) = \frac{\partial f_1}{\partial x_1} + \frac{\partial f_2}{\partial x_2} + \ldots$
$\mathcal{K}$	Class of functions. A function $f : [0, a) \to \mathbb{R}^+$ is said to belong to class $\mathcal{K}$ if it is strictly increasing and $f(0) = 0$.
$\mathcal{K}_\infty$	Class of functions. A function $f : [0, a) \to \mathbb{R}^+$ is said to belong to class $\mathcal{K}_\infty$ if it belongs to class $\mathcal{K}$, $a = \infty$ and $f(r) \to \infty$ as $r \to \infty$.
$\circ$	The function $f \circ g$ is the composition of the functions f and g
$\mapsto$	Mapping
$\mathcal{L}_2$	Space of square integrable functions. $f : \mathbb{R}_+ \to \mathbb{R}$ belongs to $\mathcal{L}_2$ iff $\int_0^\infty \|f(t)\|^2 dt < \infty$
$f_T(t)$	The truncation of f to $[0, T]$. $f_T(t) = \begin{cases} f(t) & , \quad 0 \leq t < T \\ 0 & , \quad t \geq T \end{cases}$
$\mathcal{L}_{2e}$	The extension of $\mathcal{L}_2$. $f \in \mathcal{L}_{2e}$ iff $f_T \in \mathcal{L}_2$
$\mathcal{G}$	Input-output mapping
$\langle u, y \rangle_T$	Inner product on $\mathcal{L}_{2e}$. $\langle u, y \rangle_T = \int_0^T u(t) y(t) dt$
$\|u\|_T^2$	Truncated norm. $\|u\|_T^2 = \langle u, u \rangle_T$
$\mathrm{sgn}(\cdot)$	Signum function
$\tanh(\cdot)$	Hyperbolic tangent
$\sup(\cdot)$	Supremum, lower upper bound

A.5 Symbols

The equation numbers are references to where the symbol was defined or first used.

Latin Uppercase

A_c	Flow area (2.3)
$\boldsymbol{A}_{cl}$	Closed loop Jacobian (2.193)
A_1	Reference flow area. Area of impeller eye. (5.1)
A_n	Amplitude of mode number n of rotating stall (4.48)
$\boldsymbol{A}_z(\boldsymbol{z}, \overline{\boldsymbol{d}})$	Nonlinear part of error dynamics (2.140)
$\mathcal{A}$	Area of attraction (2.154)
B	Greitzer B-parameter (2.3)
$C_{\theta 1}, C_{\theta 2}$	Tangential fluid velocity at the rotor entrance and exit (4.13)
C_x, C_{a1}, C_{a2}	Axial fluid velocity (4.21)
C_1	Fluid velocity at inducer (5.2)
C_2	Fluid velocity at diffuser entry, Figure 5.5
C_h	Surface friction loss coefficient (5.27)
$\overline{\mathcal{C}}_2$, $\overline{\mathcal{C}}_3$, $\overline{\mathcal{C}}_4$	Functions used to calculate upper bound on c_3 in the proof of Theorem 2.5
$\underline{\mathcal{C}}_1$, $\underline{\mathcal{C}}_3$, $\underline{\mathcal{C}}_4$	Functions used to calculate lower bound on c_3 in the proof of Theorem 2.5
D	Hydraulic diameter (5.27)
D_1, r_1	Average inducer diameter and radius (5.4)
D_2, r_2	Diameter and radius at impeller tip, Figure 5.5
D_{t1}	Diameter at inducer tip (5.4)
D_{h1}	Diameter at impeller hub casing (5.4)
$F(\phi)$	Pressure rise coefficient in blade passage (4.20)
$G_1(\phi), G_2(\phi)$	Functions used in the proof of Theorem 2.5
$\mathcal{G}_1, \mathcal{G}_2$	Input-output mappings (3.13), (3.14)
H	Compressor characteristic semi height (2.4)
I	Spool and rotor moment of inertia (4.8)
$\hat{I}$	Integral of $\hat{U}$ (5.65)
J	Squared amplitude of rotating stall (2.1)
J_i	Mode i of squared amplitude of rotating stall (4.72)
J_{ne}	Equilibrium value of J_n (4.74)
$J_{\max}$	Maximum value of squared rotating stall amplitude (2.150)

Latin Uppercase

$K(\hat{\phi})$	Function, used in passivity analysis (3.24)
K_G	Entrance recovery coefficient (4.30)
L_c	Length of ducts and compressor (2.3)
L_I	Length of inlet duct (4.4)
L_E	Length of exit duct (4.4)
M_1, M_2, M_3	Moments calculated in Galerkin approximation (4.66)
N_s	Number of compressor stages (2.12)
N	Number of revolutions per second (5.3)
$N(\mu)$	Number of rotating stall modes (4.50)
$\boldsymbol{P}$	Positive definite constant matrix (5.67)
$\boldsymbol{P}_z$	Constant skew symmetric matrix (2.140)
$\boldsymbol{P}(\phi)$	Matrix used in proof of Theorem 2.5
Q	Supplied heat
R_n	Residue nr. n used in Galerkin approximation (4.61)
R	Mean compressor radius (2.5)
$\boldsymbol{R}$	Positive definite constant matrix (5.75)
Re	Reynolds number (5.29)
$\mathcal{R}_\Delta, \mathcal{R}_1, \mathcal{R}_2, \mathcal{R}_3$	Residual sets (2.72), (2.87), (2.116), (2.202)
$S(\boldsymbol{z})$	Storage function (2.36)
T_{01}	Inlet stagnation temperature
$U(z_1, z_2, J)$	PDF (2.185)
U	Tangential speed of rotor
U_1	Tangential speed of rotor, at diameter D_1 (5.3)
U_2	Tangential impeller tip speed, Figure 5.5
U_d	Desired tangential speed of rotor (4.3)
U_m	Upper bound on U_1 (5.50)
V_p	Plenum volume (2.3)
V_1, V_2	LFCs
$\left(\dot{V}_2\right)_i$	Term number i in $\dot{V}_2$ (2.166)
W	Compressor characteristic semi width (2.4)
$W(z_1, z_2)$	PDF
W_1	Fluid velocity relative to moving impeller blades (5.5)
W_{1b}	Component of W_1 in blade direction (5.32)
$W_{\theta 1}$	Tangential component of W_1 (5.18)
$\dot{W}_c$	Compressor power (5.7)

Latin lowercase

a	Reciprocal time lag of the compressor passage (2.2)
a	Compressor characteristic slope (2.53)
a_s	Sonic velocity
a_m	Max positive slope of compressor characteristic (2.53)
b	Constant. $U = bB$ (4.7)
c_2, c_3	Surge/stall controller gains
c	Constant. Used in convergence proof (2.90)
c_{speed}	Speed controller gain (4.76)
c_n	Slope of backflow characteristic (5.102)
$c_3^{\min}, c_3^{\max}$	Lower and upper bound on c_3 (2.189), (2.190)
c_p	Specific heat capacity at constant pressure
c_v	Specific heat capacity at constant volume
d_ϕ, d_ψ	Mass flow and pressure biases (2.37)
d_1, d_2	Surge/stall controller damping coefficients
$\overline{d}_\psi, \overline{d}_\phi$	Estimates of biases, Theorem 2.4
$\tilde{d}_\psi, \tilde{d}_\phi$	Estimation errors (2.126), (2.134)
$\tilde{\boldsymbol{d}}$	$(\tilde{d}_\psi \ \tilde{d}_\phi)^{\mathrm{T}}$
f	Friction factor (5.29)
$g(\xi, \theta)$	Disturbance of axial flow coefficient (4.28)
$h(\xi, \theta)$	Circumferential velocity coefficient (4.28)
h_1, h_2, h_3	Weight functions used in Galerkin approximation (4.63)
h	Specific enthalpy
k_1, k_2, k_3	Compressor characteristic coefficients (2.24)
k_v	Surge control law parameter (5.64)
k_p, k_i	Proportional and integral gain of speed controller (5.65)
l_c	Nondimensional compressor length (2.2)
l_i	Nondimensional length of inlet duct (2.2)
l_e	Nondimensional length of exit duct (2.2)
l	Mean flow length (5.27)
m, m_c	Compressor mass flow
m	Compressor duct flow parameter (4.45)
m_{choke}	Choking mass flow (2.45)
p	Pressure
p_p	Plenum pressure (5.1)
$\hat{p}_{max}$	Upper bound on $\hat{p}$ used to calculate δ_2 (5.82)
p_0, m_0	Equilibrium value of p_p and m (5.54)
r_n	Phase angle of mode number n of rotating stall (4.59)
q	Dimension of state space in Chapter 4
$s(\xi, \boldsymbol{z})$	Signal. Used in convergence proof (2.90)
s	Specific entropy
u	Control variable
v	Specific volume
z_1, z_2	Error variables
$\boldsymbol{z}$	State vector. $\boldsymbol{z} = (z_1 \ z_2)^{\mathrm{T}}$

Greek uppercase

$\Delta\eta_{bf}$	Loss in efficiency due to backflow (5.39)
$\Delta\eta_c$	Loss in efficiency due to clearance (5.38)
$\Delta\eta_v$	Loss in efficiency in the volute (5.40)
$\Delta\eta_d$	Loss in efficiency due to incomplete diffusion
$\Delta\phi$	Approximation error $\Delta\phi = \phi_0 - \phi_{apprx}$ (2.64)
Δh_{0c}	Ideal specific enthalpy delivered to fluid (5.9)
$\Delta h_{0c,ideal}$	Total specific enthalpy delivered to fluid (5.54)
$\Delta h_{ii}, \Delta h_{id}$	Incidence losses in impeller and diffuser (5.21), (5.26)
$\Delta h_{fi}, \Delta h_{fd}$	Friction losses in impeller and diffuser (5.27), (5.34)
Γ_t	Nondimensional turbine (drive) torque (4.10)
Γ_c	Nondimensional compressor torque (4.10)
$\mathbf{\Gamma}$	Positive definite constant matrix (2.133)
Λ_1, Λ_2	Constants in MG model (4.12), (4.46)
$\Sigma_{\mathcal{G}_1,\mathcal{G}_2}$	Feedback interconnection of $\mathcal{G}_1$ and $\mathcal{G}_2$, Theorem 3.1
Φ	Axial mass flow coefficient, annulus averaged (2.1)
$\Phi_T(\psi)$	Throttle mass flow coefficient (2.1)
$\hat{\Phi}_d$	Time varying mass flow disturbance, section 2.2.5
$\overline{\Psi}_d(\xi)$	Monotonically decreasing non negative function, Corollary 2.1
$\overline{\Phi}_d(\xi)$	Monotonically decreasing non negative functions, Corollary 2.2
Ψ	Pressure coefficient (2.1)
$\Psi_T(\phi)$	Throttle characteristic (2.9)
$\Psi_v(\phi]$	CCV characteristic (2.11)
$\Psi_c(\phi)$	Compressor characteristic (2.7)
$\Psi_e(\phi)$	Equivalent compressor characteristic (2.10)
$\Psi_s(\phi)$	In-stall characteristic (2.17)
$\Psi_{es}(\phi)$	Equivalent in-stall characteristic (2.16)
$\hat{\Psi}_d$	Time varying pressure disturbance, section 2.2.5

Greek lowercase

α	Virtual control used in backstepping
$\alpha_1, \alpha_2, \beta_1, \beta_2$	Fluid angles
$\beta_{1b}, \beta_{2b}, \alpha_{1b}, \alpha_{2b}$	Constant blade angles
β_i	Angle of incidence (5.15)
$\beta_1, \beta_2, \beta_3$	Class $\mathcal{K}_\infty$ functions (2.70), (2.71)
γ_T	Throttle gain, parameter proportional to throttle opening (2.9)
γ	CCV gain, parameter prop. to valve opening (2.11)
δ_1, δ_2	Constants (5.66), (5.81)
$\lambda, \lambda_1, \lambda_2$	Constants (5.78)
ζ_n	$\zeta_n \triangleq n\theta - r_n(\xi)$ (4.63)
η	Nondimensional x-coordinate
$\eta_0, \eta_1, \eta_2, \eta_3, \eta_4$	Constants. Used in Young's inequality
η_i	Isentropic efficiency (5.35)
θ	Angular coordinate
ϑ_1, ϑ_2	Adaption gains, Theorem 2.4
κ_1, κ_2	Constants used in passivity proofs (3.9), (3.21)
κ	Ratio of specific heats, $\kappa = \frac{c_p}{c_v}$
μ	Viscosity (4.49)
ν_1, ν_2	Constants (2.114)
ϖ	Convergence rate (5.99)
ξ	Nondimensional time (2.5)
ϱ	Constant in the MG model (2.4)
ρ	Density
ρ_{01}	Inlet stagnation density
σ	Slip factor (5.8)
ς	Constant (5.60)
τ_t	Turbine (drive) torque (4.10)
τ_c	Compressor torque (4.10)
τ_c^-, τ_c^+	Compressor torque for neg. and pos. flow (5.10)
τ_{df}	Disc friction torque (5.13)
ϕ	Local axial mass flow coefficient (4.27)
ϕ_0	Equilibrium value of ϕ (2.18)
ϕ_{apprx}	Approximation of ϕ_0 (2.64)
ϕ_{choke}	Upper bound on ϕ (2.151)
ϕ_m	Lower bound on ϕ (2.153)
$\tilde{\phi}$	Velocity potential (4.33)
$\tilde{\phi}'$	Disturbance velocity potential (2.34)
ψ_0	Equilibrium value of ψ (2.18)
ψ_{c0}	Shut off value of compressor characteristic (2.7)
ω_H	Helmholtz frequency
ω	Rotational velocity of spool (4.8)

Appendix B

Some Thermodynamic and Fluid Mechanical Relations

B.1 Flow and Pressure Coefficients

In this section various nondimensional quantities related to compressors are presented.

Flow Coefficient

The flow coefficient is defined as

$$\phi = \frac{C_x}{U}, \tag{B.1}$$

where C_x is the axial velocity and U is the blade speed. Using the ideal gas law it is found that

$$\phi = \frac{\rho_{01} R T_{01}}{p_{01}} \frac{C_x}{U} = \frac{\sqrt{RT_{01}}}{U} \frac{m\sqrt{RT_{01}}}{A p_{01}} = \frac{\sqrt{RT_{01}}}{U} F, \tag{B.2}$$

where F is known as the (nondimensional) flow function. Mention must be made to another form of nondimensional flow, *the corrected mass flow* defined as

$$m_{corr} = \frac{m\sqrt{T_{01}/T_{ref}}}{p_{01}/p_{ref}}. \tag{B.3}$$

The reference state is usually taken as sea level static. It can be shown that the corrected mass flow is related to the flow coefficient as

$$\phi = \frac{\sqrt{T_{01}/T_{ref}}}{\rho_{ref}\sqrt{R}UA} m_{corr}, \tag{B.4}$$

that is, for constant U, ϕ is proportional to m_{corr}.

Pressure Coefficient

The total to static pressure rise coefficient is defined as

$$\Psi = \frac{p_1 - p_{01}}{\rho U^2}. \tag{B.5}$$

In (Cohen *et al.* 1996) it is shown that

$$\Psi = \eta_i \frac{c_p \Delta T_{0s}}{U^2} = \eta_i \frac{\Delta h_{0s}}{U^2}, \tag{B.6}$$

where η_i is the isentropic efficiency, ΔT_{0s} is the temperature rise in the stage and h_{0s} is the enthalpy rise. The fraction $c_p \Delta T_{0s}/U^2$ is known as the temperature coefficient.

Speed Coefficient

Blade speed U can be nondimensionalized by dividing with inlet stagnation sonic velocity a_{01},

$$\frac{U}{a_{01}} = \frac{U}{\kappa R T_{01}} = \frac{D\pi N}{\kappa R T_{01}} = \frac{D\pi}{\kappa R T_{ref}} N_{corr}, \tag{B.7}$$

where $N_{corr} = N/\sqrt{T_0/T_{ref}}$ is known as the *corrected speed*. Note that by introducing the Greitzer B-parameter it is found that

$$\frac{U}{a_{01}} = \frac{D\pi}{\kappa R T_{ref}} N_{corr} = 2B\sqrt{\frac{A_c L_c}{V_p}}. \tag{B.8}$$

Thus, B can be used as nondimensional compressor speed, and it is connected to N_{corr} as

$$N_{corr} = 2B\sqrt{\frac{A_c L_c}{V_p}} \frac{\kappa R T_{ref}}{D\pi}. \tag{B.9}$$

B.2 Isentropic Processes

Let s denote specific entropy, u denote specific internal energy, $v = V/m = \rho^{-1}$ denote specific volume and $h = u + pv$ denote specific enthalpy. It can be shown (Eastop and A.McConkey 1986), that

$$ds = \frac{dQ}{T}, \tag{B.10}$$

where

$$dQ = du + pdv \tag{B.11}$$

is known as the differential form of the non-flow energy equation. It follows that

$$\begin{aligned} Tds &= du + pdv \\ Tds &= dh - vdp. \end{aligned} \tag{B.12}$$

With constant specific heat capacities c_p and c_v,

$$\begin{aligned} Tds &= c_v dT + pdv \\ Tds &= c_p dT - vdp. \end{aligned} \tag{B.13}$$

For isentropic processes, that is reversible and adiabatic, $ds = 0$, and accordingly

$$\begin{aligned} dT &= -\frac{p}{c_v} dv \\ dT &= \frac{v}{c_p} dp, \end{aligned} \tag{B.14}$$

which in turn implies

$$\frac{dp}{p} = -\kappa \frac{dv}{v}, \tag{B.15}$$

where $\kappa = \frac{c_p}{c_v}$ is the ratio of specific heats.

B.3 Mass Balance of the Plenum

The plenum process is assumed to be isentropic, which means that the differential form (B.15) of the isentropic relation is valid, so that

$$\frac{dp_p}{p_p} = -\kappa \frac{dv_p}{v_p} = \kappa \frac{d\rho_p}{\rho_p}, \tag{B.16}$$

where it has been used that

$$\rho = \frac{1}{v} \;\Rightarrow\; \frac{d\rho}{\rho} = -\frac{dv}{v}. \tag{B.17}$$

It follows that

$$\dot{p}_p = \frac{\kappa p_p}{\rho_p} \dot{\rho}_p = \kappa R T_p \dot{\rho}_p. \tag{B.18}$$

The mass balance of the plenum is

$$\dot{\rho}_p = \frac{1}{V_p}(m - m_t), \tag{B.19}$$

and it follows that

$$\dot{p}_p = \frac{\kappa R T_p}{V_p}(m - m_t) = \frac{a_s^2}{V_p}(m - m_t), \tag{B.20}$$

where $a_s = \sqrt{\kappa R T_p}$ is the plenum sonic velocity. As velocities in the plenum are assumed negligible, a_0 can be used in (B.20). The sound speed in the plenum will wary as both temperature and pressure in the plenum varies with time. In (Simon *et al.* 1993), a time mean speed of sound in the plenum, $\overline{a}_s$ was used. Another approach to avoid using the plenum sonic velocity was taken in (Greitzer 1976*a*). It was recognized that by assuming that the temperature ratios of the compression system are near unity, the quantity $\rho_p / p_p = R T_p$ is not appreciably different from ρ_{01}/p_{01}. Thus, the speed of sound at ambient conditions can be used in (B.20). This approach is also taken in this thesis.

B.4 Flow through a Nozzle

The stagnation temperature is

$$T_0 = T + \frac{1}{2c_p} C_x^2, \tag{B.21}$$

where T is the static temperature and C_x is the velocity of the flow. The Mach number is

$$M = \frac{C_x}{a_s}, \tag{B.22}$$

where

$$a_s = \sqrt{\kappa RT}, \tag{B.23}$$

is the sonic velocity. Then $C_x^2 = M^2 \kappa RT$ and it follows that

$$\frac{T_0}{T} = 1 + \frac{M^2 \kappa R}{2c_p} = 1 + \frac{\kappa - 1}{2} M^2. \tag{B.24}$$

Using the isentropic relation

$$\frac{T_0}{T} = \left(\frac{p}{p_0} \right)^{\frac{(\kappa-1)}{\kappa}}, \tag{B.25}$$

it is found that

$$\frac{p_0}{p} = \left(1 + \frac{\kappa - 1}{2} M^2 \right)^{\frac{\kappa}{\kappa-1}}. \tag{B.26}$$

The mass flow is

$$m = \rho A C_x, \tag{B.27}$$

where A is the flow crossectional area. Alternative forms are

$$\begin{aligned} m &= \rho A M a_s = A\rho\sqrt{\kappa RT} M = A \frac{p}{\sqrt{RT}} \sqrt{\kappa} M \\ &= A \frac{p_0}{\sqrt{RT_0}} \frac{p}{p_0} \sqrt{\frac{T_0}{T}} \sqrt{\kappa} M, \end{aligned} \tag{B.28}$$

where it is used that $\rho = p/RT$. Then, by the use of (B.25) and (B.26), it is found that

$$m = A \frac{p_0}{\sqrt{RT_0}} \sqrt{\kappa} M \left(1 + \frac{\kappa - 1}{2} M^2 \right)^{-\frac{\kappa+1}{2(\kappa-1)}}. \tag{B.29}$$

The critical mass flow, or choked flow, is found by inserting $M = 1$ and using the ideal gas law in the form $RT_0 = \rho_0/p_0$. This gives

$$\begin{aligned} m_{choke} &= A\sqrt{\kappa \rho_0 p_0} \left(\frac{2}{\kappa + 1} \right)^{\frac{\kappa+1}{2(\kappa-1)}} && \text{(B.30)} \\ &= A \rho_0 a_0 \left(\frac{2}{\kappa + 1} \right)^{\frac{\kappa+1}{2(\kappa-1)}}. && \text{(B.31)} \end{aligned}$$

B.5 Compressor Pressure Rise

Here equation (5.42) for the compressor pressure rise is derived. The compressor total to static isentropic efficiency can be written

$$\eta_i(m, U_1) = \frac{h_{2s} - h_{01}}{h_{02} - h_{01}}, \tag{B.32}$$

where h_{2s} is the outlet static enthalpy obtained with isentropic compression, h_{01} is the inlet stagnation, or total, enthalpy and h_{02} is the outlet stagnation, or total, enthalpy.
Considering a perfect gas, we have that $h = Tc_p$, where c_p is the specific heat capacity at constant pressure. For a perfect gas, c_p is constant. The efficiency now is

$$\eta_i(m, U_1) = \frac{T_{2s} - T_{01}}{T_{02} - T_{01}} = \frac{\frac{T_{2s}}{T_{01}} - 1}{\frac{T_{02}}{T_{01}} - 1}. \tag{B.33}$$

Using the relation for isentropic compression (B.25),

$$\eta_i(m, U_1) = \frac{\left(\frac{p_2}{p_{01}}\right)^{\frac{\kappa-1}{\kappa}} - 1}{\frac{T_{02}}{T_{01}} - 1} = \frac{T_{01}c_p\left(\left(\frac{p_2}{p_{01}}\right)^{\frac{\kappa-1}{\kappa}} - 1\right)}{c_p(T_{02} - T_{01})}. \tag{B.34}$$

For a radially vaned impeller (Watson and Janota 1982):

$$\eta_i(m, U_1) = \frac{T_{01}c_p\left(\left(\frac{p_2}{p_{01}}\right)^{\frac{\kappa-1}{\kappa}} - 1\right)}{\Delta h_{0c,ideal}}, \tag{B.35}$$

which can be rearranged to

$$\frac{p_2}{p_{01}} = \left(1 + \frac{\eta_i(m, U_1)\Delta h_{0c,ideal}}{T_{01}c_p}\right)^{\frac{\kappa}{\kappa-1}}. \tag{B.36}$$

Appendix C

Including a Close Coupled Valve in the Moore-Greitzer Model

Equation numbers starting with *MG* are references to the paper Moore and Greitzer (1986).
Equation (MG5), which gives the pressure rise over the compressor is modified to

$$\underbrace{\frac{p_E - p_1}{\rho U^2} = N_s F(\phi) - \frac{1}{2a}\left(2\frac{\partial \phi}{\partial \xi} + \frac{\partial \phi}{\partial \theta}\right)}_{\text{Equation (5) in Moore and Greitzer (1986)}} - \Psi_v(\phi), \tag{C.1}$$

where $\Psi_v(\phi)$ is the pressure drop across the CCV, and p_E now is the pressure at the exit of the CCV. Using equation (MG23), the pressure rise over the equivalent compressor is written

$$\Psi_e(\phi) = \underbrace{N_s F(\phi) - \frac{1}{2}\phi^2}_{\Psi_c(\phi)} - \Psi_v(\phi). \tag{C.2}$$

Using this, the local (in θ) and annulus averaged momentum balances (equations (MG42) and (MG43)), are modified to

$$\Psi(\xi) + l_c \frac{d\Phi}{d\xi} = \psi_c(\Phi - Y_{\theta\theta}) - \psi_v(\Phi - Y_{\theta\theta}) - mY_\xi + \frac{1}{2a}\left(2Y_{\xi\theta\theta} + Y_{\theta\theta\theta}\right) \tag{C.3}$$

and

$$\Psi(\xi) + l_c \frac{d\Phi}{d\xi} = \frac{1}{2\pi}\int_0^{2\pi} \left\{\psi_c(\Phi - Y_{\theta\theta}) - \psi_v(\Phi - Y_{\theta\theta})\right\} d\theta. \tag{C.4}$$

In the case of pure surge, that is $Y \equiv 0$, the two momentum balances are the same and is reduced to

$$\dot{\Phi} = \frac{1}{l_c}(\Psi_c(\Phi) - \Psi_v(\Phi) - \Psi), \tag{C.5}$$

which is the same expression as used in Simon (1993). The CCV has a characteristic given by

$$\Psi_v(\phi) = \frac{1}{\gamma^2}\phi^2, \tag{C.6}$$

where $\gamma > 0$ is proportional to the valve opening. Y is now represented by a single harmonic approximation

$$Y^* = WA(\xi)sin(\theta - r(\xi)) = WA(\xi)sin(\zeta), \tag{C.7}$$

where $A(\xi)$ is the time varying stall amplitude. A residue R, is defined as

$$R \stackrel{\triangle}{=} Y_\xi^* - Y_\xi. \tag{C.8}$$

The Galerkin approximation is calculated using the weight functions

$$h_1 = 1,\ h_1 = \sin\zeta,\ h_2 = \cos\zeta \tag{C.9}$$

and the inner product

$$\langle R, h_i\rangle = \frac{1}{2\pi}\int_0^{2\pi} R(\zeta)h_i(\zeta)d\zeta. \tag{C.10}$$

Calculating $\langle R, h_i\rangle = 0$ for $i = 1, 2, 3$, we get

$$M_1 = \frac{1}{2\pi}\int_0^{2\pi} \psi_e(\Phi + WA\sin\zeta)d\zeta = \Psi + l_c\frac{d\Phi}{d\xi} \tag{C.11}$$

$$M_2 = \frac{1}{2\pi}\int_0^{2\pi} \psi_e(\Phi + WA\sin\zeta)\sin\zeta d\zeta = (m + \frac{1}{a})\frac{dA}{d\xi} \tag{C.12}$$

$$M_3 = \frac{1}{2\pi}\int_0^{2\pi} \psi_e(\Phi + WA\sin\zeta)\cos\zeta d\zeta = -(\frac{dr}{d\xi}(m + \frac{1}{a}) - \frac{1}{2a})A. \tag{C.13}$$

By using (C.2) and (2.7) the moments M_i are calculated to be

$$M_1 = \frac{\pi}{2}\left(4\psi_0 - \frac{2H\Phi^3}{W^3} - \frac{2W^2A^2}{\gamma^2} - \frac{3H\Phi A^2}{W} - \frac{4\Phi^2}{\gamma^2} + \frac{6H\Phi^2}{W^2} + 3HA^2\right) \tag{C.14}$$

$$M_2 = \frac{\pi}{2}\left(-\frac{3H\Phi^2A}{W^2} - \frac{3HA^3}{4} - \frac{2AW\Phi}{\gamma^2} + \frac{6AH\Phi}{W}\right) \tag{C.15}$$

$$M_3 = 0. \tag{C.16}$$

By combining (C.11) to (C.13) with (C.14) to (C.16) and rearranging, the following differential equations, which correspond to (MG60) and (MG61), for Φ and $J = A^2$ are found:

$$\dot{\Phi} = \frac{H}{l_c}\left(-\frac{\Psi - \psi_0}{H} - \frac{1}{2}\left(\frac{\Phi}{W} - 1\right)^3 + 1 + \frac{3}{2}\left(\frac{\Phi}{W} - 1\right)\left(1 - \frac{J}{2}\right) - \frac{1}{\gamma^2}\left(\frac{W^2J}{2H} + \frac{\Phi^2}{H}\right)\right) \tag{C.17, C.18}$$

$$\dot{J} = J\left(1 - \left(\frac{\Phi}{W} - 1\right)^2 - \frac{J}{4} - \frac{1}{\gamma^2}\frac{4W\Phi}{3H}\right)\sigma. \tag{C.19}$$

The differential equations for ψ and r are left unchanged by the introduction of the CCV.

Appendix D

Numerical Values Used in Simulations

Symbol	value	Symbol	value	Symbol	value
R	0.1m	ρ	$1.15\frac{\text{kg}}{\text{m}^3}$	a_s	$340\frac{\text{m}}{\text{s}}$
l_E	8	l_I	2	L_c	3m
V_p	1.5m^3	A_c	0.01m^2	a	0.3
H	0.18	W	0.25	ψ_{c0}	0.3
I	0.03kgm^2	m	1.75		

Table D.1: Numerical values used in the simulations of Chapters 2, 3 and 4.

Symbol	value	Symbol	value	Symbol	value
D_2	0.128m	D_{t1}	0.074m	D_{h1}	0.032m
σ	0.9	p_{01}	10^5Pa	ρ_1	$1.15\frac{\text{kg}}{\text{m}^3}$
T_{01}	303K	α_1	$\pi/2$	β_{1b}	0.61
Re	100000	D	0.02m	κ	1.4
c_p	$1005\frac{\text{J}}{\text{kgK}}$	C_m	0.01	a_{01}	$340\frac{\text{m}}{\text{s}}$
V_p	0.21m^3	L_c	1.253m	J	$.001\text{kgm}^2$

Table D.2: Numerical values used in the simulations of Chapter 5.

Appendix E

Bounds on the Controller Parameters of Theorem 2.5

In this appendix the upper and lower bounds on the controller gain c_3 defined in Theorem 2.5 are calculated. The numerical values used are

Sym.	value	Sym.	value	Sym.	value	Sym.	value
$J_{\max}$	4	W	0.25	H	0.18	ψ_{co}	0.3006
ϕ_{choke}	0.8	ϕ_m	0.2				

Table E.1: Numerical values

The equilibrium value of the mass flow coefficient ϕ_0 is found by solving equation (2.63) with respect to ϕ_0. The lower bound $\underline{\mathcal{C}}_1$ defined in (2.178) is

$$\underline{\mathcal{C}}_1 = \frac{3H}{4W^2}\left(\frac{\phi_0^2}{4W} + W + \phi_0\right) - c_2. \tag{E.1}$$

Using (2.184), the upper bound $\overline{\mathcal{C}}_2$ is calculated as

$$\overline{\mathcal{C}}_2 = \frac{\phi_m - \phi_0}{\phi_m}\frac{4W}{3H}\left((\phi_0-\phi_m)\hat{\Psi}_c(\phi_0-\phi_m) - c_2(\phi_0-\phi_m)^2 - \frac{\phi_m^2}{W^2} - \frac{2\phi_m}{W}\right) + c_2 \tag{E.2}$$

With the help of symbolic toolbox in MATLAB, the following expressions are found for $\overline{\mathcal{C}}_3$, $\overline{\mathcal{C}}_4$, $\underline{\mathcal{C}}_3$ and $\underline{\mathcal{C}}_4$:

$$\underline{\mathcal{C}}_3(c_2, \phi_{choke}) = -\frac{T_0 + T_1}{2V^4 J_{\max}} \tag{E.3}$$

$$\overline{\mathcal{C}}_3(c_2, \phi_{choke}) = -\frac{T_0 - T_1}{2V^4 J_{\max}}, \tag{E.4}$$

where

$$T_0 = -4\,\phi_{choke}^2 - 8\,\phi_{choke}\,\phi_0 - 4\,\phi_0^2 + 3\,HW\,J_{\max}\,\phi_{choke}\,\phi_0$$

$$
\begin{aligned}
& -3\,W^2 H J_{\max}\,\phi_{choke} - 3\,W^2 H J_{\max}\,\phi_0 + 3\,HW J_{\max}\,\phi_{choke}^2 \\
& +2\,W^4 J_{\max}\,c_2 \\
T_1 \;=\;& -2\,\sqrt{2}\sqrt{T_2} \\
T_2 \;=\;& -\big(3\,HW J_{\max}\,\phi_{choke}^2 - 2\,\phi_{choke}^2 - 4\,\phi_{choke}\,\phi_0 \\
& -3\,W^2 H J_{\max}\,\phi_{choke} + 3\,HW J_{\max}\,\phi_{choke}\,\phi_0 \\
& +2\,W^4 J_{\max}\,c_2 - 2\,\phi_0^2 - 3\,W^2 H J_{\max}\,\phi_0\big)\,(\phi_{choke}+\phi_0)^2
\end{aligned}
$$

and

$$
\underline{\mathcal{C}}_4(c_2,\phi_m) \;=\; -\frac{T_0+T_1}{2V^4 J_{\max}} \tag{E.5}
$$

$$
\overline{\mathcal{C}}_4(c_2,\phi_m) \;=\; -\frac{T_0-T_1}{2V^4 J_{\max}}, \tag{E.6}
$$

where

$$
\begin{aligned}
T_0 \;=\;& -4\,(-\phi_m)^2 - 8\,(-\phi_m)\,\phi_0 - 4\,\phi_0^2 + 3\,HW J_{\max}\,(-\phi_m)\,\phi_0 \\
& -3\,W^2 H J_{\max}\,(-\phi_m) - 3\,W^2 H J_{\max}\,\phi_0 + 3\,HW J_{\max}\,(-\phi_m)^2 \\
& +2\,W^4 J_{\max}\,c_2 \\
T_1 \;=\;& -2\,\sqrt{2}\sqrt{T_2} \\
T_2 \;=\;& -\big(3\,HW J_{\max}\,(-\phi_m)^2 - 2\,(-\phi_m)^2 - 4\,(-\phi_m)\,\phi_0 \\
& -3\,W^2 H J_{\max}\,(-\phi_m) + 3\,HW J_{\max}\,(-\phi_m)\,\phi_0 \\
& +2\,W^4 J_{\max}\,c_2 - 2\,\phi_0^2 - 3\,W^2 H J_{\max}\,\phi_0\big)\,((-\phi_m)+\phi_0)^2
\end{aligned}
$$

As the value of ϕ_0 depends on the choice of c_2 and c_3, the gains have to be chosen first, then ϕ_0 is calculated, and finally the bounds $c_3^{\min}$ and $c_3^{\max}$ have to be calculated and checked against c_3. After some iterations of this procedure the following gains are used: $c_2 = 1$ and $c_3 = 0.55$, ϕ_0 is calculated to $\phi_0 = 0.34$ and the bounds are calculated to be

$$
\begin{aligned}
\underline{\mathcal{C}}_1(c_2,\phi_0) &= 0.52 \\
\overline{\mathcal{C}}_2(c_2,\phi_0,\phi_m) &= 2.24 \\
\underline{\mathcal{C}}_3(c_2,\phi_0,\phi_{choke}) &= 0.33 \\
\overline{\mathcal{C}}_3(c_2,\phi_0,\phi_{choke}) &= 419.34 \\
\underline{\mathcal{C}}_4(c_2,\phi_0,\phi_m) &= 0.0011 \\
\overline{\mathcal{C}}_4(c_2,\phi_0,\phi_m) &= 6.83.
\end{aligned}
$$

Now,

$$
\begin{aligned}
c_3^{\min} &= \max\{\underline{\mathcal{C}}_1,\ \underline{\mathcal{C}}_3,\ \underline{\mathcal{C}}_4\} \\
&= \max\{0.52,\ 0.33,\ 0.0011\} \\
&= 0.52,
\end{aligned} \tag{E.7}
$$

and

$$
\begin{aligned}
c_3^{\max} &= \min\{\overline{\mathcal{C}}_2(c_2,\phi_m),\ \overline{\mathcal{C}}_3(c_2,\phi_{choke}),\ \overline{\mathcal{C}}_4(c_2,\phi_m)\} \\
&= \min\{2.24,\ 419.34,\ 6.83\} \\
&= 2.24.
\end{aligned} \tag{E.8}
$$

As can be seen the choice $c_3 = 0.55$ now satisfies

$$c_3^{\min} = 0.52 < c_3 = 0.55 < c_3^{\max} = 2.24. \tag{E.9}$$